Institute for Superconducting & Electronic Materials

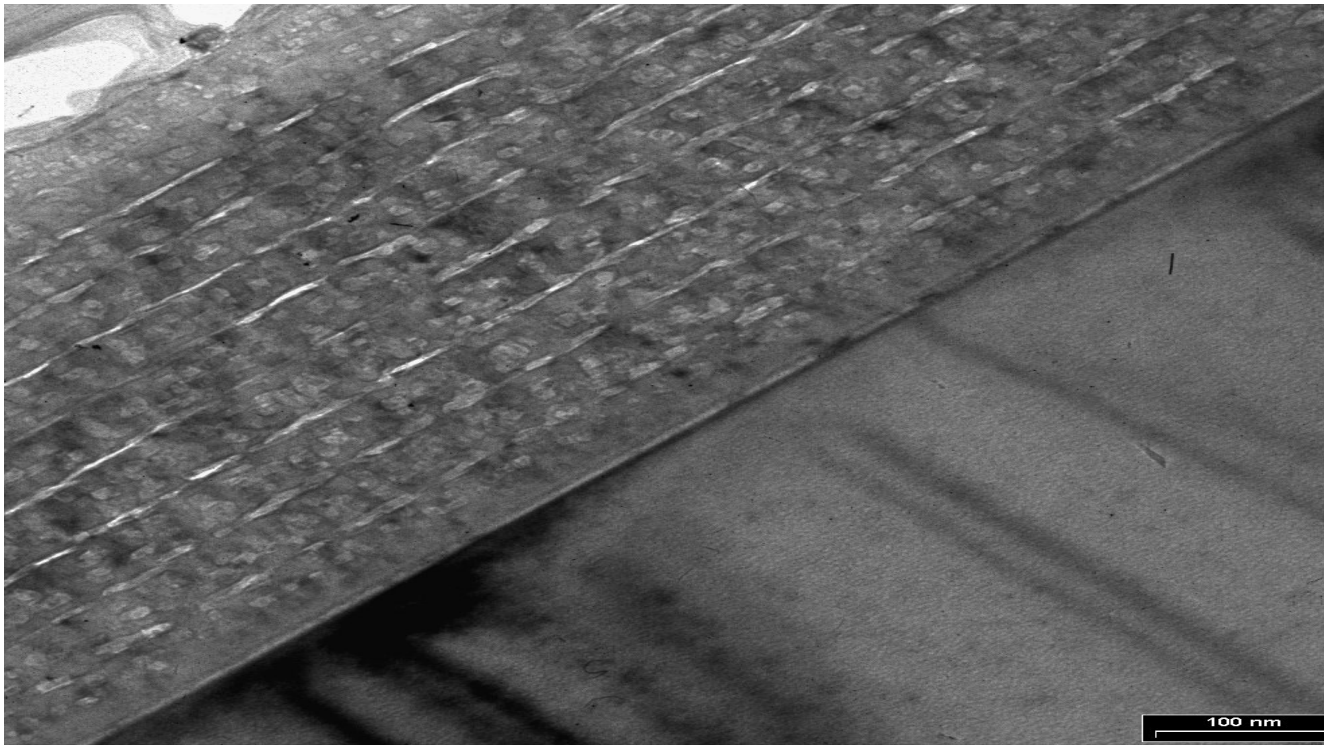

Annual Report 2004

University of Wollongong

Contents

Cover picture:
The image on the front page shows a multi layer structure of Si-doped Mg B_2 superconductur thin film from appl phys. Lett paper by Y Zhao, M Ionescu and S X Dou.

ISEM Postgraduate Student Awards

Each year ISEM selects a number of outstanding students and in recognition of their research efforts, these students are presented with a Certificate to mark their achievements, together with a cash prize.

Postgraduate Student Excellence Awards 2004

SCOTT NEEDHAM

GERMANAS PELECKIS

Postgraduate Student Merit Awards 2004

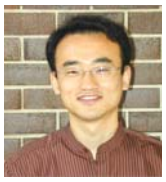

ZHENGUO (BERNIE) HUANG

DESMOND NG

OLGA SHCHERBAKOVA

MARK O'DWYER

Best Postgraduate published paper Award 2004

BRAD WINTON

Mission Statement

Establish and maintain a world-class co-operative research team in superconducting and electronic materials science and technology and stimulate the technological and commercial development of Australian Industry in this field.

Professor SX Dou
Director
e-mail: shi_dou@uow.edu.au

Prof Chao Zhang
Associate Director
e-mail: chao_zhang@uow.edu.au

Ms Christine O'Brien
Administration Officer
e-mail: cobrien@uow.edu.au

Telephone: 61 + 2 4221 5730
Facsimile: 61 + 2 4221 5731
web site: http://www.uow.edu.au/eng/ISEM

Northfields Avenue
Wollongong NSW 2522
Australia

Applied Superconductivity

Dr. J Horvat
Telephone: 61 + 2 4221 5725
Facsimile: 61 + 2 4221 5731
e-mail: jhorvat@uow.edu.au

Spintronic & Electronic Materials

Dr. X.L. Wang
Telephone: 61 + 2 4221 5766
Facsimile: 61 + 2 4221 5731
e-mail: xiaolin@uow.edu.au

Energy Materials

Prof. H.K.Liu
Telephone: 61 + 2 4221 4547
Facsimile: 61 + 2 4221 5731
e-mail: hua_liu@uow.edu.au

Dr. G.X. Wang
Telephone: 61 + 2 4221 5726
Facsimile: 61 + 2 4221 5731
e-mail: gwang@uow.edu.au

Thin Film Technology

Dr A.V.Pan
Telephone: 61 + 2 4221 4729
Facsimile: 61 + 2 4221 5731
e-mail: pan@uow.edu.au

Nanostructured Materials

Dr. K. Konstantinov
Telephone: 61 + 2 4221 5765
Facsimile: 61 + 2 4221 5731
e-mail: kostan@uow.edu.au

Terahertz Science, Thermionics & Solid State Physics

Prof. C. Zhang
Telephone: 61 + 2 4221 3458
Facsimile: 61 + 2 4221 5944
e-mail: chao_zhang@uow.edu.au

Director's Report

Prof. Shi Xue Dou
PhD, DSc, FTSE
ARC Australian Professorial Fellow

2004 is the first year of the Three Year Plan (2004-2006) of the University's Research Strength Program, which has identified the Institute for Superconducting and Electronic Materials (ISEM) as one of the key research strength areas. Our numerical target for the three years was ten ARC fellows, twenty full time researchers, forty postgraduate students enrolled, 50% of papers published in journals with an impact factor greater than 2 and $2m ARC fund per year. Our 2004 results have demonstrated that we are well on track to achieve or exceed these goals. ISEM has nine various ARC fellows, nineteen full time researchers, and thirty PGS enrolled; 39 of 73 papers were published in journals with an impact factor greater than 2; and the total ARC funding obtained in the 2004 round exceeded $3.15 million.

In the research area our institute has earned international recognition in several programs. For example, our nano-scale particle doping to enhance MgB_2 superconductor performance has been widely verified and confirmed by a number of prestigious groups as one of the most important breakthroughs since the discovery of this material. Nano-SiC doping resulted in record high critical current density and upper critical field, and these records still stand for MgB_2. Papers related to this work have been cited more than 200 times in the last two years. This work has attracted investors' interest for licensing, continuing industry support and the Australian Engineering Excellence Award in the Highly Commended category. Our institute has expanded its success in energy storage materials, spintronics, thin film technology, terahertz research, thermionics and nano-materials. *Materials Bulletin* has devoted a special article to our Battery Group's research on the application of novel nano-tubes to electrode materials. Our excellent progress in superconductivity and spintronics is evidenced by our success in winning three competitive ARC fellowships: an International Professorial Fellow, a QEII fellowship and a post-doctorial fellowship. The Physics Group, in collaboration with UNSW and the University of Oregon, has made a major breakthrough in nano-thermionics, which was published in *Physical Review Letters*. In 2004 I received the Australian Government's Centenary Medal for contributions to advancement in materials science and technology. This is not only just a personal honour to myself but also recognition of the collective effort and dedication of all members of ISEM.

In the area of staff development, our staff remains proactive in their research and career development. I am very pleased to see our next generation of early career and middle career researchers coming along as a strong team, ensuring the stability and security of ISEM. The situation of financial dependence on couple of individual senior staff has become history. I have every confidence that our institute will continue to grow in the years to come. Professor Chao Zhang was appointed as Associate Director and the head of postgraduate student training of our institute. Dr. J. Horvat was promoted to Senior Lecturer. Drs J.M. Yoo, X.L. Wang and S.H. Zhou were appointed to ARC International Professorial, QEII and APD fellowships at ISEM, respectively. Drs. D.Q. Shi, R Mendis and J.H. Kim were appointed as research fellows on ARC projects. Dr S. Shrestha was appointed research fellow on the SERDF project. After eight year's excellent administrative work Mrs B. Allen left the institute. We will remember her significant contribution to the success of ISEM. We have supported a number of visiting researchers and internship students, including the following visiting staff: Prof J.Y. Lee from Korean Advanced Institute of Science and Technology, Prof J.H. Ahn from national Andoing University, Dr. S.I. Moon from Korean Institute of Electric Technology, Prof S.Y. Ding from Nanjing University, A/Professor D. Santos from Brazil, Dr. K. Yamaura from National Institute of Materials Science Japan, A/Professor M.Y. Zhu from Shanghai University, Prof. Z.S. Ma from Peking University, Dr. G. Alvarez from Tokyo University of

Technology, and L. Yang from Shenzhen, and the following internship students: Y. Tournayre and P. Richet from French universities, and D.Y. Zhang from Jiaotong University.

Our institute made very successful ARC grant bids in the 2005 round with a total of $2,161,676 awarded for three Discovery Projects (A. Pan and S.H. Zhou; G.X. Wang and K. Konstantinov; and X.L. Wang), three ARC fellows (QEII: X.L. Wang, APD: S.H. Zhou and Int. Professorial Fellow: J.M. Yoo), two Linkage Projects (S.X. Dou, M.J. Qin, A. Pan and X.L. Wang; and S.X. Dou and A. Pan); three International Linkage Projects (H.K. Liu and V. Pan; C. Zhang and J. Cao; and M.J. Qin and S.Y. Ding); and one Linkage International Fellowship (X.L. Wang, S.X. Dou and J.M. Yoo). These represent 17.5% of the University's total ARC grants in the 2005 round. This brings our total number of ARC fellows to nine. In addition, a proposal for the conversion of solar energy to electrical energy from the Solid State Physics Group (C. Zhang and R. Lewis) has attracted joint funding from the NSW State Government (SERDF) and CSIRO. Recently, the government announced the winners of the next round of ARC Centre of Excellence; the Australian Centre for Electro-materials Science headed by Prof G. Wallace is one of them, with total ARC funding of $12 million for the next five years. The Energy Materials Program of ISEM is part of the CoE (H.K. Liu).

Our postgraduate students have made significant progress on their degree programs. D. Milliken, M. Lindsay, Ben Lough and S.H. Zhou were each awarded a PhD degree, and B. Winton, Y.P. Yao and Z.W. Zhao were each awarded a Master's degree. D. Milliken is now a research fellow at the University of Leeds, UK, M. Lindsay is now a research fellow at UNSW, while S.H. Zhou was awarded a JSPS fellowship at the National Institute of Materials Science, Japan. S. Needham and G. Peleckis won jointly the Excellent Postgraduate Student Award for 2004, Z.G. Huang, D. Ng, M. O'Dwwyer and O. Shcherbakova won the Merit Award in 2004. The winner for the Excellent Paper Award is B. Winton. X. Xu and M.S. Al Hossain were awarded an APAI scholarship, and B. Winton, M. Park and L. Yang won ISEM and match scholarships. We congratulate all our new postgraduate students on their success and welcome them to our institute.

Our laboratory infrastructure has been substantially improved during 2004. The nano-multilayer fabrication facilities have all been installed and commissioned. These include Electron Beam Evaporator (EBE) and Magnetron Sputtering units integrated with an ultra-high vacuum chamber, a surface analysis unit including XPS, Auger, UPS and ISS, a high performance JEOL SEM with LaB6 gun, EDX and BSC (backscattered detectors), and an Electron Beam Lithography (EBL) unit. These facilities were funded through the Systemic Infrastructure Initiative scheme by DIST with total funding of $1.7 million for three years and are supported by 13 institutions around Australia. These facilities will enhance the capability for nano-multilayer fabrication at ISEM. The Physics Group at ISEM has built a terahertz radiation facility, which can produce ultrashort pulses of light of less than 12 femtoseconds. This was purchased through an ARC LIEF grant involving UoW, ANU, UTS and UNSW. A multifunctional electrochemical station was installed with the support of a Pool II grant.

We are in the process of our middle term review as part of the Strength Area review. We will achieve or exceed all the goals set at the beginning of this three-year plan. However, the target to have 40 PGS enrolled remains as major challenge. This demands special attention from every member of our institute. Our strategy for next few years remains the same, that is, to consolidate our extended research programs; enhance postgraduate training; improve research staff profile and stability; increase the ARC funding success rate; foster industry links; and promote national and international collaboration.

S X Dou

Shi Xue DOU

Director

Research Grant Funds

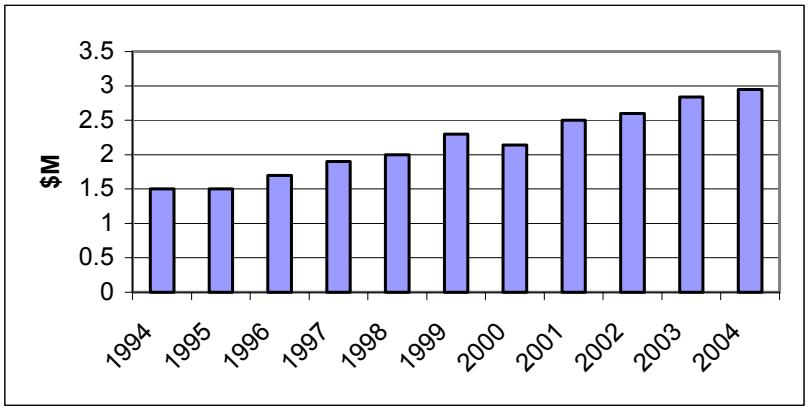

Postgraduate Student Numbers

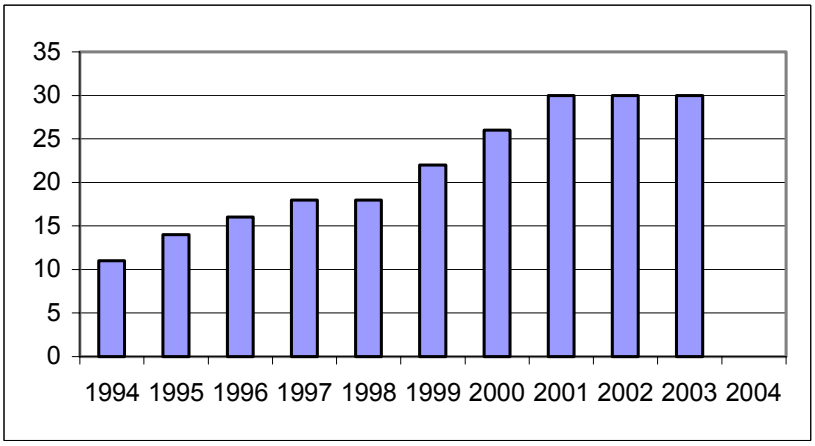

Refereed Publications (DETYA Categories)

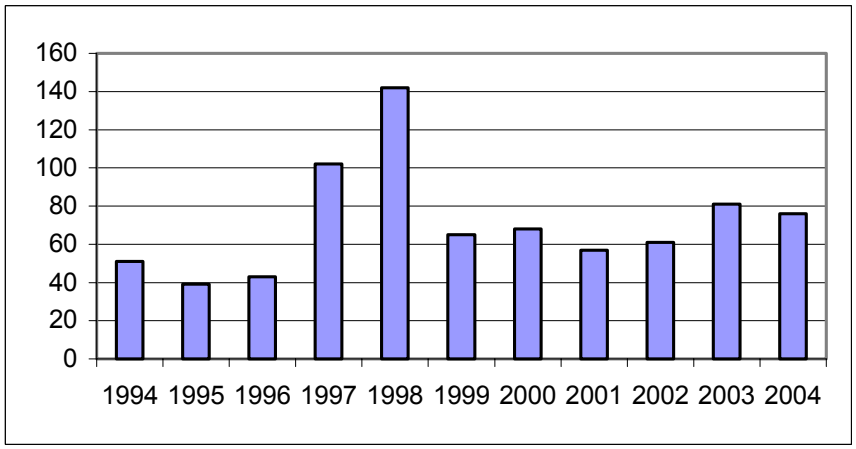

Management 2004

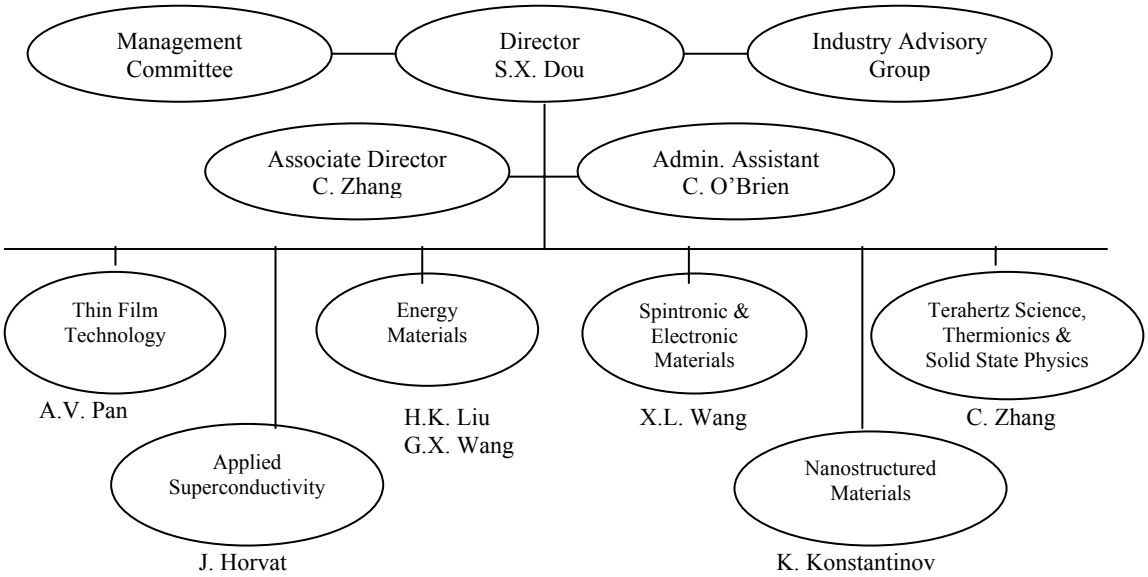

Management Committee

Chairperson:	Prof. M. Sheil	Pro Vice Chancellor, UoW
	Prof. S.X. Dou	Director, ISEM
	Prof. C. Cook	Dean, Faculty of Engineering, UoW
	Prof. C. Zhang	Associate Director, ISEM
	Prof. H.K. Liu	Research Co-Ordinator, ISEM

Industry Advisory Group

Dr T. Beales	Manager	Australian Superconductors Ltd, Metal Manufactures Ltd
Mr B. Buchtmann	Advanced Syst. Engineer	Email Limited
Mr. P.W. Dowling	Managing Director	Polarised Technologies Pty Ltd
Dr. X.F. Gao	General Manager	Lexel Batteries Co. Ltd, Shenzhen, PR China
Mr R. Neale	Managing Director	Alphatech International Ltd
Mr M. Tomsic	Managing Director	Hyper Tech Research Ltd, Ohio, USA,
Prof J.S. Wang	President	Taiyi Battery Co. Ltd., Zhuhai, PR China
Mr J.F. Wu	Marketing Manager	DLG Battery Co Ltd, Shenzhen, P.R. China
Dr. S. Zhong	Managing Director	Guangzhuo Delong Energy Technology, Guangzhuo P.R. China

Personnel

Director
Prof. S.X. Dou, Dipl, PhD, DSc, FTSE

Associate Director
Prof. C. Zhang, BSc, PhD, MA, MPhil, FAIP

Senior Program Co-Ordinators

Prof. T. Beales, BSc, PhD MM/UoW Consortium Manager

Prof. H.K.Liu, Dipl. for PGS, APF.

Prof. C. Zhang, BSc, PhD, MA, MPhil, FAIP

Dr. J. Horvat, BSc, PhD

Dr. X.L. Wang, BSc, MSc, PhD,
ARC Postdoctoral Fellow

Dr. M. Ionescu, BSc, MSc, PhD

Dr. K. Konstantinov, BSc, MSc, PhD

Dr. A.V. Pan, MSc, PhD,
ARC postdoctoral Fellow

ARC Fellows

Prof. J.H. Ahn, Assoc. Professorial Fellow

Prof. S.X. Dou, Dipl, PhD, DSc, FTSE,
Australian Professorial Fellow

Dr. Z.P. Guo, BSc, MSc, PhD,
Australian Postdoctoral Fellow

Prof. H.K. Liu, Dipl. For PGS, Dipl. AQC,
Australian Professorial Fellow

Dr. A.V. Pan, MSc, PhD,
ARC postdoctoral Fellow

Dr G.X. Wang, BSc, MSc, PhD,
ARC Postdoctoral Fellow

Dr. J. Wang, BSc, MSc, PhD,
ARC Postdoctoral Fellow

Dr. X.L. Wang, BSc, MSc, PhD,
ARC Postdoctoral Fellow

Prof. J.Y. Lee, ARC International Prof. Fellow

Dr. S. H. Zhou. BSc, MSc, PhD,
ARC Postdoctoral Fellor

Prof. J. M. Yoo, BSc, MSc, PhD,
ARC International Professorial Fellow

Research Staff

Dr. Z. Cheng, BSc, MSc, PhD

Dr. M.J. Qin, BSc, MSc, PhD

Dr. T. Silver, BSc, PhD

Dr. D. H. Wilke, BSc, PhD

Dr. J. H. Kim, BSc, Phd

Dr. R. Zeng, BSc, MSc, PhD

Dr D. Q. Shi, Bsc, Msc, PhD

Academic Staff

Prof. C. Cook, BSc, PhD, FIEAust

Prof. D. Dunne, BSc, PhD, FIEAust

Dr. C. Freeth, MSc, PhD, MAIP

Assoc Prof. R. A. Lewis, BSc (Hons), PhD, FAIP, FRMS

Dr. A.D. Martin, MSc, PhD, MAIP

Dr. R.E.M. Vickers, MSc, PhD, MAIP

Prof. P. Fisher, BSc, PhD

Visiting Staff

Prof. E.W. Collings, Ohio State University

Prof. H. Liu, Sichuan Uni, PR China

Dr. S. Kennedy, ANSTO

Dr. S. Zhong, Delong Energy Technology, China

Prof. J. Chan, Nankai University, PR China

Dr. G. Alvarez

Prof. S. Y. Ding, Nahjing University

Technical Staff

Mr. R. Kinnell

Administration Officer

Ms. Christine O'Brien

Postgraduate Students

Current

PhD	Thesis Title	Supervisors
S Bewlay	Investigation on Li-Co-Ni System for Lithium Ion Batteries	SX Dou, GX Wang
Y Chen	Investigation of Cathode Materials for Li-ion Batteries	HK Liu, GX Wang
M Farhoudi	Synthesis and characterization of transition material oxide	XL Wang, SX Dou, M. James
D Fisher	Dissipation Effect in Resonant Tunnelling through Double Barrier Structures	C Zhang
ZG Huang	Nano-materials for hydrogen storage	HK Liu, ZP Guo
S.Keshavarzi	Investigation of Vortex Dynamics of $(Tl,Pb)(Sr,Ba)_2Ca_2Cu_3O_y$ and Twinned $Sm_{1+x}Ba_{2-x}Cu_3O_{6+y}$ (x=0.04) Single Crystals	SX Dou, J Horvat MJ Qin
P Lavers	Electronic structure of perovskites	QM Qin, SX Dou
A Li	YBCO thick and thin films	M Ionescu, HK Liu
G Li	Numerical Analysis of Electromagnetic Behaviour of High T_c Superconductors in Magnetic Field	HK Liu, MJ Qin
S Needham	Anode and Cathode Materials for Lithium Ion Batteries	GX Wang, HK Liu
SH Ng	Nano-structured Materials for Electrode in Rechargeable Li-ion Battery	HK Liu, JZ Wang
M O'Dwyer	Thermionic Cooling and Power Generation	C Zhang, RA Lewis
G Peleckis	Spintronic Materials	XL Wang, SX Dou
SH Pilehrood	Electronic Properties of Semiconductor Nanostructures under Intense Terahertz Radiation	C Zhang
S Pysarenko	HTS Multi-Layers Thin Films Fabrication	AV Pan, SX Dou
M Roussel	Critical Current Density and Flux Pinning in HTS	AV Pan, SX Dou

PhD	Thesis Title	Supervisors
O Sherbakova	Two-Gap Superconductors	SX Dou, MJ Qin
M Smith	T Ray Spectroscopy	RA Lewis, C Zhang R Vickers
B Winton	An Investigation of the Surfaces of Biomaterials	SX Dou, M Ionescu R. Vickers
X Xu	Study of Multi-layer Coated Superconductors	SX Dou, MJ Qin
J Yao	Thin film microbattery	K. Konstantinov H.K. Liu
Q Yao	Studies of Novel Magnetic Ruddlesden-Popper Series Compounds	XL Wang, SX Dou
WK Yeoh	Control of Nanostructure for Enhancing Superconductor Performance through Chemical Doping	SX Dou, J Horvat
L Yuan	Nano-materials for use in Li-ion Batteries	HK Liu K Konstantinov GX Wang
Y Zhang	Effect of nano Ti doping in MgB_2	S.X. Dou, A. Pan
Y Zhao	Fabrication and Characterization of MgB_2 Films	SX Dou, M Ionescu
ZW Zhao	Novel Carbon Supported Pt and Pt alloy Catalysts for Proton Exchange Membrane Fuel Cells and Direct Methanol Fuel Cells	HK Liu, ZP Guo

Master's	Thesis Title	Supervisors
K de Silva	Diamond Growth	SX Dou, AV Pan
ZJ Lao	New Materials for Supercapacitors	K Konstantinov GX Wang
B Winton	A Study of the Magnetoresistance Effect in Bi-2212 for the Purposes of Utilisation in Magnetic Field Sensors	SX Dou, M Ionescu
Q Yao	MgB_2 Thick Films	XL Wang, SX Dou

Completions

PhD Name & Thesis Title	Awarded	Position	When Appointed
M Apperley The Fabrication of High T_c Superconductor Wire	1992	Chief Technologist Australian Superconductors Business development manager University of Sydney	1993 2004
R Baker Zeeman and Piezospectroscopy of Antimony and Aluminum in Germanium	2001	Professional Officer University of Wollongong	2003
A Bourdillion Microstructure, Phase Characterisation and Texture Processing of HTS	1992	Senior Engineer Hewlett Packard, Singapore Hewlett Packard, USA	1993 2000
Jobe Probakar Chelliah Optical spectroscopy of semiconductors	2000		
J Chen High Energy Storage Material for Rechargeable Nickel-Metal Hydride Batteries	1999	NEDO Fellow Osaka National Research Institute Professor Nankai University, China	1999 2002
N Cui Magnesium Based Hydrogen Storage Alloy Anode Materials for Ni-MH Secondary Batteries	1998	Research Fellow Alberta University, Canada Electrochemist Energizer Co, USA	1997 2000
F Darmann Characterisation of melt-texture Y-123 materials		Research Fellow ANSTO	2003
XK Fu Fabrication and Characterisation of Bi-2223 Current Lead	2002	Research Fellow Texas A&M University, USA University of Waterloo, Canada	2002 2005
F Gao Studies on the Synthesis, Characterization and Properties of Colossal Magnetoresistive (CMR) Materials	2004	Research Assistant ISEM, University of Wollongong	2004
YC Guo Investigation of Silver-clad $(Bi,Pb)_2Sr_2Ca_2Cu_3O_{10-x}$ Superconducting Tapes	1994	STA Fellow Nat. Res. Inst. Of Metals, Japan ARC Postdoctoral Fellow ISEM, University of Wollongong	1997 1998
ZP Guo Investigation on Cathode Materials for Lithium-ion Batteries	2003	ARC Postdoctoral Fellow ISEM, University of Wollongong IT, University of Wollongong	2003 2003
RJ Heron Far-infrared Studies of Semiconductors in Large Magnetic Fields	1998	Postdoctoral Fellow SUNY, Buffalo, USA	1997
QY Hu Fabrication and Enhancement of Critical Currents of Silver Sheathed $Bi,Pb_2Sr_2Ca_3Cu_3O_{10}$ Tapes	1996	Research Fellow Florida State University USA Research Scientist Argonne National Lab., USA Senior Engineer, Lucent, USA	1997 1999 2001

PhD Name & Thesis Title	Awarded	Position	When Appointed
M Ionescu Growth and Characterisation of Bi-2212 Crystals and Improvement of Bi-2212/Ag Superconducting Tapes	1998	Assistant Director ISEM, University of Wollongong Senior research scientist ANSTO	1994 2004
JX Jin $(Bi,Pb)_2Sr_2Ca_2Cu_3O_{10+x}$/Ag High T_c superconductors and their Applications in an Electrical Fault Current Limiter and an Electronic High Voltage Generator	1998	Research Fellow ISEM, University of Wollongong ARC, PDF ISEM, University of Wollongong	1997 2000
M Lerch Optical & Electrical Studies of Resonant Tunnelling Heterostructure	1998	Research Fellow Medical Physics, University of Wollongong	1999
M Lindsay Data Analysis and Anode Materials for Lithium Ion Batteries	2004	Postdoctoral Research Fellow University of New South Wales	2004
B Lough Investigations into Thermionic Cooling for Domestic Refrigeration	2004		
BL Luan Investigations on Ti_2Ni Hydrogen Storage Alloy Electrode for Rechargeable Nickel-Metal Hydride Batteries	1997	NRC Fellow National Res. Council of Canada Group Leader Shape Transfer Process Integrated Manufacturing Technologies Institute, NRC, Canada	1997 1999
J McKinnon The Fundamental Mechanisms Involved in the Production of Thin Films by Pulsed Laser	2003	Teacher New South Wales Education Department	2003
D Marinaro A Study into the Effects of Fission-Fragment Damage on Activation Energies in Ag/Bi2223 Tapes	2003	Scientist DSTO Melbourne	2003
D Milliken Uranium Doping of Silver Sheathed Bismuth-Strontium-Calcium-Copper-Oxide Superconducting Tapes for Increased Critical Current Density through Enhanced Flux Pinning	2004	Knowledge Transfer Partnership Associate University of Leeds and AVX Ltd	2005
D Shi Buffer Layers for YBCO Superconducting Films on Single Crystal YSZ Substrates and Cubic Texture Ni Substrates	2003	Research Fellow Korean Electrical Technology Institute, Korea Research Fellow ISEM, University of Wollongong	2002 2004
T Silver Near Bandedge Optical Properties Of MBE GaAs And Related Layered Structures	1999	Research Fellow ISEM, University of Wollongong	2000
S Soltanian Development of Superconducting Magnesium Diboride Conductors	2004	Pro-Vice Chancellor Kurdistan University, Iran	2005
K Song Processing And Characterisation Of Superconducting Ag/BiPbSrCaO Composite	1992	Senior Engineer South Korean Co	1993

PhD Name & Thesis Title	Awarded	Position	When Appointed
S Stewart Thermodynamic And Dielectric Properties In Modulated Two-Dimensional Electronic Systems	1998	ARC Postdoc. Fellow Teacher	1998 1999
L Sun Amorphous And Nanocrystalline Hydrogen Storage Alloy Materials For Nickel-Metal Hydride Batteries	2000	Research Associate Hydro-Quebec Research Institute, Canada Research Fellow University Sherbrooke, Canada	2000 2002
G Takacs Spectroscopy Of The Effect Of Strains And Magnetic Field On Shallow Acceptor Levels In Germanium	1999	Lab Manager 2nd Year Physics Lab	1999
K. Uprety Magnetic Hysteresis and Relaxation in Bi2212 Single Crystals Doped with Iron and Lead	2002	Research Fellow Argonne National Lab., USA	2002
N Vo Design And Characterisation Of HTS Coils	1997	Research Fellow Los Alamos Nat. Lab, USA Research Staff Intermagnetics General Co., USA	1999 1998
C Wang Cathodic Materials for Nickel-Metal Hydride Batteries	2004	Research Fellow Polymer Institute, University of Wollongong	2004
GX Wang Investigation on electrode materials for lithium-ion batteries	2001	ARC Postdoc. Fellow ISEM, University of Wollongong	2001
J Wang Development of a Novel Plate Making Processing Technique for Manufacturing Valve-Regulated Lead-Acid Batteries	2003	Research Fellow IPRI, University of Wollongong ARC Postdoctoral Fellow ISEM, University of Wollongong	2003 2004
WG Wang Fabrication And Improvement Of Silver Sheathed $(Bi,Pb)_2Sr_2Ca_2Cu_3O_{10}$ Tapes By Powder-In-Tube Technique	1998	R&D Manager Nordic Superconductor Tech. Denmark	1997
XL Wang Spiral Growth, Flux Pinning And Peak Effect In Doped And Pure Bi-2212 HTS Single Crystal	2000	Research Fellow ISEM, University of Wollongong ARC Postdoctoral Fellow ISEM, University of Wollongong ARC QEII Fellow ISEM, University of Wollongong	1999 2002 2005
A Warner A Spectroscopic Study of Acceptors in Germanium	1997	Consultant Computer Industry	1999
JA Xia Characterisation of Melt-Texture of YBCO HTS	1994	Research Fellow Solar Cell Ltd	1995
JM Xu Phase Formation and Transformation in the R-Fe-T System (R=Nd, Gd, Tb, Dy, Er, Ho, T and Lu, T=Si, Ti & Zr	1997	Research Fellow St. George Bank, Australia	1998
J Yau Ag/Bi-2223 Tape Processing and Mechanical Properties	1994	Assistant Professor City Polytechnical University	2000

PhD

Name & Thesis Title	Awarded	Position	When Appointed
M Yavus Powder Processing of Bi-Pb-Sr-Ca-Cu-O Superconducting Materials	1997	Ass. Professor Texas A&M University, Texas USA Ass. Research Professor Tohoku University, Sendai, Japan Ass. Professor University of Waterloo, Canada	2000 1997 2004
B Zeimetz High Temperature Superconducting Tapes & Current Leads	1998	Research Fellow Cambridge Univ., U.K.	1999
R Zeng Processing and characterisation of Bi-2223/Ag superconducting tapes	2000	Research Fellow ISEM, University of Wollongong	2000
S Zhong Investigation on Lead-Calcium-Tin-Aluminium Grid Alloys for Valve-Regulated Lead-Acid batteries	1998	ARC Postdoc. Fellow ISEM, University of Wollongong CEO, Leadcel Dynamic Energy Ltd, P.R. China CEO, Guangzhou Delong Energy Tech Ltd	1997 2002 2003
SH Zhou Processing and Characterisation of MgB_2 Superconductors	2004	STA Fellow Nat. Res. Inst. Of Metals, Japan ARC Postdoc. Fellow ISEM, University of Wollongong	2004 2005

Masters

Name & Thesis Title	Awarded	Position	When Appointed
F Chen The Influence of Selenium on Lead-Calcium-Tin-Aluminium	1998	PhD candidate University of Sydney, Australia	1999
M Farhoudi AC Loss in Ag/Bi-2223 Tape in AC Field	2002	PhD candidate ISEM, University of Wollongong	2003
K Ishida Landau Spectra of ZnH and Neutral Zn in Germanium	2004		
JX Jin $(Bi,Pb)_2Sr_2Ca_2Cu_3O_{10+x}$/Ag High T_c Superconductors and their Applications in an Electrical Fault Current Limiter and an Electronic High Voltage Generator	1994	Research Fellow ISEM, University of Wollongong ARC, PDF ISEM, University of Wollongong	1997 2000
P Lavers The Mobility of Large Anions in Crystals with the Fluorite Structure	2004	PhD Candidate ISEM, University of Wollongong	2004
S Lee Multilayer Thermionic Cooling in GaAs-$Al_xGa_{1-x}As$ Heterostructures	2003		
A Li Fabrocation and Characterisation of Novel Substrates and Superconducting Thick Films	2002	PhD Candidate ISEM, University of Wollongong	2002
M Ling	2001		

Masters Name & Thesis Title	Awarded	Position	When Appointed
Mechanism of Outgrowth in Multifilament Bi-2223 tape			
E. Sotirova Investigation of Colossal Magnetoresistance Materials	2001	Learning Centre Employee Communications Assistant Star CD Pty Ltd	2002
K Uprety Vortex Properties of Bi-HTS	1999	PhD Candidate ISEM, University of Wollongong Research Fellow Argonne National Lab., USA	2000 2003
JZ Wang Investigations on Anode Materials For Rechargeable Lithium-Ion Batteries	1999	PhD Candidate ISEM, University of Wollongong Research Fellow IPRI, University of Wollongong	2000 2003
G Yang Effect of Element Substitution on Superconductivity	1997	Research Fellow University of Melbourne	2000
J Yao Carbon Based Anode Materials for Lithium-Ion Batteries	2004	PhD Candidate ISEM, University of Wollongong	2004
N Zahir A New Method for Production and Study of Electrical Properties of Carbon Foam	1996	PhD Candidate Queensland University	1997
Z. Zhang The Comparative Research on the Ag-alloy Sheathed Bi-2223 Tapes	2003	Senior Staff China-URC Ltd, Shanghai. PR China	2003
ZW Zhao Nano-oxides Fabricated in-situ by Spray Pyrolysis Technique as Anode Materials for Lithium Secondary Batteries	2004	PhD Candidate ISEM, University of Wollongong	2004

National and International Links

The Institute has established a national and international multi-disciplinary collaborative network. This has led to information exchange, co-supervision of PhD students, joint grant proposals and joint publications with more than 40 research teams around the world. Current collaborative organizations are listed below:

Australia

Australian Nuclear Science & Technology Organisation	Dr. S. Kennedy, Dr. M. James, Dr M. Reinhard
University of Sydney	Dr. S. Ringer, Dr. R. Keast
Curtin University of Technology	A/Prof. J Low
Macquarie University	A/Prof. E. Goldys
University of Technology, Sydney	Prof. G. Smith
Monash University	Dr. Y.B. Cheng, Krishnamurthy
University of Melbourne	Prof. D. Jamieson
University of New South Wales	Dr. R. Ramer, Prof.M.S.Kazakos, Prof. P. Munroe, Prof. S. Li
University of Western Sydney	Prof. M.M. Wilson
University of Queensland	Prof. G.Q.M. Lu

International

Atomic Institute of Austrian Universities, Vienna, Austria	Prof. H.W. Weber
Brookhaven National Lab	Dr. X.Q. Yang, Dr. Y.M. Zhu
Dalhousie University, Canada	Prof. J. Dahn
Houston University, USA	Prof. R. Weinstein
Institute for Metal Physics, Kiev, Ukraine	Prof. V. Pan
Los Alamos National Lab	Drs A. Serquis and X.Z. Liao
Ludwig Boltzmann Institut für Festkörperphysik, University of Vienna, Austria.	Dr. W. Lang
Max-Planck Institute for Metals Research, Germany	Dr. E.H. Brandt
Max-Planck Institute for Solid State Physics, Germany	Prof. U. Habermeier
Nankai University, PRC	Prof. J. Chen, Prof. Y.H. Tang
Nanjing University	Prof. S.Y. Ding, Prof. W.M. Chen
National Andong University	Prof. J.H. Ahn
Northeatern University, Shenyang, PRC	Prof. X.D. Sun
Ohio State University, Columbus, OH, USA	Dr. E.W. Collings, Dr. M. Sumption
Osaka National Reseach Institute, Japan	Dr. T. Sakai
University of Auckland	Prof. W. Gao
University of Cincinnati	Prof. D. Shi
University of Wisconsin	Prof. D. Larbalestier, Dr. A. Polyanskii
University of Zagreb, Zagreb, Croatia	Prof. E. Babic, I. Kusevic
Yamagata University, Japan	Dr. S. Kambe, Prof. Ohshima
Kyushu Institute of Technology	Prof. T. Masushita
Institute of Physics, Chinese Academy	Prof H.H. Wen
University of Geneva	Prof. R. Flukiger
Korean Advanced Institute of Science & Technology	Prof. J.Y. Lee
Imperial College	Dr. Cohen,
Philips Research Laboratories and Technical University Eindhoven, The Netherlands	Prof. Dr PHL Notton

Progress Reports for Projects funded by the Australian Research Council

1. Progress Report on ARC Centre of Excellence Research

Progress Report on the program of energy conversion and storage within the ARC Centre for Nanostructured Electromaterials **(Project ID:** CE0348245)

Years funded: 2003 2004 2005 2006 2007
Chief Investigator: H.K. Liu
Research Fellow: Guoxiu Wang
PhD student: See How Ng

Nanocrystalline Si-MCMB composite anode:

Since MCMB (mesocarbon microbeads) anode materials have the best cyclability among all the various types of carbon anode materials the combination of MCMB and Si may result in Si-MCMB composite anode materials with high capacity and satisfactory rechargeability. Based on this hypothesis, we prepared nanocrystalline Si-MCMB composite materials by high-energy ball milling. Nanocrystalline Si with an average particle size of 80 nm was obtained from Nanostructured & Amorphous Materials Inc., USA, which were prepared by laser driven silane gas reaction. MCMB was supplied by Osaka Gas Co. Japan. MCMB powders have an average particle size of 10 mm. The mixtures were ball milled for 5, 10, and 20 h, respectively, three batches of Si-MCMB composites. The electrochemical properties of Si-MCMB composites were measured via cells testing.

Scanning electron microscopic observation showed that the spherical shape of MCMB particles was retained via moderate ball milling. Their electrochemical properties as anodes in lithium-ion cells were systematically evaluated.

We have found that the ball-milling conditions have an impact on the capacity and cyclability of nanocrystalline Si-MCMB composites. The optimized Si-MCMB composite anode demonstrated a reversible capacity of 1066 mAh/g with good cyclability.

WS_2 nanotubes in lithium-ion cells:

The one-dimensional (1D) nanotube materials have a variety of potential applications ranging from quantum computers to nano-scale biomedical sensors. Thin-films of fullerene-like MoS_2 nanoparticles were found to have ultra-low friction and wear. It has been reported that MoS_2 nanotubes have a moderate hydrogen storage capacity and $MoS_{2-x}I_y$ nanotubes have demonstrated a reversible lithium intercalation capacity of 385 mAh/g. Lithium-ion batteries are the most advanced power sources for modern portable electronic devices. The development of next generation lithium-ion batteries with high energy relies on the new electrode materials. For the first time, we have studied the lithium intercalation properties of WS_2 nanotubes in lithium-ion cells.

TEM images of WS_2 nanotubes demonstrate that nanotubes stick together to form bundles. The outer diameter of the WS_2 nanotubes is about 25 nm. High-resolution TEM images of WS_2 nanotubes shows the tip of a straight WS_2 nanotube with an outer diameter of ~ 20 nm. This nanotube has a nonspherical open tip and a clear-cut outside wall. The tip of another WS_2 nanotube has an onion-like cluster structure. A more magnified HRTEM image of a WS_2 nanotube shows the interlayer spacing is about 0.6 nm, corresponding to the (002) plane.

The WS_2 nanotubes demonstrated significantly different electrochemical properties, compared to the crystalline WS_2 powders. The WS_2 nanotube electrodes show stable cyclability over a wide voltage range. Nanotube materials could provide a class of versatile electrode materials for lithium-ion batteries with improved electrochemical characteristics.

$LiM_xFe_{1-x}PO_4$ (M = Mg, Zr, Ti) phosphates:

A series of $LiM_xFe_{1-x}PO_4$ (M = Mg, Zr, Ti) phosphates were synthesized via a sol-gel method. TEM observations show that $LiM_xFe_{1-x}PO_4$ particles consist of nanosize crystals, ranging from 40 nm to 150 nm. HRTEM analysis reveals that a layer of amorphous carbon was coated on the surface of the $LiM_xFe_{1-x}PO_4$ particles, which substantially increases the electronic conductivity of $LiM_xFe_{1-x}PO_4$ electrodes. The doped $LiM_xFe_{1-x}PO_4$ powders are phase pure. Near full capacity (170 mAh/g) was achieved at the C/8 rate at room temperature for $LiM_xFe_{1-x}PO_4$ electrodes. The doped $LiM_xFe_{1-x}PO_4$ electrodes demonstrated better electrochemical performance than that of undoped $LiFePO_4$ at a high rate.

In order to distinguish the doping effect on the electrochemical performance of lithium iron phosphates, we performed high rate cycling. The doped sample demonstrated better performance than the undoped one at high charge/discharge rate. This effect becomes easily distinguishable at the high charge/discharge rate of 10C. When the electrodes are charged and discharged at high rates, the polarisation of the electrodes due to electronic conductivity becomes an influential factor determining the kinetics of the electrochemical reaction of the electrodes. Lithium insertion and extraction in $LiFePO_4$ electrodes is accompanied by electron transfer not only on the particle surface but also inside the crystals. Since the doping effect induces the increased semiconductivity of $LiFePO_4$, which enhances the electronic conductivity of the electrode materials on the crystal level, electron transfer in doped $LiFePO_4$ would be more facilitated than in undoped $LiFePO_4$. This is because the individual undoped $LiFePO_4$ crystals are still insulating. Therefore, the doped samples demonstrated better overall electrochemical performance at high rate.

Publications from the program of energy conversion and storage within the ARC Centre for Nanostructured Electromaterials in 2004:

G. X. Wang, Jane Yao, and H. K. Liu, "Characterization of Nanocrystalline Si-MCMB Composite Anode Materials", ***Electrochemical and Solid-State Letters***, **7(**8), A250-A253 (2004) impact factor: 2.742

G.X. Wang, Steve Bewlay, Jane Yao, H.K. Liu and S.X. Dou, "Tungsten disulfide nanotubes for lithium storage", ***Electrochemical and Solid-State Letters***, 7(10) A321-A323 (2004) impact factor: 2.742

G.X. Wang, Steve Bewlay, Jane Yao, J.H. Ahn, S.X. Dou, H.K. Liu, "Characterization of $LiM_xFe_{1-x}PO_4$ (M = Mg, Zr, Ti) cathode materials prepared by the sol-gel method", ***Electrochemical and Solid-State Letters***, 7(12) A503-A506 (2004) impact factor: 2.742

2. Progress Reports on ARC Large/Discovery Projects

First principles for development of high temperature superconducting wires

Funded:	2002	2003	2004	2005	2006
Project ID:	DP0211240				
Chief Investigators:	S.X. Dou, J. Horvat				
Assoc. Investigators:	H. Weber, E. Collings, J. Habermeier				
Postgrad Students:	S. Keshavarzi, M. Roussel				

Optimization of the final heat treatment for the improvement of the superconducting properties of Bi-2223 multifilamentary tapes: A set of Bi-2223/Ag tapes was produced using the powder in tube technique and two heat treatments. The second heat treatment consisted of first heating at 825˚C and then at temperatures ranging from 725 to 800˚C. It appears that a final temperature of 750˚C results in best critical current density. However, the best microstructure was obtained by slow cooling after the first step sintering.

Critical currents and vortex pinning in U/n treated Bi2223/Ag tapes: Critical currents J_c (T,B) for virgin and ^{235}U doped Bi2223/Ag tapes irradiated with thermal neutrons (U/n treated) were measured. Below 97 K vortex pinning in U/n treated tapes increased with matching field B_φ. Since the rate of increase of field of peak in pinning force density vs. field depends on T, one can tune the maximum enhancement at desired T.

Improvement of J_c and H_{c2} of MgB_2 by doping: Resistive transition measurements for MgB_2 wires doped with 10% SiC were carried out. The highest values of H_{irr} and H_{c2} were obtained for wires with 15nm SiC heated at 725^{o}C for 30 minutes (29 T and >33 T, respectively). Doping of MgB_2 with carbon nano-tubes (CNT) resulted in improvement of field dependence of J_c and H_{c2}, which was weaker than for the nano-SiC doping. CNTs in samples sintered at T>900°C disappear to a large degree, resulting in the best field dependence of J_c. This would indicate that improvement of vortex pinning and J_c occurs because the carbon released from CNT at high temperature dopes into MgB_2 . This improvement is stronger than with nano-C doping.

Vortex dynamics in pure and SiC-dopedMgB_2: Hysteresis loop and magnetization relaxation measurements have been performed on a pure and a SiC-doped MgB_2 samples. The normalized volume pinning forces determined from the hysteresis loop are observed to scale as a function of the reduced magnetic field ($h = H/H_{irr}$) which peaks at $h_{max} \approx 0.2$. This result implies that the dominating pinning mechanism in both materials is the pinning by normal surface defects. Logarithmic dependence of the vortex activation energy on the current was obtained.

Improvement of J_c by ferromagnetic sheath: The improvement of J_c by ferromagnetic sheath (Horvat et al. Appl. Phys. Lett. 80 (2002) 829) was suggested to be a consequence of interaction between the external magnetic field and the self-field produced by the current that flows through the sample (Kovac et al., Supercond. Sci. Technol. **16** (2003)1195). This model was verified in a series of experiments testing its basic principles. These experiments showed that the proposed model is not in agreement with the observed improvement of J_c by the ferromagnetic sheath.

Sample size dependence of the magnetic J_c: Magnetically obtained J_c in MgB_2 exhibited sample size dependence of J_c. A systematic study showed that the porous structure of MgB_2 results in the observed artefact of sample size effect of magnetic J_c (Horvat et al., J. Appl. Phys. 96(2004)4342). This finding challenges many claims of high J_c in the literature, when J_c is derived from magnetic measurements.

Growth, Periodical Modulation Structure and Heat Treatment of $(Tl,Pb)(Sr,Ba)_2Ca_2Cu_3O_y$ Single Crystals: $(Tl,Pb)(Sr,Ba)_2Ca_2Cu_3O_y$ single crystals were grown by a self-flux method. The c-lattice parameter was determined to be 1.55 nm by X-ray precession technique. SEM photos show a layer-by-layer growth mechanism. A periodic modulation structure with 200 nm in width and about 0.7~0.8 nm in height was observed by using atomic force microscope. It was proven that the modulation structure and the Tl to Pb ratio are responsible for large J_c of Tl-1223 single crystal**.**

Cryogenic magnetic field sensor based on the magnetoresistive effect in bulk Bi2212 + USr_2CaO_6: The resistivity measurements of melt-textured Bi2212 + 6 wt% USr_2CaO_6 show high sensitivity of the resistivity to applied magnetic fields, in particular below 3T and in temperature range between 45 K and 85 K. A cryogenic sensor was built and tested at 77 K in low fields. It shows a good sensitivity and a small (≅1%) hysteresis of resistivity when the applied field was cycled between 0 T and 1 T.

Enhancement and elucidation of flux pinning in doped Bi-Sr-Ca-Ci-O high temperature superconducting single crystals

Funded:	2002	2003	2004
Project ID:	DP0211328		
Chief Investigators:	X.L. Wang		
APD:	X.L. Wang		

1) Magnetoresisitivity and J_c as a function of temperature ($4.2 < T < 100$ K) and magnetic field (B< 5 T) are studied for the first time for $Bi_2Sr_2Ca_2Cu_3O_{10}$ single crystals successfully grown using the travelling solvent floating zone method. It has been found that below a characteristic field B*, J_c as a function of applied field exhibits a field-independent plateau associated with a single vortex pinning regime. A strong temperature dependence of the B* is suggested to be due to thermally activated pinning of individual vortices. Analysis of resistive transition broadening revealed that thermally activated flux flow is found to be responsible for the resistivity contribution in the vicinity of T_c. The activation energy U_0 is 800 K in low field and scales as $B^{-1/6}$ for B<2 T and drops to 200 K with $B^{-1/2}$ for B>2T.

2). Studies of crystal growth, structures, superconductivity and flux pinning were carried out on $(Bi_{1.64}Pb_{0.36})Sr_2Ca_{1-x}RE_xCu_{2-y}Zn_yO_8$ (RE=Y, Gd; x=0, 0.05, 0.11, 0.33; y=0, 0.02) single crystals grown by the self-flux method. X-ray diffraction, transport and magnetic measurements were performed for purposes of characterisation. Structures were analysised using the Rietveld refinement method. It has been revealed that Pb substituted for Bi and Gd or Y for Ca. The c lattice parameter and T_c systemically decreased as the RE doping level increased. Flux pinning was also studied by measuring the hysteresis loops at different temperatures and different fields. A peak effect was observed in all doped samples. Results show that at low temperatures, the peak field is smaller than in solely Pb doped crystals and decreases as x increases (x>0.1). It has been also found that below a characteristic field B, J_c as a function of applied field exhibits a field-independent plateau associated with a single vortex pinning regime. A strong temperature dependence of B is suggested to be due to thermally activated pinning of individual vortices. The vortex dynamics of the doped crystals was also studied by measuring magnetization relaxation. A paper is under preparation.

3). Influence of surface barrier on the third harmonics AC susceptibility (X3) was studied numerically. The surface barrier is described by a critical current density in surfaces which is higher than the inside one. The numerical results based on the model are closer to the well known experimental data probing the harmonics as a function of temperature (or field). Besides, the surface barrier will lead to new peaks in the real and imaginary parts of the third harmonics, which are the signature of the surface barrier.

4). Flux pinning studies have also been carried out for rare-earth based HTS materials. Measurements of the magnetic critical current density showed that it was possible to fabricate single grains with a high J_c at high temperatures and fields by means of proper control of starting powders.

5). With the emergence of newly discovered magnesium diboride, I have continued to carry out nano-Si doping effect on flux pinning of MgB2 in cooperation with the international collaborator under the support of the APD fellowship. The magnetoresistivity and critical current density of well characterized Si-nanoparticle doped and undoped Cu-sheathed MgB_2 tapes have been studied. We found that $B_{irr}(T)$ variation is typical for high-temperature superconductors with columnar defects (a kink occurs near the matching field Bf and is very different from a smooth Birr(T) variation in undoped MgB2 samples).

Papers published and accepted.

1) X.L. Wang, et al., Journal of Applied Physics, in press;
2) X. B. Xu, et al., Journal of Applied Physics, in press;
3) L. Zhang, et al., Journal of applied physics. In press;
4) I. Kusevic, et al., "Correlated vortex pinning in Si-nanoparticle doped MgB2", Solid State Communications 132 (2004) 761–765;

About Citation:

1) X.L. Wang, et al, Physica C 385 (2003)461-465 (cited more than 9 times.

2). X.L. Wang, et al., published in Journal of Applied Physics 95, 6699 (2004), was selected for the June 1, 2004 issue of Virtual Journal of Applications of superconductivity.

Analysis, simulation, fabrication and characterization of reliable, robust and scalable compact cooling elements based on semiconductor nanostructures

Funded:	2003	2004	2005
Project ID:	DP0343516		
Chief Investigators:	C. Zhang, R.A. Lewis		
Postgrad students:	B.C. Lough, Z. Dou, S.P. Lee		

Project summary: Modern electronic, microelectronic and optoelectronic devices generally work better when they are cooler. We aim to develop a semiconductor nanostructure cooling element that directly integrates into existing devices. The solid-state cooling element will be reliable, robust, scalable and operate in any orientation. The basis of operation is thermionic emission - electrons are the working fluid. Our project combines (1) analysis and simulation, (2) fabrication of nanostructures and (3) experimental test-benching using optical and electrical methods. The outcome of this research has the potential to revolutionize cooling of modern electronic and photonic systems, from computer motherboards to mobile phones.

Non-linear dynamics in electronic systems and devices under intense terahertz radiation

Funded:	2004	2005	2006
Project ID:	DP0452713		
Chief Investigators:	C. Zhang, R.A. Lewis, X.C. Zhang, R.E. Vickers		

Project summary: Non-linear interactions allow for a detailed and intricate probing of materials. Sufficiently high-power light directed at a subject can yield spectroscopic data about multiple material parameters, providing a unique diagnostic tool for many applications. We propose to study the non-linear dynamic properties of electronic systems and devices under various external conditions. A thorough understanding of non-linear properties will accelerate development of new optoelectronic devices in the terahertz frequency regime. Examples of these devices are oscillators and sensors.

Fabrication, Charge and Spin Ordering, Magnetoresistance, and polaron effects in nano-size and single crystals of novel transition metal perovskite oxide

Funded:	2003	2004	2005
Project ID:	DP0345012		
Chief Investigator:	X.L. Wang, M. Ionescu, Z.X. Cheng		
Partner Investigator:	Dr.M James, Prof. R.S. Liu, Prof. W. Lang		
Postgraduate students:	M. Farhoudi		

1). Doping effects on the structure and physical properties has been studied systematically for $Gd_{1-x}Sr_xCoO_3$ compounds. Crystal structures have been refined by the Rietveld refinement program. The spin states of Co^{3+} and Co^{4+} have also been determined.

2). A novel Roddlesden-Popper homologous series $Sr_{n+1}Co_nO_{3n+1}$ (n=1,2,3,4 and ∞) compounds were successfully synthesized by a high pressure and high temperature technique. Structure refinement revealed that these compounds crystallize in tetragonal structures, while the compound n = ∞ is cubic. These compounds are ferromagnetic with the Curie temperature decreasing from 255 K for n=1 to about 200 K for n=2-4 and down to 175 K for $SrCoO_3$. Co^{4+} ions present as intermediate spin states for n=1 to 4, but in the low spin state in $SrCoO_3$. Negative magnetoresistance was observed for Sr_2CoO_4 and found to be larger than that for $SrCoO_3$.

3). Far-infrared phonon modes in the cobaltite/manganites A(Co0.5Mn0.5)O3, where A is a lanthanide, have been studied in magnetic fields up to 17.5 T. The phonon energies in the compounds with A = La, Nd or Ho show little change with applied magnetic field. In contrast, with A=Yb, all the phonon modes exhibit a splitting when a magnetic field is applied.

4). Structures and magnetic properties of $Ho_2Co_{1-x}MnxO_6$ (x=0-1) have been well studied in detail. It was found that the ferromagnetic transition Tc decreases as x decreases. The Infra-red spectrum have been systematically studied.

5). We have demonstrated that $SrCoO_{3-x}$ can be stabilized into phase pure peroskite forms by introduction of small amounts ~ 5% of certain rare earth ions (Sm3+-Yb3+). La3+ and Pr3+ crystallize with the same isostructural trigonal structure as Sr6Co5O1; while the Nd3+ composition shows a mixture of both structure types. Magnetisation measurements show that these materials undergo transitions to a spin-glass state at temperatures below 150 K, and that significant coupling occurs between the rare earth ions and the mixed $Co^{3+/4+}$ ions. Magnetisation measurements as a function of applied field versus field reveals that below the transition temperature ferromagnetic ordering takes place at relative large fields.

6) The perovskite-based rare earth cobaltates $Ln_{0.33}Sr^{0.67}CoO_3$ (Ln=Y3+, Ho3+ and Dy 3+) have been synthesized. Synchrotron X-ray diffraction study has revealed the presence of a complex, previously unreported, perovskite-related superstructure phase. Coupled Ln/Sr and O/vacancy ordering and associated structural relaxation is shown to be responsible for the observed superstructure.

7).Single phase perovskite-based rare earth cobaltates ($Ln_{1-x}Sr_xCoO_{3-\delta}$) ($Ln$=$La^{3+}$, Pr^{3+}, Nd^{3+}, Sm^{3+}, Gd^{3+}, Dy^{3+}, Y^{3+}, Ho^{3+}, Er^{3+}, Tm^{3+} and Yb^{3+}; $0.67 \leqslant x \leqslant 0.9$) have been synthesized and their structures have been extensively characterised using X-ray diffraction, electron diffraction, and oxygen contents determinations. This work was done in cooperation with ANU, Australia.

8). In cooperation with the group at the University of technology, Sydney, a three-dimensional (3D) magnetic property testing system has been completed and successfully used to measure 3D hysteresis loops of soft magnetic material.

The following papers have been published or accepted:

1). X.L. Wang, et al, Journal of Applied Physics, in press; 2).W. Lin, H.W. Lu, J.G. Zhu, and J.J. Zhong, X.L. Wang, Journal of Applied Physics, in press; 3). Lewis RA, et al, Journal of Magnetism & Magnetic Materials, vol.272-276, pt.1, May 2004, pp.616-17; 4).M. James, et al, Solid State Sciences, 6(7), 655-662 (2004); 5). D. J. Goossens, et al., " Phys. Rev. B, 69, 134411 (2004); 6) M. James, et al., J. Solid State Chem., 177, 1886-1895 (2004); 7) Z.X.Cheng, et al., Journal of magnetism and magnetic materials, 283(2-3) (2004) 143-149; 8) Z. X. Cheng, et al., Journal of Crystal Growth, Dec 2004.

Control of nano-structure for enhancing the performance of magnesium diboride superconductor by chemical doping

Funded:	2004	2005	2006
Project ID:	DP0449629		
Chief Investigators:	S.X. Dou, M.J. Qin		
Partner Investigators:	D.C. Larbalestier, R.L. Flükiger, L.F. Cohen		
Postgrad. Students	W.K. Yeoh, O. Sherbakova, Y. Zhang		

Enhancement of H_{c2} and J_c using nano-doping: We carried out a systematic study on the effect of sintering temperature on the phase formation, critical current density, upper critical field and irreversibility field of nano SiC doped MgB_2. A systematic correlation between the sintering temperature, normal state resistivity, RRR, J_c, H_{c2}, and H_{irr} has been found in all samples of each batch. Samples sintered at lower temperature have a very fine and well-consolidated grain structure while samples sintered at high temperature contain large grains with easily distinguishable grain boundaries. Low temperature sintering resulted in a higher concentration of impurity precipitates, larger resistivity, higher J_c up to 15 T and lower T_c values. These samples show higher H_{c2} and H_{irr} at T near T_c but lower H_{c2} in the low temperature regime. Nano-precipitates were the dominant mechanism responsible for higher H_{c2} at T near T_c while impurity scattering due to C substitution for B is responsible for higher H_{c2} in the low temperature regime for samples sintered at higher temperature.

Effect of ferromagnetic element doping on T_c and J_c: we have used iron doping to control pinning properties of MgB_2 superconductors. Neither free Fe particles nor FeB compound was detected at 1% Fe doping by either TEM or XRD, suggesting that Fe substituted for Mg in the lattice. The level of Fe substitution for Mg is estimated to occur at a level lower than 1% of Mg, and this substitution is proposed to be responsible for the decrease in transition temperature with Fe doping. Because of the high reactivity of nano-scale Fe particles, Fe doping is largely in the form of FeB at a Fe doping level of 2% while Fe_2B was

detected at 10% Fe doping. The detrimental effect of nano-scale Fe doping on $J_c(H)$ is attributable to both the Fe substitution for B in the lattice structure and the inclusions of Fe and FeB which act as weak links at grain boundaries.

Effect of ultrasonic irradiation: ultrasonic irradiation has been applied to our iron doped samples. MgB_2, MgB_2+10wt% Fe, MgB_2+100wt% Fe samples are used in this study. SEM pictures indicate that as the amount of Fe is increased, the grains become finer. However, magnetic hsystesis loop measurements at 5 K shows no enhancement of Jc for MgB_2+10wt% Fe sample, compared to pure MgB_2 sample. Also no Tc change has been observed for these samples. More experiments will be conducted in the coming year to clarify this topic.

Effect of Ball-milling: we have applied the ball-milling technique to MgB_2+10wt% Fe powders to refine the structure. XRD measurements indicate a larger FWHM of the 100 peak as the milling time is increased (2, 5, 10, 15, 20, and 30 min). SEM measurements show a finer grain size as the milling time is increased and better mixture of iron in the MgB_2 powder. Further magnetic and transport measurements will be performed to study this effect.

Nano-carbon doping to improve J_c and H_{c2}: Carbon doping has been used to enhance significantly the upper critical field, however, its effect on pinning properties has not been fully understood yet. In this project, we studied both carbon substitutional and additional MgB_2 samples. The behaviour of the critical current density is much more complicated, at low temperatures (5 K), withthe substitutional sample $MgB_{1.9}C_{0.1}$ first, then MgB_2+10at%C and then MgB_2+7at%C, pure MgB_2 sample shows poor field performance, but highest critical current density at fields lower than 5 T. As the temperature is increased, J_cs of MgB_2+10at%C and MgB_2+10at%C samples drop quickly; $MgB_{1.9}C_{0.1}$ still shows the highest J_c at 20 K, but at 30 K, pure sample shows the highest J_c.

High-pressure synthesized MgB_2 with high critical currents: High-pressure synthesized (HPS) MgB_2–based material shows at 20 K up to 3 T $j_c \geq 100$ kA/cm^2 and up to 5 T $j_c \geq 10$ kA/cm^2. The Mg-B (most likely MgB_2) inclusions in the Mg-B-O superconductive "matrix" greatly affect the SC characteristics: the samples with higher j_c and H_{irr} exhibit the higher content of the inclusions. At lower synthesis temperatures the amount of Mg-B inclusions is higher. Additions of Ta, Ti, Zr and nano-SiC can increase j_c of HPS MgB_2. The main effect of Ta, Ti and Zr seems to be due to the absorption of impurity hydrogen at low synthesis temperatures to form TaH, Ta_2H, TiH_2, ZrH_2, which prevents harmful MgH_2 impurity phase from appearing and may prevent hydrogen from being introduced into the material structure.

Hydrogen storage materials for energy conversion applications

Funded:	2004	2005	2006
Project ID:	DP0449660		
Chief Investigators:	H.K. Liu, Z.P. Guo (APD)		
Partner Investigators:	J. Lee, A. Zuettel, P.H. Notten		
Postgrad. Student:	Z.G. Huang		

The effect of nickel content on the electrochemical properties of $Mg_{1.9}Cu_{0.1}Ni_\chi$ (χ = 1.8, 1.9, 2.0, 2.1) hydrogen storage alloys has been investigated. A high discharge capacity of 490 mAhg^{-1} was observed for χ = 1.8. As to capacity degradation, 66.7 % of initial capacity was lost after 15 cycles for χ = 1.8, while only 47.2 % for χ = 2.1. Clearly high nickel content can reduce the extent of discharge capacity degradation. CV, EIS and the linear polarization curves indicate that the improvement of the electrochemical performance can be explained by the following facts: the high electrocatalytic activity of Ni in alloys; the suppression of the formation of $Mg(OH)_2$ on the surface of electrodes; and the high rate of absorption and desorption of hydrogen, as evidenced from exchange current density, increases almost ten times to 133 mAg^{-1} when χ = 2.1.

Enhancement of electrochemical performance of nonstoichiometric amorphous Mg_2Ni_x electrodes by different carbon coating has also been done. Nonstoichiometric amorphous Mg_2Ni_x alloys were synthesized by mechanically milling crystalline Mg_2Ni alloy with Ni powders (since excess Ni is beneficial to the amorphization of the alloy). In comparison with the stoichiometric material, the nonstoichiometric Mg_2Ni_x

phase showed a higher discharge capacity because of the amorphization of the alloy. Surface modification with different carbon materials was also carried out for further improvement of its electrode performance. CV indicates that CNTs and graphite can help maintain redox reaction current and subsequently improve the cycle performance. In addition, CNTs and graphite can reduce the charge-transfer reaction resistance on the alloy surface. The linear polarization curves show that the exchange current density, namely the rate of hydriding/dehydriding, has been greatly increased through CNT and graphite coating. The hydrogen diffusion rate has also been estimated by the potential-step method. It is found that the CNT and graphite coating significantly increases the diffusion coefficient. All of these are attributed to the high electrocatalytic activation of CNT and graphite and the suppression of $Mg(OH)_2$ formation. In contrast, carbon black coating has no such positive effect because carbon black may partially screen the alloy surface and consequently decreases the number of active sites for H adsorption.

The electrochemical behavior and the reversible hydrogen storage capacity of SWNT-papers have been firstly investigated by CV, linear micropolarization, constant current charge/discharge, etc. The effect of thickness and the addition of carbon black on hydrogen adsorption/desorption were also investigated. The thin SWNT-paper electrode exhibits a discharge capacity of 104 $mAhg^{-1}$ with good reversibility. The electrical conductivity decreases with increasing thickness of SWNT paper, and the addition of carbon black could improve the contact between the carbon tubes, thus improving the electrical conductivity. The charge/discharge mechanism of SWNT paper could be affected by the thickness of the SWNT paper and the addition of carbon black. For the thick SWNT paper and SWNT paper containing carbon black electrodes, the electrochemical reactions were controlled by the charge transfer process on the surface and by a proton diffusion process at the thin SWNT-paper electrode. The electrochemical charge-discharge mechanism occurring in SWNT paper electrodes is somewhere between that of carbon nanotubes and metal hydride electrodes, and consists of the charge-transfer reaction and diffusion step.

Three papers have been submitted to peer-reviewed Journals:

- Z. G. Huang, Z. P. Guo, H. K. Liu, S. X. Dou, " Effect of Ni Content On the Structural and Electrochemical Properties of the $Mg_{1.9}Cu_{0.1}Ni_{\chi}$ hydride alloys" submitted to Journal of Solid-State Chemistry.
- Z.P. Guo, S.H. Ng, J.Z. Wang, Z.G. Huang, H.K. Liu et al. "Electrochemical Hydrogen Storage in Single-Walled Carbon Nanotube Paper", submitted to Carbon.
- Z.P. Guo, Z. G. Huang, Z.W. Zhao, X. Menard, H.K. Liu, "Enhanced Electrochemical Properties of Nonstoichiometric Amorphous $Mg_2Ni_{1.3}$ Electrodes", submitted to Journal of Applied of Electrochemistry.

Development of high-temperature superconducting coated conductors by pulsed-laser deposition technique for future long-length applications

Funded:	2004	2005	2006
Project ID:	DP0451267		
Chief Investigators:	A.V. Pan (APD), M. Ionescu		

The aim of the project is to develop a novel technology for manufacturing flexible coated conductors with the help of a pulsed laser deposition technique and the characterisation and understanding of the electromagnetic properties of the coating on flexible and single crystal substrates.

A number of $YBa_2Cu_3O_7$ thin superconducting films have been grown on different single crystal substrates under different conditions using pulsed-laser deposition and magnetron sputtering techniques. Employing magnetization measurements, critical current density (J_c) dependences on the applied magnetic field (B_a) have been obtained for the films. The analysis of the $J_c(B_a)$ behaviour suggests that the range of the B_a-independent J_c plateau depends on the interplay between the vortex pinning of certain, particularly effective defects and thermally activated depinning of individual vortices. The latter process is found to be the main factor responsible for the temperature dependence of the size of the J_c-plateau. This temperature behaviour is independent of the properties of the films and their orientation with respect to the field. The absolute J_{c0}

value at $B_a \rightarrow 0$ T is, in contrast to the plateau, more sensitive to pinning media transparency to the supercurrent flow.

Further measurements of magnetic field, angular and temperature dependencies of the critical current density by SQUID magnetometry, ac magnetic susceptibility, and transport techniques in single-crystalline epitaxial YBCO films enabled us to describe the mechanism of vortex depinning from growth-induced linear defects quantitatively. The model developed takes into account a distribution of domain size as well as the dislocation spacing within domain boundaries in the films. The structural parameters of YBCO films extracted from $J_c(B_a; T)$-curves as a result of this quantitative description is consistent with those obtained from X-ray diffraction studies.

Temperature dependences of the magnetic moment have been measured in $YBa_2Cu_3O_7$ thin films over a wide magnetic-field range ($5<Ha<10^4$ Oe). In these films a paramagnetic signal known as the paramagnetic Meissner effect has been observed. The experimental data on the films, which have strong pinning and high critical current densities ($Jc \sim 3\times10^6$ A/cm^2 at 77 K), are shown to be highly consistent with the theoretical model proposed by Koshelev and Larkin (Phys. Rev. B **52**, 13 559, 1995). This finding indicates that the origin of the paramagnetic effect is ultimately associated with nucleation and inhomogeneous spatial redistribution of magnetic vortices in a sample that is cooled down in a magnetic field. It is also shown that the distribution of vortices is extremely sensitive to the interplay of film properties and the real experimental conditions of the measurements.

- **A. V. Pan**, Y. Zhao, M. Ionescu, S. X. Dou, V. A. Komashko, V. S. Flis, and V. M. Pan, Thermally activated depinning of individual vortices in $YBa_2Cu_3O_7$ superconducting films prepared under different conditions, Physica C **407**, 10-16 (2004).
- D. A. Luzhbin, **A. V. Pan**, V. A. Komashko, V. S. Flis, V. M. Pan, S. X. Dou, and P. Esquinazi, Origin of paramagnetic magnetization in field-cooled $YBa_2Cu_3O_{7-\delta}$ films, Phys. Rev. B **69**, 024506 (2004).
- Yu. V. Fedotov, E. A. Pashitskii, S. M. Ryabchenko, A. V. Semenov, **A. V. Pan**, S. X. Dou, C. G. Tretiachenko, V. A. Komashko, Yu. V. Cherpak, V. M. Pan, Field behavior of the critical current in quasi-single-crystalline YBCO films, Physica C **401**, 316-319 (2004).
- **A. V. Pan**, S. X. Dou and V. M. Pan, Low field vortex behaviour in various superconductors, International Cryogenic Materials Conference (ICMC04), February 10-14, 2004, Wollongong, Australia.
- V. M. Pan, V. A. Komashko, V. L. Svetchnikov, C. G. Tretiatchenko, Yu. V. Cherpak, **A. V. Pan**, S. X. Dou, E. A. Pashitskii, S. M. Ryabchenko, A. V. Semenov, Yu. V. Fedotov, Nano-structure and high critical current density of HTS $YBa_2Cu_3O_{7-\delta}$ films, International Cryogenic Materials Conference (ICMC04), February 10-14, 2004, Wollongong, Australia. **(INVITED)**

3. Progress Report on SPIRT/Linkage Programs

.

Fabrication and Characterisation of Magnesium Diboride Superconducting Wires

Funded:	2002	2003	2004
Project ID:	P0219629		
Chief Investigator:	S.X. Dou, X.L. Wang, M. Ionescu		
Partner Investigator:	S. Sumption		
Industry partners:	Hyper Tech Research Inc. OH USA, Alphatech International Ltd. Sydney		

1).High-quality bulk MgB_2 exhibits a structure of voids and agglomeration of crystals on different length scales. Because of this, the superconducting currents percolate between the voids in the ensuing structure. Magnetic measurements reveal that the superconducting currents circulate on at least three different length scales, of ~1 mu m, ~10 mu m, and whole of the sample (~millimeter). Each of these screenings contributes to the measured irreversible magnetic moment. The analysis of the field dependence of Delta m for samples of subsequently decreasing size showed that the critical current obtained using the simple critical state model is erroneous. This leads to the artifact of the sample size-dependent critical current density J_c and irreversibility field. Our data analysis enables the separation of the contribution of each of the screening currents to Delta m. The currents flowing around the whole of the sample give a dominant contribution to moment m in the intermediate fields 4 T at 20 K) and they can be used to obtain the value of J_c from the critical state model, which corresponds to the transport J_c. The stretched exponential field dependence of these currents is similar to the one obtained for high-temperature superconductors, and it seems to be connected with the percolation of the currents.

2) Sample size dependent magnetic critical current density has been observed in magnesium diboride superconductors. At high fields, larger samples provide higher critical current densities, while at low fields, larger samples give rise to lower critical current densities. The explanation for this surprising result is proposed in this study based on the electric field generated in the superconductors. The dependence of the current density on the sample size has been derived as a power law j varies as R/sup 1/n/ [n is the n factor characterizing E-j curve E=E/sub c/(j/j/sub c/)/sup n/]. This dependence provides one with a method to derive the n factor and can also be used to determine the dependence of the activation energy on the current density.

3) The critical current density was measured at 4.2 K for MgB_2 strands with and without SiC additions. It was found that in situ processed strands with 10% SiC additions heat treated at 700-800 degrees C showed improved irreversibility field and bulk pinning strengths as compared to control samples; an increase in H_{irr} of 1.5 T was noted. Heat treatment to 900 degrees C gave even larger improvements, with Hirr reaching 18 T and F_p values maximizing at 20 GN m3.

4) Bulk and Fe sheathed wires doped with different nano-SiC particle sizes have been made and heat treated at temperatures ranging from 580^{o}C to 1000^{o}C. A systematic correlation between the sintering temperature, normal state resistivity, RRR, J_c, H_{c2}, and H_{irr} has been found in all samples of each batch. Samples sintered at lower temperature have a very fine and well-consolidated grain structure while samples sintered at high temperature contain large grains with easily distinguishable grain boundaries. Low temperature sintering resulted in a higher concentration of impurity precipitates, larger resistivity, higher J_c up to 15 T and lower T_c values. These samples show higher H_{c2} and H_{irr} at T near T_c but lower H_{c2} near T = 0 than samples sintered at high temperature. It is proposed that huge local strains produced by nano-precipitates and grain boundary structure were the dominant mechanism responsible for higher H_{c2} at T near T_c. However, higher impurity scattering due to C substitution is responsible for higher H_{c2} in the low temperature regime for samples sintered at higher temperature. In addition to high H_{c2}, it is also proposed that the large number of nano impurities serve as pinning centres and improve the flux pinning, resulting in higher J_c values at high magnetic fields up to 15 T.

Papers published and accepted:

1) Journal of Applied Physics, 96(2004)4342-51; 2).Phys. Rev.B, 69 (2004)12507-1-4; **3)** Superconductor Science & Technology, vol.17, no.10, Oct. 2004, pp.1180-4; 4) Superconductor Science and Technology, accepted.

Developing new cathode materials for Li-ion batteries using Australian mineral resources

Funded:	2002	2003	2004
Project ID:	LP0214179		
Chief Investigators:	S.X. Dou, G.X. Wang		
Partner Investigators:	J.Y. Lee, S.J. Kennedy		
Industry Partners:	Sons of Gwalia, OM Group		

Layered $Li[Li_{0.3}Cr_{0.1}Mn_{0.6}]O_2$ cathode material with a hexagonal structure was synthesized by a solid-state reaction. The structural changes of this material were studied using a synchrotron based *in situ* x-ray diffraction technique during charge/discharge cycles. The results of *in situ* x-ray diffraction indicated that the layer structure and the hexagonal symmetry of this material was preserved through the phase transition between H1 and H2 during the charge/discharge cycling. Cyclic voltammograms show a single pair of oxidation and reduction peaks, consistent with a reversible phase transition between H1 and H2 observed from the *in situ* x-ray diffraction data. Based on the *in situ* XRD spectra collected during the charge/discharge process and the cyclic voltammograms, a reversible phase transformation between hexagonal phases H1 and H2 has been identified for $Li[Li_{0.3}Cr_{0.1}Mn_{0.6}]O_2$ cathode material. Since this phase transition takes place within the hexagonal symmetry and the changes in lattice parameters are much smaller than in other layered systems, the integrity of the crystal structure is preserved during cycling. The $Li[Li_{0.3}Cr_{0.1}Mn_{0.6}]O_2$ electrode delivered a discharge capacity of 145 mAh/g.

Single-phase spherical $LiCo_{0.25}Ni_{0.75}O_2$ compounds were prepared from lithium compounds and spherical $Co_{0.25}Ni_{0.75}$ $(OH)_2$ precursor by sintering at high temperature. The spherical $Ni_{1-x}Co_x(OH)_2$ precursor was synthesized by coprecipitation of Ni- and Co- sulfates in the mixed solution with NaOH and NH_4OH. The PH value of the solution was precisely controlled by NaOH and NH_4OH. LiOH and $Ni_{0.75}Co_{0.25}$ $(OH)_2$ powders were then mixed uniformly with a molar ratio of 1:1.04 $Ni_{0.75}Co_{0.25}$: Li and sintered in a steam of oxygen flow at different temperature of 650ºC, 700ºC, 750ºC, 800ºC, and 850ºC for 12 hrs. $LiCo_{0.25}Ni_{0.75}O_2$ sintered at 750°C has good morphology and uniform particle size. $LiCo_{0.25}Ni_{0.75}O_2$ electrodes were cycled in the voltage window of 3.0V to 4.3V at a current density of $0.4mA/cm^2$ at room temperature. The initial reversible discharge capacity is 167.4mAh/g. It demonstrated that the spherical $LiCo_{0.25}Ni_{0.75}O_2$ has high specific capacity and high reversibility of during charge and discharge. Furthermore, the spherical $LiCo_{0.25}Ni_{0.75}O_2$ can be a promising further commercial material due to its higher tap-density than normal $LiCo_xNi_{1-x}O_2$ powder.

In order to reduce the cost of $LiCoO_2$ cathode materials, lithium nickel based oxides were developed as alternative cathode materials for lithium-ion batteries. The $LiCoO_2$ electrode demonstrated excellent cyclability compared to the $LiNiO_2$ electrode. The $LiCoO_2$ electrode delivered an initial discharge capacity of 141 mAh/g. On the other hand, the $LiNiO_2$ electrode reached 181 mAh/g capacity in the first discharge. The first discharge capacities for $LiNi_xCo_{1-x}O_2$ solid solutions were between those of $LiCoO_2$ and $LiNiO_2$. The rechargeability for the $LiNi_{0.5}Co_{0.5}O_2$ and $LiNi_{0.25}Co_{0.75}O_2$ electrodes is still good with capacity fading rate of 0.3 mAh/g and 0.18 mAh/g per cycle, respectively. A mechanism for the capacity fade of $LiNi_xCo_{1-x}O_2$ electrodes on cycling could include the following factors: (i) a structural change due to lithium insertion/extraction causes contraction and expansion of the unit cell, which may lead to the formation of fractures in the particles of the active materials; (ii) In the charged state, MO_2 reacts with the organic electrolyte, inducing dissolution of M ions into the solution. $LiNiO_2$ has been found to experience several topotactic phase trsformations during lithium insertion and extraction. However, $LiCoO_2$ does not behave in this way. Therefore, in the $LiNi_xCi_{1-x}O_2$ solid solutions, Co can stabilize the layered structure for lithium ioninsertion and extraction. On the other hand, the binding energy of the Co-O bond is higher than that of the Ni-O bond. The strong Co-O skeleton could contribute to the stability of the electrode in the charged state.

- G.X. Wang, Z.P. Guo, X.Q. Yang, J. McBreen, H.K. Liu and S.X. Dou, "Electrochemical and in situ Synchrotron x-ray diffraction studies of $Li[Li_{0.3}Cr_{0.1}Mn_{0.6}]O_2$ cathode materials" Solid State Ionics **167/1-2** (2004) 183 – 189.
- Yao Chen**,** G.X. Wang**,** J.P. Tian and H.K. Liu, "Preparation and properties of Spherical $LiCo_{0.25}Ni_{0.75}O_2$ as a Cathode for Lithium Ion Batteries" Electrochimica Acta 50 (2004) 433 - 439.

- G.X. Wang, Steve Bewlay, Matthew Lindsay, K. Konstantinov, Z.P. Guo, Jane Yao, H.K. Liu & SX Dou, "Energy storage materials for lithium-ion batteries" Materials Forum **27** (2004) 33 – 44

Investigation of nano-materials for use in lithium rechargeable batteries

Funded:	2002	2003	2004
Project ID:	LP0219309		
Chief Investigators:	Prof. H.K. Liu, S. Zhong		
Partner Investigator:	Prof. J. Ahn		
APA(I) Award:	L. Yuan		
Industry Partners:	Sons of Gwalia Ltd, OM Group, Lexel Battery Ltd		
Postgrad. Students:	Z.W. Zhao, M. Lindsay		

A series of Sn-coated graphite composite materials for lithium-ion batteries were prepared by microencapsulating nanosize Sn particles in graphite. As the nanosize Sn particles can homogeneously disperse in the graphite matrix via electroless chemical reduction, the lithium storage capacities of tin-graphite composite show a great improvement. Since Sn is an active element to lithium, Sn can react with lithium to form $Li_{4.4}Sn$ alloys, a reaction accompanied by a dramatic volume increase, whereas the ductile graphite matrix provides a perfect buffer layer to absorb this volume expansion. Therefore, the integrity of the composite electrode was preserved during lithium insertion and extraction. Cyclic voltammetry was employed to identify the reaction process involved in lithium insertion and extraction in the graphite structure, as well as lithium alloying with tin. We believe that the tin-graphite composites provide a new type of anode material for lithium-ion batteries with an increased capacity.

Co_3O_4, Ni-Co_3O_4 mixture and Ni- Co_3O_4 were obtained from the solid state reaction. The synthetic temperature and time, were varied for optimized electrochemical properties of Co_3O_4. As the irreversible capacity of Co_3O_4 may be due to the solid electrolyte interface (SEI) film formation on surface and incomplete decomposition of Li_2O during the discharge process, SEI film formation cannot be restrained without the development of a special electrolyte, and there has been little research on the proper electrolyte composition, whereas in our research, Ni will be used for the catalytic activity to facilitate Li_2O decomposition. Thus, in order to improve the low initial coulombic efficiency of Co_3O_4 (69%), Ni was added to Co_3O_4 using two methods like physical mixing and mechanical milling. It is found that adding the same amount of Ni, the mechanical milling showed better improvement in initial coulombic efficiency than physical mixing. The charge–discharge mechanism of Co_3O_4 was considered with the morphologies of Ni–Co_3O_4 mixture obtained by physical mixing and Ni–Co_3O_4 composite prepared by mechanical milling.

A series of SnO_2-carbon nano-composites were synthesized by in situ spray pyrolysis of a solution of $SnCl_2{\cdot}2H_2O$ and sucrose at 700 ^oC. The process results in super fine nanocrystalline SnO_2, which is homogeneously distributed inside the amorphous carbon matrix. The SnO_2 was revealed as a structure of broken hollow spheres with porosity on both the inside and outside particle surfaces. This structure promises a highly developed specific surface area. X-ray diffraction (XRD) patterns and transmission electron microscope (TEM) images revealed the SnO_2 crystal size is about 5–15 nm. These composites show a reversible lithium storage capacity of about 590 mAh/g in the first cycle. The discharge curve of the composite indicates that lithium is stored in crystalline tin, but not in amorphous carbon. However, the conductive carbon matrix with high surface area provides a buffer layer to cushion the large volume change in the tin regions, which contributes to the reduced capacity fade compared to nonacrystalline SnO_2 without carbon.

Publications from this project in 2004 are listed below:

- G.X. Wang, Jane Yao, Jung-Ho Ahn, H.K. Liu and S.X. Dou, "Electrochemical properties of nanosize Sn-coated graphite anodes in lithium-ion cells", Journal of Applied Electrochemistry 34: 187–190, 2004.

- Y.M. Kang, K.T. Kim, J.H. Kim, H.S. Kim, P.S. Lee, J.Y. Lee, H.K. Liu and S.X. Dou "Electrochemical properties of Co_3O_4, Ni-Co_3O_4 mixture and Ni-Co_3O_4 composite as anode materials for Li ion secondary batteries", *Journal of Power Sources* **133** 252-259 (2004)

- L. Yuan, K. Konstantinov, G.X. Wang, H.K. Liu, S.X. Dou, "Nano-structured SnO2-carbon composites obtained by in situ spray pyrolysis method as anodes in lithium batteries", J. Power Sources, in press

Fabrication of Magnesium Diboride (MgB_2) thick films

Years funded:	2002	2003	2004
Amount funded:	$22,545	$22,545	$22,545
Total funding:	**$67,635**		
Project ID:	LP0228370		
Chief Investigator:	Dr X L Wang		
APA(I) Award(s):	Q.W. Yao		
Industry Partner(s):	SFC Enterprises Pty Ltd		

1. **Structures and superconducting properties of C and Al co-doped MgB_2 for the first time.** Polycrystalline $Mg_{1-x}Al_xB_{2-x}C_x$ samples with x=y=0, 0.05, 0.1, 0.2, 0.3, 0.4 were prepared using an in-situ reaction method and sintered at temperatures from 700 up to 950 ^oC. The phases, lattice parameters, microstructures, superconductivity and flux pinning were characterized by XRD, TEM, and magnetic measurements. Rietveld refinement results indicated that the Al and C occupied Mg and B positions, respectively. It was found that both the lattice parameters and the T_c decreased monotonically with increasing doping level. The effect of the Al and C co-doping on the flux pinning and the upper critical fields are also systematically measured studied.

2. **Bulks, thick films and metal clad MgB2 superconductors were prepared by a one step in-situ reaction of magnesium and boron at ambient pressure.** Samples with different grain sizes ranging from 300 um down to 20 nm were synthesized by using different Mg precursor powders with different particle sizes and by controlling the sintering conditions. The effect of grain size on the critical current density has been investigated. Results show that the Jc and its field dependence are improved significantly when the grains sizes of the MgB_2 are significantly reduced. Our best samples show a high Jc of 1.1 x 10^6 in zero field at 30 K, 4 x 10^6 A/cm^2 in zero field and 10^6 A/cm^2 in 2.2 T at 15 K, and above 10^5 A/cm^2 in 5.2 T at 5 K. A large number of grain boundaries and nano-precipitates are suggested to be effective pinning centers.

3. **MgB_2 polycrystalline bulk samples with addition of 5 and 10 wt.% nano-sized Al_2O_3 powders were prepared by solid state reaction using pre-reacted MgB_2.** All the samples were sintered at 850 degrees C for 40 min in Ar. All the samples were characterized by X-ray diffraction, scanning electron microscopy and magnetic measurements. Results show that the critical current density and irreversibility fields decrease significantly with increasing Al_2O_3 level. J_c values were decreased significantly by more than one order of magnitude. The T_c drops slightly from 37.9 to 36.6 K, but acquires a very wide transition width of more than 20 K. Furthermore, the amount of MgO was found to increase with increasing Al_2O_3 level, probably indicating that Mg was replaced by Al, with the excess Mg forming extra MgO. The field dependence of J_c for all the samples was also studied.

The following papers have been published:

- Q.W. Yao, X.L. Wang, S. Soltanian, A.H. Li, J. Horvat, and S.X. Dou, "Fabrication, microstructure and critical current density of pure and Cu doped MgB_2 thick films on stainless substrate by short-time in-situ reaction", Ceramic International, 30 (2004) 1603-1606,
- *X.L. Wang*, Q. W, Yao, J. Horvat, M.J. Qin, and S.X. Dou, "Significant improvement of critical current density in MgB_2/Cu short tapes through nano-SiC doping and short-time in-situ reaction", Supercopnductor Science and Technol. 17 (2004) L21.
- Q.W. Yao, X.L. Wang, A.H. Li, P.R. Munroe, and S.X. Dou, "Effect of nano-Y-ZrO_2 addition on the microstructure and critical current density of MgB_2 superconductors", International Journal of Nanoscience. 4&5 (2004) 563-569.

- .X.L. Wang, et al., "Significant enhancement of critical current density in MgB2 through nano-SiC, Si and C doping", *[invited],* Physica C, 408-410 (2004) 63-67.
- Q.W. Yao, X.L. Wang, A.H. Li, S.X. Dou, X. Peng, M. Bhatia, M.D. Sumption, E.W. Collings, "Structures and superconducting properties of C and Al co-doped MgB_2", 17th International Symposium on Superconductivity , Japan, Nov, 2004.
- M. Delfany, X.L. Wang, S. Soltanian, J. Horvat, H.K. Liu, S.X. Sou, Ceramics International 30 (2004) 1581-3.

Lithium/sulfur rechargeable battery for power applications

Funded:	2004	2005	2006
Project ID:	LP0453698		
Chief Investigators:	H.K. Liu, J.Z. Wang (APD), G. Wang		
Industry Partner:	Guangzho Delong Energy Technology Pty Ltd		

Nanosize ZnS powders were prepared at room temperature by dropping simultaneously 20 ml of 1M zinc sulfate solution and 1 M sodium sulphide solution into distilled water containing 0.1 M ethylene diamine tetra acetic acid. The suspension was centrifuged at 4000r. min^{-1} for 15mins, and the precipitate was washed using de-ionised water with the assistance of an ultrasonic disintegrator. This procedure was repeated for three times to remove any adsorbed ions. The precipitate was finally dried at 100^{o}C in a vacuum oven for 10 h. The resulting powder was annealed at 450 ^{o}C to improve the crystallinity. The x-ray diffraction peaks for as-prepared ZnS powders are very broad, indicating nanocrystalline nature. After annealing treatment, the intensities of diffraction peaks increase substantially, reflecting the increased crystallinity. The average crystal size of zinc sulphide powders was determined by using the Traces Program according to the Scherrer formula. The crystal size is 3.41 nm for as-prepared ZnS powders, and 11.12 nm for annealed powder. TEM images of ZnS powders show that the pristine crystals have an average crystal size of a few nanometers. The small crystals stick together, forming agglomerates.

The charge and discharge curves for ZnS electrodes show that the first cycle of both electrodes exhibits high irreversible capacity, which may be attributed to the irreversible reaction of the formation of the SEI layer. The irreversible capacity of the annealed sample was slightly smaller than the as-prepared ZnS sample. During the subsequent cycle, the potential of the discharge plateaus is between 0.8 V and 0.0 V versus Li/Li^{+}, which is suitable for anode materials for lithium-ion batteries. The potential of charge plateaus exist in the range of 0 -1.5V. The charge and discharge curves of ZnS electrodes exhibit several discharge and charge plateaus, which involve a series of different reactions as demonstrated in CV measurements. The discharge capacity for the cells made from annealed and non-annealed samples was measured. It can be seen that the initial reversible discharge capacities of the two samples are all quite high, about 730 mAh/g and 660 mAh/g for non-annealed and annealed samples respectively. The capacity declined rapidly to about 400 mAh/g in fifteen cycles and maintained stable for more than forty cycles. The results indicate that ZnS nanopowders are promising anode materials for lithium-ion batteries.

Nanosize cobalt sulfides were synthesized through the chemical reaction method, which was the same method by which ZnS was synthesised. The as-prepared CoS nanopowders were characterized by X-ray diffraction, Scanning electron microscopy and electrochemical testing. The x-ray diffraction pattern showed that CoS powder prepared via the chemical reaction method was amorphous phase. SEM images of the synthesised CoS showed that the particle sizes are homogenous and the grain sizes are around 50 nm. CoS electrodes exhibited a reversible lithium storage capacity of about 400 mAh/g with stable cyclability. The results show that the CoS nanopowders are promising cathode materials for lithium secondary batteries.

Publication from this project in 2004:

- Jiazhao Wang, Guoxiu Wang, LI Yang, See How Ng and Hua Kun Liu, "An investigation on electrochemical behaviour of nanosize sulphide electrode in lithium-ion cells", Journal of Solid State Electrochemistry, submitted

Large-scale rechargeable lithium battery for power storage and electric vehicle applications

Funded:	2004 2005 2006
Project ID:	LP0453766
Chief Investigators:	G. Wang, H.K. Liu, K. Konstantinov, J. Ahn, B. Ammundsen
APA(I) Award:	J. Yao
Industry Partners:	Pacific Lithium NZ Ltd, Sopo Battery Energy Co.
Postgrad. Students:	S. Needham

This project started on March, 2004. We have achieved significant progress on the development of new anode materials and cathode materials for lithium energy storage.

Nanostructured Si-C composite materials were prepared by dispersing nanocrystalline Si in carbon aerogel and subsequent carbonization. A typical carbon gel was formed by mixing 0.29 M resorcinol and 0.57 M formaldehyde. The pH value was adjusted to be in the range of 6.5 – 7.4 by adding $NH_3.H_2O$ solution. The mixture solution was put in an ampoule, sealed and heated on a hot plate. The temperature was maintained at 85 °C. The solution changed progressively from clear to milk white to yellow to orange as the reaction progressed. When the solution became viscous, nanocrystalline Si powders were added, and dispersed through magnetic stirring. The ampoule was kept at 85 °C for 10 hours and then carbon aerogel was formed with Si dispersed inside the gel. The obtained gel was then sintered at 650 ° under flowing argon to yield Si-C composites, containing 40% by weight in carbon. Through this process, nanosize Si was homogeneously distributed in a carbon matrix. The Si-C composites exhibit a reversible lithium storage capacity of 1450 mAh/g when used as anodes in lithium-ion cells. The nanostructured Si-C composite electrodes demonstrated good cyclability. The Si-C composites could provide a novel anode material for lithium-ion batteries.

Stoichiometric and non-stoichiometric Mg-doped lithium iron phosphates were synthesised via spray-pyrolysis, followed by sintering at high temperature for crystallization. The ingredient chemicals Li_2CO_3 (99.95%), $FeC_2O_4.4H_2O$ (99%), $NH_4.H_2PO_4$ (97%), and $Mg(C_2H_3O_2)_2.4H_2O$ (99%) were dissolved in dilute nitric acid to form a homogeneous solution, in which Li^+, Mg^{2+}, Fe^{2+} and $[PO_4]^{3-}$ ions were mixed at molecular level. The mixed solution was peristalsic pumped into a homemade spray-pyrolysis furnace operating at 400 °C. Argon gas was used as the carrier gas for spraying solution to prevent the oxidation of Fe^{2+}. The loose precursor powders were collected by a cyclone. After spray pyrolysis, the precursor powders were then sintered at 750 °C for 10 hours. The spray pyrolysis process allows the homogeneous mixing of the ingredient reactants at atomic level. The electronic conductivities of the Mg-doped lithium iron phosphates have been drastically improved by four orders of magnitude, comparing to the undoped $LiFePO_4$. The electrochemical properties of as-prepared lithium iron phosphates were systematically measured by cyclic voltammetry and constant current charge/discharge cycling tests.

- G.X. Wang, J.H. Ahn, Jane Yao, Steve Bewlay, H.K. Liu, "Nanostructured Si-C composite anodes for lithium-ion batteries" Electrochemistry Communication 6(7) (2004) 689 – 692**.**

- G.X. Wang, S.L. Bewlay, K. Konstantinov, H.K. Liu, S.X. Dou and J.H. Ahn, "Physical and electrochemical properties of doped lithium iron phosphate electrodes" Electrochimica Acta 50 (2004) 441 – 445.

- S.L. Bewlay, K. Konstantinov, G.X. Wang, S.X. Dou and H.K. Liu, "Conductivity improvements to spray-produced Li $FePO_4$ by addition of a carbon tube", Materials Letters 58 (2004) 1788-1791.

4. Progress Reports on International Linkage Award Projects

Investigation of a series of metallic substrate materials** suitable **for developing long Y-Ba-Cu-O superconductors

Funded:	2002	2003	2004
Project ID:	LX0211084		
Australian Investigator:	H.K. Liu – University of Wollongong		
Partner Investigator:	D.L. Shi – University of Cincinnati		

Researchers from Institute for Superconducting and Electronic Materials, the University of Wollongong (UoW) & the Dept. Mat. Sci. & Eng., University of Cincinnati (UC) in USA have strong collaborations through this joint research on a series of metallic substrate materials. The research work has contributed to the development of the second generation of high temperature superconducting wire technology. International research experience for junior researchers and development of new collaborations between senior researchers from UoW in Australia and UC in the USA have been achieved.

Despite great success in the TFA methods of depositing $YBa_2Cu_3O_x$ (YBCO) thin films for coated conductors, critical issues involved in removing $BaCO_3$ have not entirely been settled. There could possibly be other ways of dealing with carbon that remains in the film. We have recently developed a fluorine-free sol–gel synthesis with several important advantages, including precursor solution stability, improved film density, and elimination of HF during processing. With this approach, high-quality YBCO films have been developed on single crystal substrates with the transport J_cs up to 106 A cm−2. In this study, the precursor solution stoichiometry was altered and its effects on superconducting properties were studied. The fluorine-free sol–gel-derived films on the $LaAlO_3$ (LAO) substrate exhibited epitaxial growth with excellent in- and out-of-plane texture. Experimental details are reported on the sol–gel synthesis chemistry and XRD and TEM characterization of the YBCO thin films. Also discussed is the underlying formation mechanism of the YBCO phase during synthesis.

During the mutual visits, Prof. Shi (UC), Prof. Liu (UoW), Dr. M. Ionescu (UoW), A. Li (PhD candidate, UoW) and Y. Zhao (PhD candidate, UoW) have worked together on YBCO thin films using the pulsed laser deposition technique, and discussed project collaboration. Prof. Shi's two PhD students (Y. Xu and HB Yao) also communicated with the researchers at UoW. A joint paper was published in Supercond. Sci. Technol. Two joint papers were presented at the ICMC conference.

Donglu Shi, Yongli Xu , Haibo Yao, Z Han, Jie Lian,Lumin Wang, Aihua Li, H.K. Liu and S. X. Dou, "The development of YBa2Cu3O*x* thin films using a fluorine-free sol–gel approach for coated conductors", Supercond. Sci. Technol. **17** (2004) 1420–1425

Donglu Shi and Yongli Xu Aihua Li, Michal Ionescu, Hua Kun Liu, S.X. Dou, Haibo Yao and Z. Han "Synthesis and characterization of epitaxial YBCO thin films prepared by a fluorine-free sol-gel method for coated conductors", presented at ICMC topical workshop 2/2004

A.H. Li, M. Ionescu, H.K. Liu, D.L. Shi and S.X. Dou, "Microstructure and phase evolution in $Yba_2Cu_3O_y$ films grown on various substrates fabricated via a non-fluorine sol-gel route", presented at ICMC topical workshop 2/2004

Magneto-optical imaging of super-current flow in superconducting tapes and wires

Funded:	2004	2005	2006
Project ID:	LX0453582		
Chief Investigators:	Prof. S.X. Dou, A.V. Pan – University of Wollongong		
	Prof. T.H. Johansen – University of Oslo		

This project is aimed at establishing the connections between local and global superconducting current-carrying abilities in magnesium diboride and high temperature superconducting tapes and wires with the help of local high-resolution magneto-optical imaging combined with transport current technique.

In the first year of the project, two of the project goals have received careful analysis:

1. We have investigated the development of the overcritical state in MgB_2 superconducting wires sheathed in iron. For these purpose, Iron sheathed superconducting MgB_2 wire samples were studied with the help of magneto-optical (MO) imaging in order to visualize local effects induced by a ferromagnetic iron screen (the sheath) around the superconducting MgB_2 core. MO experiments were also carried out in the wires with transport currents applied. The magnetic flux distribution within the superconducting core of the wire was unusually modified in the case where the current is applied in the field-cooled state. The observed phenomenon was evaluated in terms of the magnetic interaction between the ferromagnetic screen and the superconducting core. This interaction enables a super-current redistribution within the core, so that the super-current paths are pushed to the middle of the core. This redistribution is consistent with the explanation of experimentally observed overcritical currents in the wires, which are higher than the "conventional" critical current density achieved in the wires without a ferromagnetic sheath.

2. We studied the process of optimization of the Bi-2223 superconducting tape fabrication procedure with the help of magneto-optical imaging. In this research, a set of Ag-sheathed Bi-2223 ($Bi_{1.72}Pb_{0.34}Sr_{1.85}Ca_{1.99}Cu_3O_x$) tapes was produced using the powder in tube technique and two heat treatments separated by a mechanical deformation. For the second heat treatment, a two-step annealing process was used with the first step at 825˚C and the second at different temperatures from 725 to 800˚C; an additional tape was produced by a slow cooling ramp after annealing at 825˚C. These tapes were studied with local MO imaging. This "local' technique provides results which correlate with and clarify the results obtained by other "global" techniques such as measurements involving XRD, magnetization, transport critical current J_C, and critical temperature T_C. The MO results show better superconducting properties (higher J_C, good shielding properties) for the slow cooled sample and for the sample that was annealed at 750˚C during the second step. Reasons for the observed behaviour were explained in terms of the rate control of the healing process of the cracks in the liquid phase of the superconducting core formation, in terms of enhanced crystallization of Bi-2223 from the liquid phase and the secondary phases, and in terms of distribution of remanent secondary phases.

- V. Pan, S. Dou, and T. H. Johansen, Magneto-optical imaging of magnetic screening in superconducting wires, in NATO Science Series II: Mathematics, Physics and Chemistry, Vol. 142: *Magneto-Optical Imaging*, (Kluwer A. P., Dordrecht), pp. 141-148 (2004).

- M. Roussel, A. V. Pan, R. Zeng, H. K. Liu, S. X. Dou, and T. H. Johansen, Optimization control of Bi-2223 superconducting tape fabrication procedure by magneto-optical imaging, in NATO Science Series II: Mathematics, Physics and Chemistry, Vol. 142: *Magneto-Optical Imaging*, (Kluwer A. P., Dordrecht), pp. 125-132 (2004).

Two more papers are currently being finalized.

Simulation and Characterisation of opto-thermionic cooling devices

Funded:	2003	2004	2005
Project ID:	LX0348004		
Chief Investigators:	A/Prof. C. Zhang, A/Prof. R.A. Lewis – University of Wollongong		
	Prof. K.A. Chao – Lund University, Sweden		

Project summary: Opto-thermionic devices combine thermionic emission and laser cooling to achieve the maximum cooling power and highest thermal efficiency. These devices are ultra small, very reliable and fully integratiable. Many important problems need to be solved to improve the performance of this new class of solid-state cooling devices. One is to understand and manipulate the electron-hole radiative recombination and minimize the Auger process in reduced dimensionality devices such as quantum wells. Researchers at Wollongong and Lund will collaborate on theoretical analysis, computer simulation and electrical/optical measurements to solve this problem.

Selected Abstracts

Conductivity improvements to spray-produced $LiFePO_4$ by addition of a carbon source, *S.L. Bewlay, K. Konstantinov, G.X. Wang, S.X. Dou, H.K. Liu,* Materials Letters 58 (2004) 1788.

We present order-of-magnitude conductivity data for "carbon-included" lithium iron phosphate (LFP) powders lightly pelletised as used as cathodes in Li-ion batteries. The powders were synthesised by a spray pyrolysis method, with a short ameliorating sinter to optimise phase purity. Carbon was introduced into the materials by adding stoichiometric amounts of sucrose into the starting ingredients. We obtained X-ray diffraction patterns and electrical conductivity estimates for carbon contents of between 0 and 31 wt.%. The resultant conductivities spanned almost seven orders of magnitude.

Preparation and properties of spherical $LiNi_{0.75}Co_{0.25}O_2$ as a cathode for lithium-ion batteries, *Y. Chen, G.X. Wang, J.P. Tian, K. Konstantinov, H.K. Liu,* Electrochimica Acta 50 (2004) 435.

Spherical $LiNi_{0.75}Co_{0.25}O_2$ compounds were synthesized by sintering spherical $Ni_{0.75}Co_{0.25}(OH)_2$ and LiOH center dot H_2O precursors at various temperatures in an oxygen atmosphere. A pure phase $LiNi_{0.75}Co_{0.25}O_2$ could be identified. SEM observation showed that the $LiNi_{0.75}Co_{0.25}O_2$ particles are spherical in shape and are composed of many small crystals. Magnetic susceptibility measurements reveal that the spherical $LiNi_{0.75}Co_{0.25}O_2$ compounds have a more ordered layered structure than that of non-spherical $LiNi_{0.75}Co_{0.25}O_2$. The spherical $LiNi_{0.75}Co_{0.25}O_2$ cathodes demonstrated a stable electrochemical performance in lithium-ion cells with a high reversible capacity of 167mAh/g and good cyclability.

Effect of progressive substitution of La^{3+} by Bi^{3+} on the structure, magnetic and transport properties of $La_{0.67}Sr_{0.33}MnO_3$, *Z.X. Cheng, T.M. Silver, A.H. Li, X.L. Wang, H. Kimura,* Journal of Magnetism and Magnetic Materials 283 (2004) 143.

Polycrystalline $La_{0.67-x}Bi_xSr_{0.33}MnO_3$ (x = 0, 0.1, 0.2, 0.3 and 0.67) was prepared by solid-state reaction. The effects of La-substitution by Bi with a typical polarized lone pair electron character on the structure, magnetic and transport properties are presented. The results show that the polarized lone pair $6s^2$ electrons have a dramatic effect on these properties. Structure refinements by the Rietveld method show that the substitution elongates the *a*- and *c*-axes, and eventually changes the structure from rhombohedral to tetragonal. At the same time, the elongated Mn^{3+}-O-Mn^{4+} chain weakens the double exchange between adjacent Mn^{3+} and Mn^{4+} ions via the O bridge. As a consequence, the ferromagnetic coupling temperature decreases from 370 K down to 330 K as x increases to 0.3 from 0, and down to 270 K when La is totally replaced by Bi. With an increasing substitution level, the saturation moment (M_s) decreases from the near theory value of 3.67 μ_B down to 2.5 μ_B for x = 0.3, and 0.08 μ_B for the totally substituted sample. The sample with x = 0.67 shows a very weak ferromagnetic property. However, M_s should not change if only the unchanged Mn^{3+}/Mn^{4+} ratio is considered in the $La_{0.67-x}Bi_xSr_{0.33}MnO_3$ system. The decrease in M_s can only be explained by an enhanced anti-ferromagnetic coupling that is simultaneous with the weakening of the ferroelectric dc coupling by Bi. With increasing Bi content, the resistivity increases, and the temperature of the semiconductor to metallic transition also rises. Eventually the totally substituted sample becomes an insulator.

The morphology, periodical modulation structure and effects of heat treatment on the superconductivity of (Tl, Pb)(Sr, Ba)-1223 single crystals, *Z.X. Cheng, X.L. Wang, S. Keshavarzi, M.J. Qin, T.M. Silver, H.K. Liu, H. Kimura, S.X. Dou,* Supercond. Sci. Technol. 17 (2004) 696.

Surface morphologies and microstructures of (TI, Pb)(Sr, Ba)-1223 single crystals were investigated by using a scanning electronic microscope (SEM) and an atomic force microscope (AFM). The SEM images showed that a T1-1223 single crystal grown by self-flux obeys a layer-by-layer growth mechanism. Periodic modulation structures 200 nm in width and about 0.7-0.8 nm in height were observed using an AFM. Heat treatments in different atmospheres of argon and oxygen at 500 ºC were carried out with different treatment times. T_c and J_c have been improved through optimized heat treatment for 3 h in argon gas. Crystals were also heat treated in PbO. Results showed that the magnetic properties were significantly improved, with large increases in T_c and J_c, indicating that the ratio of T1 to Pb in the crystal is another important factor in addition to the oxygen content in affecting the superconducting properties. The modulation structure is probably responsible for the strong flux pinning in (TI, Pb)(Sr, Ba)-1223 crystals and the large J_c.

Characterization and growth of magnesium diboride single crystals, *Z.X. Cheng, X.L. Wang, A.V. Pan, K.K. Liu, S.X. Dou*, J. Crystal Growth 263 (2004) 218.

Single crystals of magnesium diboride with maximum dimensions of 200 x 200 x 60 mum^3 have been successfully grown from copper flux in iron capsules. MgB_2 crystallized separately in a system with the composition Mg40Cu40B20, and large single crystals were grown. Crystals grow together in the system with the composition Mg35Cu40B25, and MgB_4 is found in this system due to excess B content. MgB_2 crystallizes in very small particles in a system with the composition Mg50Cu40B10. MgB_2 single crystals show strongly polarized light properties, and thus are easily discriminated from other kinds of accompanying crystals and from their surroundings. Magneto-optical microscopy gives direct evidence of superconducting properties of MgB_2 crystals. Further measurements of ac-susceptibility show that crystals begin the superconducting transition at 39.1 K with a transition width of 1.3 K.

Nano-sized Al_2O_3 doping effects on the critical current density of MgB_2 superconductors, *M. Delfany, X.L. Wang, S. Soltanian, J. Horvat, H.K. Liu, S.X. Dou,* Ceramics International 30 (2004) 1581.

MgB_2 polycrystalline bulk samples with addition of 5 and 10 wt.% nano-sized Al_2O_3 powders were prepared by solid state reaction using pre-reacted MgB_2. All the samples were sintered at 850ºC for 40 min in Ar. All the samples were characterized by X-ray diffraction, scanning electron microscopy and magnetic measurements. Results show that the critical current density and irreversibility fields decrease significantly with increasing Al_2O_3 level. J_c values decreased significantly by more than one order of magnitude. The T_c drops slightly from 37.9 to 36.6 K, but acquires a very wide transition width of more than 20 K. Furthermore, the amount of MgO was found to increase with increasing Al_2O_3 level, probably indicating that Mg was replaced by Al, with the excess Mg forming extra MgO. The field dependence of J_c for all the samples is also presented.

Nanoscale-SiC doping for enhancing J_c and H_{c2} in superconducting MgB_2, *S.X. Dou, V. Braccini, S. Soltanian, R. Klie, Y. Zhu, S. Li, X.L. Wang, D. Larbalestier,* J. Appl. Phys. 96 (2004) 7549.

The effect of nanoscale-SiC doping of MgB_2 was investigated in comparison with undoped, clean-limit, and Mg-vapor-exposed samples using transport and magnetic measurements. It was found that there are two distinguishable but related mechanisms that control the critical current-density-field $J_c(H)$ behavior: increase of upper critical field H_{c2} and improvement of flux pinning. There is a clear correlation between the critical temperature T_c, the resistivity ρ, the residual resistivity ratio RRR=R(300 K)/R(40 K), the irreversibility field H*, and the alloying state in the samples. The H_{c2} is about the same within the measured field range for both the Mg-vapor-treated and the SiC-doped samples. However, the $J_c(H)$ for the latter is higher than the former in a high-field regime by an order of magnitude. Mg vapor treatment induced intrinsic scattering and contributed to an increase in H_{c2}. SiC doping, on the other hand, introduced many nanoscale precipitates and disorder at B and Mg sites, provoking an increase of ρ(40 K) from 1 $\mu\Omega$ cm (RRR=15) for the clean-limit

sample to 300 μΩ cm (RRR=1.75) for the SiC-doped sample, leading to significant enhancement of both H_{c2} and H* with only a minor effect on T_c. Electron energy-loss spectroscope and transmission electron microscope analysis revealed impurity phases: Mg_2Si, MgO, MgB_4, BO_x, $Si_xB_yO_z$, and BC at a scale below 10 nm and an extensive domain structure of 2-4-nm domains in the doped sample, which serve as strong pinning centers.

Field behavior of the critical current in quasi-single-crystalline YBCO films, *Y.V. Fedotov, E.A. Pashitskii, S.M. Ryabchenko, A.V. Semenov, A.V. Pan, S.X. Dou, C.G. Tretiatchenko, V.A. Komashko, Y.V. Cherpak, V.M. Pan,* Physica C 401 (2004) 316.

Magnetic field, angular and temperature dependencies of the critical current density were measured by SQUID-magnetometry, ac magnetic susceptibility, and transport techniques in single-crystalline epitaxial YBCO films. The mechanism of vortex depinning from growth-induced linear defects consistently quantitatively describes the measured $J_{(c)}$(H)-dependencies. The model takes into account a distribution of domain size as well as the dislocation spacing within domain boundaries. Structure parameters of YBCO films extracted from $J_{(c)}$(H||c,T)-curves and X-ray diffraction studies agree.

Virgin magnetization of a magnetically shielded superconductor wire: Theory and experiment, *Y.A. Genenko, S.V. Yampolskii, A.V. Pan,* Appl. Phys. Lett. 84 (2004) 3921.

On the basis of exact solutions to the London equation, the magnetic moment of a type II superconductor filament surrounded by a soft-magnet environment is calculated and the procedure of extracting the superconductor contribution from magnetic measurements is suggested. A comparison of theoretical results with experiments on MgB_2/Fe wires allows the estimation of the value of critical current for the first magnetic flux penetration.

Structural and magnetic properties of $Y_{0.33}Sr_{0.67}CoO_{2.79}$, *D.J. Goossens, K.F. Wilson, M. James. A.J. Studer, X.L. Wang,* Phys. Rev. B 6913 (2004) 4411.

The perovskite-based oxide $Y_{0.33}Sr_{0.67}CoO_{2.79}$ has been magnetically and structurally characterized. The material shows a unit cell of 2x2x4 simple perovskite cubes with space group I4/mmm. This is a different structure to that observed in the much-studied (La,Sr)CoO_3 oxides. Oxygen stoichiometry is established through thermogravimetric analysis and correlated with ac and dc magnetic measurements and magnetic neutron diffraction. Hysteresis with field and temperature is observed in the dc magnetization measurements, yet the absence of an imaginary component in the ac susceptibility suggests a time-independent cause for these effects such as the presence of independently ordering ferromagnetic regions due to compositional inhomogeneities within the (single-phase) sample. Rietveld magnetic refinements suggest that the Co moments are arranged antiferromagnetically below 320 K, with the ferromagnetic regions existing within the long-range ordered antiferromagnetic matrix. The staggered moments are (anti)parallel with the c axis and of magnitude 2μ(B), a moment most typical of intermediate spin Co^{3+}. The material does not enter a spin glass or cluster glass phase, but appears to undergo a broad spin-state transition below 100 K.

Characterization of nanoparticles of $LiMn_2O_4$ synthesized by a one-step intermediate temperature solid-state reaction, *Z.P. Guo, J.H. Ahn, H.K. Liu, S.X. Dou,* J. Nanoscience and Nanotechnology 4 (2004) 162.

Nanoparticles of lithium manganese oxide ($LiMn_2O_4$) with a spinel structure have been synthesized by a one-step intermediate temperature solid-state reaction. The influence of the molar ratio of citric acid to the metal ions on the physicochemical properties of $LiMn_2O_4$ powders in air has been analyzed by means of X-ray diffraction and electron microscope techniques. The electrochemical behavior of the material has been examined by charge/discharge tests and cyclic voltammetry. Test results reveal that $LiMn_2O_4$ particles with lower molar ratios of citric acid to metal ions (1:2) are highly crystalline and highly electrochemically

reversible, with better cycle capabilities when compared with a sample with a higher molar ratio (2:1). The $LiMn_2O_4$ powders obtained by this method have a uniform morphology with a narrow size distribution.

Nanopinning in high-temperature superconductors, *J. Horvat,* in Encyclopedia of Nanoscience and Nanotechnology 7. Ed: H.S. Nalwa, American Science Publishers, 207-218 (2004).

High-temperature superconductivity is one of the most studied phenomena in the last 20 years. This is because of its potential to bring the fascinating world of superconductivity into our every-day life. However, soon after the discovery of high-temperature superconductivity it became clear that two main obstacles have to be overcome: vortex pinning and grain connectivity. Improvement of vortex pinning in *high-temperature superconductors* (HTS) is in the domain of nanotechnology, because of their special intrinsic physical properties. This contribution outlines improvement of vortex pinning in HTS by introduction of nano-size *pinning centres*. Because of wide range of intended readership, the contribution will begin with simple description of basic principles of superconductivity and vortex pinning. The focus will gradually shift to more specific topics, being intended for more advanced readers

Interaction of Superconductor with magnetic sheath as a way for improvement of critical current in MgB_2/Fe superconductor, *J. Horvat,* in *Focus on Superconductivity*, Edited by B. P. Martins, Nova Science Publishers, 2004, pp.175-190.

Magnesium diboride superconducting wires give the largest critical current density (J_c) when produced with iron sheath. Because iron is ferromagnetic, it is expected to improve the field dependence of J_c by shielding of the external field for low magnetic fields. However, transport and magnetic measurements of J_c reveal that J_c in MgB_2/Fe is improved far beyond the effect of simple magnetic shielding. The transport measurements in external field show that J_c initially decreases with the field. This is followed by an increase for intermediate fields and again a decrease for high fields, resembling the "peak effect". The value of J_c in the field range of this peak effect is higher than the J_c without iron sheath. The field range of improved J_c widens with decreasing the temperature, shifting to the higher values of the field. The explanation of this phenomenon is suggested in terms of a model predicting the occurrence of overcritical state, as a result of interaction between partly vortex filled superconductor and a magnet. In this model, the currents are pushed into vortex-free volume of the superconductor, effectively increasing its value of loss-free current. The occurrence of the overcritical state is supported by magnetic measurements of J_c.

Superconducting screening on different length scales in high-quality bulk MgB_2 superconductor*, J. Horvat, S. Soltanian, A.V. Pan, X.L. Wang,* J. Appl. Phys. 96 (2004) 4342.

High-quality bulk MgB_2 exhibits a structure of voids and agglomeration of crystals on different length-scales. Because of this, the superconducting currents percolate between the voids in the ensuing structure. Magnetic measurements reveal that the superconducting currents circulate on at least three different length-scales, of ~1 micrometre, ~10 micrometre and whole of the sample (~millimetre). Each of these screenings contributes to the measured irreversible magnetic moment (Δm). The analysis of the field dependence of Δm for samples of subsequently decreasing size showed that the critical current obtained using the simple critical state model is erroneous. This leads to the artefact of the sample size-dependent critical current density J_c and irreversibility field. Our data analysis enables the separation of the contribution of each of the screening currents to Δm. The field dependence of each of the currents follows a *stretched exponential form*. The currents flowing around whole of the sample give a dominant contribution to Δm in the intermediate fields ($1T < H < 4T$ at 20K) and they can be used to obtain the value of J_c from critical state model, which corresponds to the transport J_c. The stretched exponential field dependence of these currents is similar to the one obtained for high-temperature superconductors, and it seems to be connected with the percolation of the currents.

Effect of sample size on magnetic J_c for MgB_2 superconductor, *J. Horvat, S. Soltanian, X.L. Wang, S.X. Dou,* Appl. Phys. Lett. 84 (2004) 3109.

A strong effect of sample size on magnetic $J_c(H)$ was observed for bulk MgB_2 when J_c is obtained directly from the critical state model. Thus obtained zero-field J_c (J_{c0}) decreases strongly with the sample size, attaining a constant value for the samples larger than a few millimetres. On the other hand, the irreversibility field (H_{irr}) defined at J_c = 100 A/cm^2 increases with the sample size. The decrease of J_{c0} is described in terms of voids in the bulk MgB_2 samples and superconducting screening around the cells of superconducting material between these voids (35 μm), because of concentration of the current in the narrow bridges connecting the cells. For samples larger than a few millimetres, the value of magnetic J_c is in agreement with the transport J_c and it is restricted by the voids. The critical state model is not suitable for obtaining J_c for small bulk MgB_2. The increase of H_{irr} with the sample size is an artefact of defining H_{irr} by the value of J_c at which an additional superconducting screening on 1μm scale dominates Δm.

Enhancement of critical current density in $YBa_2Cu_3O_{7-\delta}$ thin films grown using PLD on YSZ (001) surface modified with Ag nano-dots, *M. Ionescu, A.H. Li, Y. Zhao, H.K. Liu, A. Crisan, J.* Phys. D – Appl. Phys. 37 (2004) 1824.

Y123 thin films were grown by pulsed laser deposition (PLD) on YSZ (001) substrate. Prior to the film deposition, a discontinuous layer of Ag was deposited on the substrate, also using PLD, in the form of separate islands. Atomic force microscopy (AFM) investigation of the Ag layer showed that its morphology consisted of self-assembled islands of nanometre size, randomly distributed on the surface of the substrate, called nano-dots. The Y123 superconducting films grown on such a surface were characterized using AFM, x-ray diffraction, secondary electron microscopy, ac susceptibility and dc magnetization. The results show that there is no significant difference in surface morphology, crystallographic orientation, phase composition or superconducting transition temperature between the Y123 films grown on YSZ (001) with an Ag nano-dots layer and a control Y123 film grown on a virgin YSZ (001) surface. On the other hand, at 77 K, the magnetic critical current density (J_{cm}) was three times higher for the Y123 film grown on YSZ with the modified (001) surface than for the film grown on YSZ with a virgin (001) surface. At 5 K the enhancement of J_{cm} was approximately seven times, at both low and high fields. This suggests an increase in pinning, caused presumably by point defects formed in the Y123 film above the Ag islands.

Large magnetoresistive effect in bulk Bi2212 with small additions of USr_2CaO_6, *M. Ionescu. B. Winton, T. Silver, S.X. Dou. R. Ramer,* J. Phys. D – Appl. Phys. 37 (2004) 1727.

A large magnetoresistive (MR) effect was observed in Bi2212 in which USr_2CaO_6 was added in a proportion of 6 wt%. The resistivity of melt-textured (MT) Bi2212 + 6 wt% USr_2CaO_6 possesses a high sensitivity to applied dc fields, as compared to pure Bi2212, in particular at low fields, below 3 T, and in a temperature range between 45 and 85 K. In this temperature range, the MR effects of MT Bi2212 + 6 wt% USr_2CaO_6 display a maximum that may be tuned to a particular temperature within the above range, by changing the amount of added non-superconducting compound. X-ray results show that during the melt-texturing process of this mixture, the USr_2CaO_6 phase is stable and the reaction with Bi2212 matrix is minimal, in spite of a small decrease in the superconducting transition temperature. A cryogenic sensor was build and tested at 77 K in low fields. It shows high sensitivity and no hysteresis of resistivity when the applied field was cycled between 0 and 1 T.

Cryogenic magnetic field sensor based on the magnetoresistive effect in bulk Bi2212+USr_2CaO_6, *M. Ionescu, B. Winton, T. Silver, R. Ramer,* Appl. Phys. Lett. 84 (2004) 5335.

A large magnetoresistive (MR) effect was observed in melt-textured (MT) Bi2212 in which USr_2CaO_6 was added in a proportion of 6 wt %. The resistivity measurements of MT Bi2212+6 wt % USr_2CaO_6 show high sensitivity to applied dc fields, as compared to pure Bi2212, in particular at low fields, below 3 T, and in a temperature range between 45 K and 85 K. In this temperature range, the MR effect of MT Bi2212+6 wt %

USr_2CaO_6 is two orders of magnitude larger than the MR effect in pure Bi2212, and displays a maximum that may be tuned to a particular temperature within the above range, by changing the amount of added nonsuperconducting compound. A cryogenic sensor was built and tested at 77 K in low fields. It shows a good sensitivity and small (~1%) hysteresis of resistivity when the applied field was cycled between 0 T and 1 T.

Oxygen vacancy ordering and magnetism in the rare earth stabilised perovskite form of $SrCoO_{3-\delta}$, *M. James, D. Cassidy, K.F. Wilson, J. Horvat, R.L. Withers,* Solid State Sciences 6 (2004) 655.

We have demonstrated that $SrCoO_{3-\delta}$ can be stabilised into phase pure perovskite forms by the introduction of small amounts ~5% of certain rare earth ions (Sm^{3+}-Yb^{3+}). At the same doping levels, La^{3+} and Pr^{3+} crystallise with the same isostructural trigonal structure as $Sr_6Co_5O_{15}$; while the Nd^{3+} composition shows a mixture of both structure types. Powder X-ray diffraction showed only a simple cubic perovskite structure, however, a combination of electron and neutron diffraction has revealed a tetragonal (P4/mmm) a(p) x a(p) x 2a(p) superstructure. Strontium and the rare earth ions are disordered over a single site, while the oxygen vacancies are localised on the apical 02 sites. Magnetisation measurements show that these materials undergo transitions to a spin-glass state at temperatures below 150 K, and that significant coupling occurs between the rare earth ions and the mixed $Co^{3+/(4+)}$ ions. Magnetisation measurements as a function of applied field reveals that below the transition temperature ferromagnetic ordering takes place at relatively large fields.

Electrochemical properties of Co_3O_4, Ni-Co_3O_4 mixture and Ni-Co_3O_4 composite as anode materials for Li ion secondary batteries, *Y.M. Kang, K.T. Kim, J.H. Kim, H.S. Kim, P.S. Lee, J.Y. Lee, H.K. Liu, S.X. Dou,* J. Power Sources 133 (2004) 252.

By varying the synthetic temperature and time, Co_3O_4 with highly optimized electrochemical properties was obtained from the solid state reaction of $CoCO_3$. As a result, Co_3O_4 showed a high capacity around 700 mAh/g and stable capacity retention during cycling (93.4% of initial capacity was retained after 100 cycles). However, its initial irreversible capacity reached about 30% of capacity. Several phenomenological examinations in our previous results told us that the main causes of low initial coulombic efficiency, that is, large initial irreversible capacity, were solid electrolyte interphase (SEI) film formation on the surface and incomplete decomposition of Li_2O during the first discharge process. SEI film formation cannot be restrained without the development of a special electrolyte, and there has been little research on the proper electrolyte composition, whereas in our research, Ni had the catalytic activity to facilitate Li_2O decomposition. Thus, in order to improve the low initial coulombic efficiency of Co_3O_4 (69%), Ni was added to Co_3O_4 using two methods, physical mixing and mechanical milling. When adding the same amount of Ni, the mechanical milling showed an improvement in initial coulombic efficiency, 79%, but physical mixing had no effect. Finally, when the charge-discharge mechanism of Co_3O_4 was considered and the morphologies of the Ni-Co_3O_4 mixture obtained by physical mixing and the Ni-Co_3O_4 composite prepared by mechanical milling were compared, it was revealed that the initial coulombic efficiency of Ni-Co_3O_4 composite depends on the contact area between the Ni and the Co_3O_4.

Vortex dynamics in pure and SiC-doped MgB_2, *S. Keshavarzi, M.J. Qin, S. Soltanian, H.K. Liu, S.X. Dou,* Physica C 408-410 (2004) 601.

Hysteresis loop and magnetization relaxation measurements have been performed on a pure and a SiC-doped MgB_2 samples. The normalized volume pinning forces determined from the hysteresis loop are observed to scale as a function of the reduced magnetic field ($h = H/H_{irr}$) with peaks at h_{max} approximately 0.2. This result implies that the dominating pinning mechanism in both materials is the pinning by normal surface defects. From magnetization relaxation measurements, the current dependence of the activation energy is found to be logarithmic.

New approach for synthesis of carbon-mixed $LiFePO_4$ cathode materials, *K. Konstantinov, S. Bewlay, G.X. Wang. M. Lindsay, J.Z. Wang, H.K. Liu, S.X. Dou, J.H. Ahn,* Electrochimica Acta 50 (2004) 421.

For the first time, carbon-mixed $LiFePO_4$ (LFP) cathode materials have been prepared by spray solution technology. Nominal addition of 15 or 20 wt.% C was used in order to simulate the industrial practice for preparation of electrode materials. The prepared powders consist of a single $LiFePO_4$ phase: small crystallites with a highly developed surface area, beneficial for the surface electrochemical processes limited by the low Li diffusion. The combination of spray technology and carbon addition increased the specific surface area above 20 m^2/g at a relatively high sintering temperature (700 ºC). The initial discharge capacity was up to 140 mAh/g compared to 125 mAh/g for conventionally prepared (using a solid state reaction) $LiFePO_4$ electrode materials.

In-situ production of nano-structured ceramics by spray solution technique, *K. Konstantinov, Z. W. Zhao, L. Yuan, H. K. Liu and S. X. Dou,* Proc. Advanced Materials for Energy Conversion II, TMS Annual Conference 15-18 March 2004, Charlotte, USA, pp. 331-338.

Various nano-structured M_xO_y ceramics, e.g. CoO, Co_3O_4, SnO_2, and NiO, have been prepared in-situ by a spray pyrolysis method. The effects of the temperature and sintering time on nano-crystallinity, phase composition, and other physical or electrochemical parameters have been studied in detail. Different methods including X-ray diffraction, gas sorption analysis (for estimation of BET surface area), and TEM and SEM techniques, combined with EDX analysis and standard battery testing methods have been used to characterized the powders obtained. We have demonstrated that the method used is flexible and universal, and it permits good control of the crystal size and phase product, allowing in-situ production of simple or complex ceramics possessing specific surface areas that are generally larger than for the corresponding materials obtained via conventional technology. The obtained materials have promising potential applications as anode battery materials, catalysts or capacitors.

Correlated vortex pinning in Si-nanoparticle doped MgB_2, *I. Kusevic, E. Babic, O. Husnjak, S. Soltanian, X.L. Wang, S.X. Dou,* Solid State Comm. 132 (2004) 761.

The magnetoresistivity and critical current density of well characterized Si-nanoparticle doped and undoped Cu-sheathed MgB_2 tapes have been measured at temperatures T greater than or equal to 28 K in magnetic fields B less than or equal to 0.9 T. The irreversibility line $B_{irr}(T)$ for doped tape shows a stepwise variation with a kink around 0.3 T. Such $B_{irr}(T)$ variation is typical for high-temperature superconductors with columnar defects (a kink occurs near the matching field B_ϕ) and is very different from a smooth $B_{irr}(T)$ variation in undoped MgB_2 samples. The microstructure studies of nanoparticle doped MgB_2 samples show uniformly dispersed nanoprecipitates, which probably act as a correlated disorder. The observed difference between the field variations of the critical current density and pinning force density of the doped and undoped tape supports the above findings.

Critical currents and vortex pinning in U/n treated Bi2223/Ag tapes, *I. Kusevic, E. Babic, D. Marinaro, S.X. Dou, R. Weinstein,* Physica C 408-410 (2004) 524.

Critical currents $J_c(T, B)$ for virgin and four U-235 doped Bi2223/Ag tapes irradiated with thermal neutrons (U/n treated) were measured in the temperature range $T \geq 50$ K and magnetic field $B \leq 1$ T. Below 97 K vortex pinning in U/n treated tapes increases with matching field B-phi, as evidenced by a weaker B dependence of J_c on increasing B_ϕ. Hence, the field B-max ($F_{pmax} = J_cB_{max}$) and the irreversibility field $B_{irr}(F_p \rightarrow 0)$ of U/n treated tapes are enhanced compared to those for virgin tape. Since the rate of the enhancement of B_{max} and B_{irr} with B_ϕ depends on T, one can tune the maximum enhancement at desired T.

Irreversibility fields and pinning potentials in U/n treated Bi2223/Ag tapes, *I. Kusevic, E. Babic, D. Marinaro, S.X. Dou, R. Weinstein,* Physica C 408-410 (2004) 643.

The magnetoresistance R(T, B) of virgin and four U-235 doped Bi2223/Ag tapes irradiated with thermal neutrons (U/n treated) has been measured in the temperature range $T \geq 50$ K and magnetic field $B \leq 1$ T. For $B \geq 20$ mT the pinning potentials U_0 of U/n treated tapes were enhanced compared to that of virgin tape. The relative enhancement $U_0(B, U/n)/U_0(B, virg.)$ increased with matching field B_ϕ and persisted to higher B at higher B_ϕ. For U/n treated samples, U-0 showed universal variation with B/B_ϕ : $U_o(B <\sim B_\phi)$ proportional to (B-phi/B)(proportional to) with alpha approximate to 0.5 and faster variation at higher B. The resistive irreversibility fields B-irr(T) of all U/n treated samples for T less than or similar to 100 K were also enhanced: B-irr (T, U/n)/B-irr (T, virg.) increased with B-phi and the enhancement persisted to lower T for higher B-phi. The maximum enhancements of B_{irr} scale well with the corresponding enhancements of $U_0(B)$.

Magnetospectroscopy of Zn-doped InP to 30 T, *R.A. Lewis, Y.J. Wang,* Int. J. Mod. Phys. B 18, 3839.

While the III-V alloy InP finds increasing applications in high-power and high-speed electronics, optical fiber communications, and radiation detection, the knowledge of its impurity states, especially in magnetic fields, remains sparse. Fig. 1 summarizes present knowledge of the Zn acceptor states in InP in zero and applied field. The unperturbed energies of acceptor states have been calculated by Baldereschi and Lipari.[1-3] The ground-state energy has recently been calculated by Wang and Chen.[4] Energies of the Zn acceptor have been determined experimentally by Kubota et al.[5] using photoluminescence (PL) and by Wenzel et al.[6] using electronic Raman scattering (ERS). Magnetospectroscopy[7,8] has previously been conducted to 17.5 T; the present work extends this to 30 T.

Phonon spectra of cobaltite/manganites in strong magnetic fields, *R.A. Lewis, Y.J. Wang, F. Gao, X.L. Wang, S.X. Dou,* J. Magnetism and Magnetic Materials 272-276 (2004) 616.

Far-infrared spectroscopy has been employed to determine phonon modes in the cobaltite/rnanganites $A(Co_{1/2}Mn_{1/2})O_3$, where A is a lanthanide, in magnetic fields up to 17.5 T. The phonon energies in the compounds with A = La, Nd or Ho show little change with applied magnetic field. In contrast, with A = Yb, all the phonon modes exhibit a splitting when a magnetic field is applied. It is thought that this field dependence of the phonon energies is related to the metamagnetism of $Yb(Co_{1/2}Mn_{1/2})O_3$.

Zeeman spectroscopy of Be impurity in GaAs to 30 T, *R.A. Lewis, Y.J. Wang, M. Henini,* Physica B 346 (2004) 483.

Absorption measurements have been made in fields to 30 T of the far-infrared optical transitions associated with the Be impurity in GaAs. The order and magnitude of the splitting of the ground state has been clarified by low-field (to 6 T) photo-thermal ionisation spectroscopy measurements of the C line. In light of the new high-field data the G line is now believed to comprise two unresolved components. At high magnetic field (above 25 T) a new feature appears which increases in energy with field at a much greater rate than the other transitions; this is thought to originate in valence-band Landau levels.

Amorphous and nanocrystalline Magnesium–Nickel Alloys for Ni-MH Batteries, *H.K. Liu,* in Encyclopedia of Nanoscience and Nanotechnology. Edited by H. S. Nalwa, American Scientific Publishers, **4,** 775-790 (2004), (Review Chapter).

The Nickel-Metal Hydride (Ni-MH) battery is one of the key competitors in the rechargeable battery market, not only for advanced information and telecommunication systems, but also for next generation vehicles in which energy must be used efficiently with low emissions to the environment. The key materials for this high-tech battery are the hydrogen storage alloys. The current efforts, recent advances and the expectations

for the future of the novel amorphous and nanocrystalline magnesium(Mg) – nickel(Ni) alloys as electrode materials in Ni-MH batteries are reviewed in this paper.

Origin of paramagnetic magnetization in field-cooled $YBa_2Cu_3O_{7-\delta}$ films, *D.A. Luzhbin, A.V. Pan, V.A. Komashko, V.S. Flis, V.M. Pan, S.X. Dou, P. Esquinazi,* Phys. Rev. B 6902 (2004) 4506.

Temperature dependences of the magnetic moment have been measured in $YBa_2Cu_3O_{7-\delta}$ thin films over a wide magnetic-field range ($5 \leq H \leq 10(4)$ Oe). In these films a paramagnetic signal known as the paramagnetic Meissner effect has been observed. The experimental data in the films, which have strong pinning and high critical current densities ($J_c \sim 2x10^6$ A/cm^2 at 77 K), are shown to be highly consistent with the theoretical model proposed by Koshelev and Larkin [Phys. Rev. B 52, 13 559 (1995)]. This finding indicates that the origin of the paramagnetic effect is ultimately associated with nucleation and inhomogeneous spatial redistribution of magnetic vortices in a sample which is cooled down in a magnetic field. It is also shown that the distribution of vortices is extremely sensitive to the interplay of film properties and the real experimental conditions of the measurements.

Overcritical state in superconducting round wires sheathed by iron, *A.V. Pan, S.X. Dou,* J. Appl. Phys. 96 (2004) 1146.

Magnetic measurements carried out on MgB_2 superconducting round wires have shown that the critical current density $J_c(B_a)$ in wires sheathed by iron can be significantly higher than that in the same bare (unsheathed) wires over a wide applied magnetic field B_a range. The magnetic behavior is, however, strongly dependent on the magnetic history of the sheathed wires, as well as on the wire orientation with respect to the direction of the applied field. The behavior observed can be explained by magnetic interaction between the soft magnetic sheath and superconducting core, which can result in a redistribution of supercurrents in the flux filled superconductor. A phenomenological model explaining the observed behavior is proposed.

Magneto-optical imaging of magnetic screening in superconducting wires, *A.V. Pan, S.X. Dou, T.H. Johansen,* Magneto-Optical Imaging 142 (2004) 141.

Iron sheathed superconducting MgB_2 wires were investigated with the help of magneto-optical (MO) imaging technique in order to visualize local effects induced by ferromagnetic iron screen (sheath) into the superconducting MgB_2 core. MO experiments were also carried out in the wires with transport currents applied. The magnetic flux distribution within the superconducting core of the wire has been shown to be unusually modified in the case when the current is applied in the field-cooled state. The observed phenomenon is discussed in terms of magnetic interaction between the ferromagnetic screen and the superconducting core. This interaction enables a super-current redistribution within the core, so that the super-current paths are pushed to the middle of the core. This redistribution is consistent with the explanation. of experimentally observed overcritical currents in the wires, which are higher than the conventional critical current density. Presented at NATO Advanced Research Workshop on Magneto-Optical Imaging, Øystese, Norway, Aug. 28-30, 2003.

Decoupling transition of two coherent vortex arrays within the surface superconductivity state, *A.V. Pan, P. Esquinazi,* Phys. Rev. B 7018 (2004) 4510.

In magnetic fields applied within the angular range of the surface superconductivity state a magnetically anisotropic layered medium is created in structurally isotropic, sufficiently thick niobium films. Surface (Kulik) vortices residing in the superconducting sheaths on both main film surfaces in tilted fields are shown to undergo a decoupling transition from a coherent to an independent behavior, similar to the behavior observed for a Giaever transformer. At the transition a feature in pinning properties is measured, which implies different pinning for the lattice of surface vortices coherently coupled through the normal layer and for two decoupled vortex arrays in the superconducting surface sheaths.

Nature of high critical current density in HTS $YBa_2Cu_3O_{7-\delta}$ films, *V. M. Pan, V. A. Komashko, V. L. Svetchnikov, C. G. Tretiatchenko, Yu. V. Cherpak, A. V. Pan, S. X. Dou, E. A. Pashitskii, S. M. Ryabchenko, A. V. Semenov, Yu. V. Fedotov, H.W. Zandbergen,* in Applied Superconductivity: Proceedings of the 6th European Conference on Applied Superconductivity, Sorrento, Italy, 14-18 Sept. 2003. Edited by A. Andreone, G.P. Pepe, R. Cristiano and G. Masullo. Institute of Physics Conference Series no. 181 (2004) pp. 245-253.

By highly advanced structural analysis, HTS YBCO films have been shown to form the nano-scale network of low-angle domain boundaries (LABs), consisting of natural linear defects (out-of-plane edge dislocations). The domains are 30-300 nm large and misoriented by ~1°. The average in-plane density of dislocations is up to 10^{11} cm^{-2}. LABs are quite ordered rows of parallel dislocations capable of providing strong pinning for vortices because the dislocations have non-superconducting cores surrounded by localized regions of suppressed T_c. However, supercurrent density can be limited by transparency of the dislocations, determining the effective depairing current density, whereas gaps between dislocations would remain transparent for supercurrent flow across LABs. As a consequence, two J_c-limiting mechanisms governed by depairing/transparency and by depinning can be anticipated. The variation of linear defect density and defect spatial distribution would lead to the realization of a certain J_c-limitation mechanism. Magnetic field, angular and temperature dependencies of $J_c(H,T)$ have been measured by SQUID magnetometer, ac susceptibility and dc transport current techniques in YBCO films, epitaxially-grown by off-axis dc magnetron sputtering, having $J_c(77\ K) > 2$ MA/cm^2. The model of vortex depinning from linear defects has been developed and shown to well describe the measured $J_c(H,T)$ quantitatively. The model takes into account a statistic distribution of dislocation domain sizes, as well as interdislocation spacing within boundaries. On the other hand, the crossover of $J_c(H)$ from a plateau-like behavior at $H \rightarrow 0$ to its logarithmic degradation at higher fields can indicate the existence of the transparency-controlled J_c-limitation in the low-field region.

Thermally activated depinning of individual vortices in $YBa_2Cu_3O_7$ superconducting films, *A.V. Pan, Y. Zhao, M. Ionescu, S.X. Dou, V.A. Komashko, V.S. Flis, V.M. Pan,* Physica C 407 (2004) 10.

A number of $YBa_2Cu_3O_7$ thin superconducting films have been grown on different single crystal substrates under different conditions using pulsed-laser deposition and magnetron sputtering techniques. Employing magnetization measurements, critical current density (J_c) dependences on the applied magnetic field (B_a) have been obtained for the films. The analysis of the $J_c(B_a)$ behaviour suggests that the range of the B_a-independent J_c plateau depends on the interplay between the vortex pinning of certain, particularly effective defects and thermally activated depinning of individual vortices. The latter process is found to be the main factor responsible for the temperature dependence of the size of the J_c-plateau. This temperature behaviour is independent of the properties of the films and their orientation with respect to the field. The absolute J_{c0} value at B_a --> 0 T is, in contrast to the plateau, more sensitive to pinning media transparency to the supercurrent flow.

Iron-sheath influence on the superconductivity of MgB_2 core in wires and tapes, *A.V. Pan, S.H. Zhou, S.X. Dou,* Supercond. Sci. Technol. 17 (2004) S410.

The magnetic systems of superconducting wires and tapes, consisting of a magnesium diboride (MgB_2) superconducting core surrounded by a ferromagnetic iron (Fe) sheath, have been investigated. The interaction of the superconductor with the soft magnetic environment has been experimentally shown to lead to significant enhancement of dissipation-free super-current densities. The maximum densities of the super-currents can exceed the critical current densities obtained in the same 'bare' wire (with its iron sheath removed) by more than one order of magnitude under the same experimental conditions. This current density enhancement is referred to as the overcritical state, which has been observed over a wide range of magnetic fields applied transversely to the wire. No overcritical currents are observed for the longitudinal field

orientation. The irreversibility field is shown to be considerably suppressed by the influence of the iron sheath for both field orientations. Different geometries of the wire cross section have been investigated.

Investigation of Fe valence in $LiFePO_4$ by Mossbauer and XANES spectroscopic techniques, *A.A.M. Prince, S. Mylswamy, T.S. Chan, R.S. Liu, B. Hannoyer, M. Jean, C.H. Shen, S.M. Huang, J.F. Lee, G.X. Wang,* Solid State Comm. 132 (2004) 455.

A crystalline form of $LiFePO_4$ has been synthesized by solid-state reaction using LiOH, $FeC_2O_4.2H_2O$ and $(NH_4)(2)HPO_4$ under reducing (5% H_2 and 95% Ar) atmosphere. The sample was characterized by X-ray diffraction (XRD), Mossbauer and Xray absorption near-edge spectroscopic (XANES) methods. The crystal parameters were derived from Rietveld's refinement of the XRD data. The oxidation state of Fe was investigated by Mossbauer and Fe K-edge XANES spectral techniques.

Sample-size dependence of the magnetic critical current density in MgB_2 superconductors, *M.J. Qin, S. Keshavarzi, X.L. Wang, H.K. Liu, S.X. Dou,* Phys. Rev. B 6901 (2004) 2507.

Sample size dependent magnetic critical current density has been observed in magnesium diboride superconductors. At high fields, larger samples provide higher critical current densities, while at low fields, larger samples give rise to lower critical current densities. The explanation for this surprising result is proposed in this study based on the electric field generated in the superconductors. The dependence of the current density on the sample size has been derived as a power law proportional to $R^{1/n}$ [n is the n factor characterizing the E-j curve $E=E_c(j/j(c))(n)$]. This dependence provides one with a method to derive the n factor and can also be used to determine the dependence of the activation energy on the current density.

The optimization control of Bi-2223 superconducting tape fabrication procedure by magneto-optical imaging, *M. Roussel, A. V. Pan, R. Zeng, H. K. Liu, and S. X. Dou,* Magneto-Optical Imaging 142 (2004) 125.

A set of Ag-sheathed Bi-2223 ($Bi_{1.72}Pb_{0.34}Sr_{1.85}Ca_{1.99}Cu_3O_x$) tapes was produced using the powder in tube technique and two heat treatments separated by a mechanical deformation. For the second heat treatment, a two step annealing process was used with the first step at 825˚C and the second at different temperatures from 725 to 800˚C, an additional tape was produced by a slow cooling ramp after annealing at 825˚C. These tapes were studied by the way of magneto-optical imaging (MOI). This "local' technique provides results which correlate and clarify the results obtained by other "global" techniques (XRD, magnetization, critical current J_C, critical temperature T_C). The MO results show better superconducting properties (higher J_C, good shielding properties) for the slow cooled sample and for the sample which was annealed at 750˚C during the second step. Presented at NATO Workshop on Magneto-Optical Imaging, 28-31st August 2003 Øystese, Norway.

Flux jumps in magnesium diboride, *D.V. Shantsev, P.E. Goa, F.L. Barkov, A.V. Bobyl, T.H. Johansen, W.N. Kang, S.I. Lee, M. Kühberger, G. Gritzner, M. Roussel, S.X. Dou,* Magneto-Optical Imaging 142 (2004) 223.

Magneto-optical imaging was used to study flux penetration into MgB_2 films in a slowly increasing perpendicular applied field. A variety of flux jumps and avalanches have been observed at temperatures below 10K. At small fields, jumps with typical size of 20 μm and regular shape occur at random location along the flux front. Above some threshold field of 2-10 mT, big dendritic jumps with dimensions comparable to the sample size (mm scale) take place. The jumps are developing extremely fast, result in highly-branching irreproducible flux patterns, and effectively suppress the apparent critical current. Both type of jumps are believed to result from thermo-magnetic instability. Presented at NATO Workshop on Magneto-Optical Imaging, 28-31st August 2003 Øystese, Norway.

The development of $YBa_2Cu_3O_x$ thin films using a fluorine-free sol-gel approach for coated conductors, *D.L. Shi, Y.L. Xu, H.B. Yao, Z. Han, J. Lan, L.M. Wang, A.H. Li, H.K. Liu, S.X. Dou,* Supercond. Sci. Technol. 17 (2004) 1420.

Despite great success in the TFA methods of depositing $YBa_2CU_3O_x$ (YBCO) thin films for coated conductors, critical issues involved in removing $BaCO_3$ have not entirely been settled. There could be other possible ways of dealing with carbon that remains in the film. We have recently developed a fluorine-free sol-gel synthesis with several important advantages including precursor solution stability, improved film density, and elimination of HF during processing. With this approach, high-quality YBCO films have been developed on single crystal substrates with the transport J_ss up to 10^6 A cm^{-2}. In this study, the precursor solution stoichiometry was altered and its effects on superconducting properties were studied. The fluorine-free sol-gel-derived films on the $LaAlO_3$ (LAO) substrate exhibited epitaxial growth with excellent in- and out-of-plane texture. Experimental details are reported on the sol-gel synthesis chemistry and XRD and TEM characterization of the YBCO thin films. Also discussed is the underlying formation mechanism of the YBCO phase during the synthesis.

Uranium doping and thermal neutron irradiation flux pinning effects in MgB_2, *T.M. Silver, J. Horvat, M. Reinhard, P. Yao, S. Keshavarzi, P. Munroe, S.X. Dou,* IEEE Trans. Appl. Supercond. 14 (2004) 33.

The U/n method is a well-established means of improving flux pinning and critical current performance in cuprate superconductors. The method involves the doping of the superconductor with U-235 followed by irradiation with thermal neutrons to promote fission. The resultant columnar damage tracks produced by the energetic fission products pin flux vortices and improve critical current performance in magnetic fields. No such improvement could be observed when, the U/n method was applied to the MgB_2 superconductor. No fission tracks could be observed in TEM, even for samples that were irradiated at the highest fluence. Gamma-ray spectroscopy indicated that fission had occurred in the expected way. The likely resistance of MgB_2 to the formation of fission tracks is highly relevant to attempts to improve flux pinning and superconducting performance in this material through the introduction of columnar defects.

Effects of nanosized adsorbing material on electrochemical properties of sulfur cathodes for Li/S secondary batteries, *M.S. Song, S.C. Han, H.S. Kim, J.H. Kim, K.T. Kim, Y.M. Kang, H.J. Ahn, S.X. Dou, J.Y. Lee,* Journal of the Electrochemical Society 151 (2004) A791.

In order to prevent polysulfide dissolution into liquid electrolytes and to promote the Li/S redox reaction ($16Li+S_8$<---->Li_2S_n<---->Li_2S), nanosized $Mg_{0.6}Ni_{0.4}O$, which has the catalytic effect of chemical bond dissociating and is expected to have an adsorbing effect due to the effect of retaining liquid electrolyte of MgO in a Li/iron sulfide secondary battery,[16] was prepared by the sol-gel method as an electrochemically inactive additive for an elemental sulfur cathode for Li/S rechargeable batteries. The Li/S battery using an elemental sulfur cathode with nanosized $Mg_{0.6}Ni_{0.4}O$ added showed the improvement of not only the discharge capacity but also cycle durability (maximum discharge capacity: 1185 mAh/g sulfur, C-50/C-1=85%). The rate capability of the sulfur cathode was also increased with the addition of the nanosized $Mg_{0.6}Ni_{0.4}O$. From the results, it is confirmed that the nanosized $Mg_{0.6}Ni_{0.4}O$ had the polysulfide adsorbing effect and the catalytic effect of promoting Li/S redox reaction. Furthermore, it is found that the nanosized $Mg_{0.6}Ni_{0.4}O$ also increased the porosity of the sulfur cathode.

Irreversibility field and flux pinning in MgB_2 with and without SiC additions, *M.D. Sumption, M. Bhatia, S.X. Dou, M. Rindfleisch, M. Tomsic, L. Arda, M. Ozdemir, Y. Hascicek, E.W. Collings,* Supercond. Sci. Technol. 17 (2004) 1180.

The critical current density (J_c) was measured at 4.2 K for MgB_2 strands with and without SiC additions. In some cases measurements were performed on long (1 m) samples wound on barrels, the transport results being compared to the results of magnetic measurements. Most measurements were performed on short samples in fields of up to 18 T. It was found that in situ processed strands with 10% SiC additions heat treated at 700-800ºC showed improved irreversibility fields (H_{irr}) and bulk pinning strengths (F_p) as

compared to control samples; an increase in H_{irr} of 1.5 T was noted. Heat treatment to 900ºC gave even larger improvements, with H_{irr} reaching 18 T and F_p values maximizing at 20 GN m^{-3}.

Nanostructured Si-C composite anodes for lithium-ion batteries, *G.X. Wang, J.H. Ahn, J. Yao, S. Bewlay, H.K. Liu,* Electrochemistry Communications 6 (2004) 689.

Nanostructured Si-C composite materials were prepared by dispersing nanocrystalline Si in carbon aerogel and subsequent carbonization. Through this process, nanosize Si was homogeneously distributed in a carbon matrix. The Si-C composites exhibit a reversible lithium storage capacity of 1450 mAh/g when used as anodes in lithium-ion cells. The nanostructured Si-C composite electrodes demonstrated good cyclability. The Si-C composites could provide a novel anode material for lithium-ion batteries.

Physical and electrochemical properties of doped lithium iron phosphate electrodes, *G.X. Wang, S.L. Bewlay, K. Konstantinov, H.K. Liu, S.X. Dou, J.H. Ahn,* Electrochimica Acta 50 (2004) 443.

Stoichiometric and non-stoichiometric Mg-doped lithium iron phosphates were synthesised via spray-pyrolysis, followed by sintering at high temperature for crystallization. The spray pyrolysis process allows the homogeneous mixing of the ingredient reactants at atomic level. The electronic conductivities of the Mg-doped lithium iron phosphates have been drastically improved by 4 orders of magnitude, compared to the undoped $LiFePO_4$. The electrochemical properties of as-prepared lithium iron phosphates were systematically measured by cyclic voltammetry and constant current charge/discharge cycling tests.

Tungsten disulfide nanotubes for lithium storage, *G.X. Wang, S. Bewlay, J. Yao, H.K. Liu, S.X. Dou,* Electrochemical and Solid State Letters 7 (2004) A321.

WS_2 nanotubes were synthesized by sintering amorphous WS_3 at high temperature under flowing hydrogen. High-resolution transmission electron microscopy observation revealed that the as-prepared WS_2 nanotubes have an open end with an inner hollow core of about 4.6 nm. We studied the lithium intercalation behavior of WS_2 nanotubes. The WS_2 nanotubes demonstrated a stable cyclability in a wide voltage range (0.1-3.1 V vs. Li/Li+). The nanotubes could provide a new class of electrode materials for lithium-ion batteries.

This paper has been highlighted as a breakthrough in the field in MRS Bulletin, November Issue, 2004 p787 – 789). An excerpt of the comments follows:

In the October issue of Electrochemical and Solid-State Letters (p. A321), G.X. Wang, S. Bewlay, J.Yao, H.K. Liu and S.X. Dou from the University of Wollongong, Australia reported a major breakthrough in utilising such WS_2 nanotubes for storing lithium in Li-ion batteries. Li-ion batteries are the most commonly used type of rechargeable batteries in portable electronic devices. Wang's research team has focused on how lithium in stored in WS_2 nanotubes, which respresents an important process in using these materials as electrodes or anodes in rechargeable batteries. The researchers synthesised WS_2 nanotubes from amorphous WS_3 at high temperature in a hydrogen atmosphere. They report a very high yield of – 80%. Characterisation of the materials by transmission electron microscopy with field emission indicated that the nanotubes have a length of a few hundred nanometers, have open tips, a diameter between 30 nm and to nm, with wall thickness of ~ 15 nm. The hollow core measured roughly 4.6 nm. Electrochemical properties were assessed based on coin cell testing. Wang and co-workers identified electrochemical properties of the WS_2 nanotubes that differ significantly from WS_2 as a powder material. The WS_2 nanotube electrode delivered a lithium insertion capacity correlating to 8.6 mol lithium per mol WS_2 nanotube whereas the lithium insertion capacity was 0.6 mol lithium per mol crystalline WS_2. The researchers attribute the nanotube capability to its 1D topology and open structure. They further found that the WS_2 nanotubes show stable cyclability over a wide voltage range (0.1 – 3.1 V vs. Li/Li^+), so that batteries built with these materials will be tolerant for overcharge and overdischarge. Based on their results, the researchers said that WS_2 nanotubes may be an attractive material for usage in electrochemical applications. In particular, they said, the capacity for storing Li is much enhanced in the nanotube modification of the material than the crystalline powder materials.

Characterization of $LiM_xFe_{1-x}PO_4$ (M=Mg, Zr, Ti) cathode materials prepared by the sol-gel method, *G.X. Wang, S. Bewlay, J. Yao, J.H. Ahn, S.X. Dou, H.K. Liu,* Electrochemical and Solid State Letters 7 (2004) A503.

A series of $LiM_xFe_{1-x}PO_4$ (M = Mg,Zr,Ti) phosphates were synthesized via a sol-gel method. Transmission electron microscopy observations show that $LiM_xFe_{1-x}PO_4$ particles consist of nanosize crystals, ranging from 40 to 150 nm. High-resolution TEM analysis reveals that a layer of amorphous carbon was coated on the surface of the $LiM_xFe_{1-x}PO_4$ particles, which substantially increases the electronic conductivity of $LiM_xFe_{1-x}PO_4$ electrodes. The doped $LiM_xFe_{1-x}PO_4$ powders are phase pure. Near full capacity (170 mAh/g) was achieved at the C/8 rate at room temperature for $LiM_xFe_{1-x}PO_4$ electrodes. The doped $LiM_xFe_{1-x}PO_4$electrodes demonstrated better electrochemical performance than that of undoped $LiFePO_4$ at high rate.

Electrochemical and in situ synchrotron X-ray diffraction studies of $Li[Li_{0.3}Cr_{0.1}Mn_{0.6}]O_2$ cathode materials, *G.X. Wang, Z.P. Guo, X.Q. Yang, J. McBreen, H.K. Liu, S.X. Dou,* Solid State Ionics 167 (2004) 183.

Layered $Li[Li_{0.3}Cr_{0.1}Mn_{0.6}]O_2$ cathode material with a hexagonal structure was synthesized by a solid-state reaction. The structural changes of this material were studied using a synchrotron-based in situ X-ray diffraction (XRD) technique during charge/discharge cycles. The results of in situ X-ray diffraction indicated that the layer structure and the hexagonal symmetry of this material were preserved through the phase transition between H1 and H2 during the charge/discharge cycling. When cycled in the voltage range of 2.0-4.5 V, the changes in lattice parameters a and c are smaller than those for the $LiNiO_2$, layered material. When charged to a high voltage at 5.1 V, the hexagonal phase H3, which is commonly formed at voltages higher than 4.3 V in $LiNiO_2$ with a very short c-axis, is not observed in the $Li[Li_{0.3}Cr_{0.1}Mn_{0.6}]O_2$ cathode, indicating a possible high thermal stability in the fully charged state. Cyclic voltammograms show a single pair of oxidation and reduction peaks, consistent with a reversible phase transition between H1 and H2 observed from the *in situ* X-ray diffraction data.

Electrochemical properties of nanosize Sn-coated graphite anodes in lithium-ion cells, *G.X. Wang, J. Yao, J.H. Ahn, H.K. Liu, S.X. Dou,* J. Appl. Electrochem. 34 (2004) 187.

A series of Sn- coated graphite composite materials for lithium-ion batteries were prepared by microencapsulating nanosize Sn particles in graphite. The nanosize Sn particles are homogeneously dispersed in the graphite matrix via electroless chemical reduction. The tin- graphite composite showed a great improvement in lithium storage capacity. Since Sn is an active element to lithium, Sn can react with lithium to form $Li_{4.4}Sn$ alloys, a reaction accompanied by a dramatic volume increase, whereas the ductile graphite matrix provides a perfect buffer layer to absorb this volume expansion. Therefore, the integrity of the composite electrode is preserved during lithium insertion and extraction. Cyclic voltammetry was employed to identify the reaction process involved in lithium insertion and extraction in the graphite structure, as well as lithium alloying with tin. The tin-graphite composites provide a new type of anode material for lithium-ion batteries with an increased capacity.

Characterization of nanocrystalline Si-MCMB composite anode materials, *G.X. Wang, J. Yao, H.K. Liu,* Electrochemical and Solid State Letters 7 (2004) A250.

Nanocrystalline Si-mesocarbon microbead (MCMB) composite anode materials were prepared by ball milling. Scanning electron microscopic observation showed that the spherical shape of MCMB particles can be retained via moderate ball milling. Ball-milling conditions have an impact on the capacity and cyclability of nanocrystalline Si-MCMB composites. The optimized Si-MCMB composite anode demonstrated a reversible capacity of 1066 mAh/g with good cyclability. A reaction model has been proposed to explain the reaction mechanisms of lithium insertion and extraction in the Si-MCMB electrode.

Electrochemical characteristics of tin-coated MCMB graphite as anode in lithium-ion cells, *G.X. Wang, J. Yao, H.K. Liu, S.X. Dou, J.H. Ahn,* Electrochimica Acta 50 (2004) 515.

Several Sn-coated MCMB (mesocarbon microbead) graphite anode materials were prepared by microencapsulating nanosize Sn particles in MCMB. The nanosized tin particles are homogeneously dispersed in MCMB graphite matrix via electroless in situ chemical reduction. X-ray diffraction and EDS measurement confirms the presence of Sn in the MCMB matrix. Systematic electrochemical testing has been performed on the Sn-coated MCMB graphite electrodes. The tin-coated MCMB graphite electrodes demonstrated an improvement in lithium storage capacity. The reaction process of lithium intercalation and de-intercalation in MCMB structure and lithium alloying with tin has been identified by cyclic voltammetry measurement. The micro-encapsulation of Sn in MCMB graphite can enhance the electrochemical properties of MCMB graphite anodes.

A novel cureless pure lead oxide plate for valve-regulated lead-acid batteries, *J. Wang, G.X. Wang, Y. Chen, C.Y. Wang, H.K. Liu,* J. Appl. Electrochem. 34 (2004) 1127.

Pure lead oxide has been tested as a starting material for VRLA lead-acid batteries. The influence of the acid-to-oxide ratio and the paste density on the plate formation and battery performance has been investigated. The results show that the plates can be directly formed without undergoing the conventional plate curing process if pure lead oxide is used. The new process shows significant advantages in simplifying the conventional plate making processes for lead acid batteries and reducing the production cost and time.

Significant enhancement of critical current density and flux pinning in MgB_2 with nano-SiC, Si, and C doping, *X.L. Wang. S. Soltanian, M. James, M.J. Qin, J. Horvat, Q.W. Yao, H.K. Liu, S.X. Dou,* Physica C 408-410 (2004) 63.

Polycrystalline MgB_2 samples with addition of 0-10 wt% powders of SiC, Si and C were prepared by an in situ reaction process. The phases, microstructures, and flux pinning were characterized by XRD, TEM, and magnetic measurements. It was observed that the samples doped with nano-sized SiC have best pinning performance, while nano-Si or nano-C powders showed a similar improved field dependence of the critical current over a wide temperature range compared with both undoped samples and samples doped with coarse SiC and Si powders. Both magnetic and transport J_c were as high as 3000-20,000 A/cm^2 in 8 T at 5 K, one or two orders of magnitude higher than for undoped MgB_2. T_c only dropped 2 K and remained unchanged with high doping levels for these doped samples. X-ray diffraction results indicated that Si and SiC had reacted with Mg to form Mg_2Si. Neutron diffraction and Rietveld analysis showed no evidence of Si doping into the lattice in the Si doped MgB_2 samples. Nano-particle inclusions, such as Mg_2Si, precipitates of MgO, and unreacted nano-particles observed using TEM, are proposed to be responsible for the enhancement of flux pinning in high fields. A strong effect of sample size on magnetic $J_c(H)$ was also observed for bulk MgB_2.

Growth, microstructures, and superconductivity of $Bi_{2-x}Pb_xSr_2Ca_{1-y}Gd_yCu_2O_{8+z}$ single crystals, *X.L. Wang, E. Takayama-Muromachi, A.H. Li. Z.X. Cheng, S. Keshavarzi, M.J. Qin, S.X. Dou,* J. Appl. Phys. 95 (2004) 6699.

$Bi_{2-x}Pb_xSr_2Ca_{1-y}Gd_yCu_2O_{8+\delta}$ (x=0.34 and y=0.18, 0.34) crystals were grown by the self-flux method. The crystals have a cleavage thickness of only half unit cell up to two unit cells with T_c only dropping 20 K as y is increased from 0.18 to 0.34 for as-grown crystals. However, T_c increased to almost the same value of about 80 K after annealing in air regardless of the Gd doping levels. The co-doping produced enhanced flux pinning compared to the sole Gd doping. A secondary peak effect presented in crystals with x=0.34 and y=0.34 was explained by phase segregations containing Gd-rich clusters.

Significant improvement of critical current density in coated MgB_2/Cu short tapes through nano-SiC doping and short-time in situ reaction, *X.L. Wang. Q.W. Yao, J. Horvat, M.J. Qin, S.X. Dou,* Supercond. Sci. Technol. 17 (2004) L21.

Pure and 10 wt% nano-SiC doped MgB_2/Cu tapes were fabricated using the coating and pressing method. Samples were sintered by an in-situ reaction process. It was observed that the nano-SiC doped tapes were significantly reacted with the Cu sheath at 700ºC, while pure samples have less reactivity with Cu under the same conditions. However, for sintering at 667ºC for just 6 min, the reaction with Cu was significantly reduced for the nano-SiC doped samples and led to very high critical current densities of more than 1 MA cm^{-2} in zero field at $T \leq 10$ K. The J_c values exceed 10^5 A cm^{-2} for 30 K in zero field, 20 K in 2 T and $T \leq 10$ K in 4 T. These J_c values are of one to two orders of magnitude higher than those of the pure MgB_2/Cu short tapes, are the best reported J_c values for Cu sheathed wires and tapes and are comparable to the J_c values reported for MgB_2/Fe tapes. These nano-SiC doped MgB_2/Cu tapes also exhibited very small flux jumping at 5 K. Such a high J_c value and its field performance together with its possible high thermal stability make the Cu-sheathed MgB_2 tapes an attractive candidate for large-scale applications.

Optical absorption in terahertz-driven quantum wells, *M. Xi, J.C. Cao, C. Zhang,* Journal of Applied Phys. 95 (2004) 1191.

The optical absorption spectra in a quantum well driven both by an intense terahertz (THz) and by an optical pulse are theoretically investigated within the theory of density matrix. We found that the optical absorption spectra and the splitting of the excitonic peaks splitting can be controlled by changing the THz field intensity and/or frequency. The Autler–Towns splitting is a result of the THz nonlinear dynamics of confined excitons, which is in agreement with the experiments. In addition, the dependence of the optical absorption on the quantum well width and the carrier density is also discussed.

- High-field magnetotransport in a two-dimensional electron gas in quantizing magnetic fields and intense terahertz laser fields, *W. Xu, R.A. Lewis, P.M. Koenraad, C.J.G.M. Langerak,* **J. Phys. – Cond. Mat. 16 (2004) 89.**

We present a combined experimental and theoretical study of interactions between two-dimensional electron gases (2DEGs) and terahertz (THz) free-electron lasers in the presence of quantizing magnetic fields. It is found both experimentally and theoretically that when an intense THz field and a quantizing magnetic field are applied simultaneously to a GaAs-based 2DEG in the Faraday geometry, a strong cyclotron resonance (CR) effect on top of the magnetophonon resonances can be observed by transport measurements at relatively high temperatures. With increasing radiation intensity and/or decreasing temperature, the peaks of the CR are broadened and split due to magnetophoton-phonon scattering.

Cu and nano-SiC doped MgB_2 thick films on Ni substrates processed using a very short-time in situ reaction, *Q.W. Yao, X.L. Wang, J. Horvat, S.X. Dou,* Physica C 402 (2004) 38.

Pure and doped MgB_2 thick films were fabricated on Ni substrates by applying a coating mixture of powders of elemental magnesium and boron with varying amounts of elemental Cu and nano-SiC powders, followed by a high pressure press, and sintering at 840 or 900 ºC for just a few minutes, and then quenching in liquid nitrogen. For films sintered at 900 ºC, critical current densities $J_c$were achieved as high as 1.4 x 10^6/cm^2at 20 K and 2.3 x 10^5A/cm^2at 20 K and 2 T for the pure and SiC added films. Films doped with 5 wt.% of Cu powders were observed to have better adherence to the Ni substrate without degradation in T_c and J_c was found to be slightly decreased, but still remained as high as 7 x 10^5 A/cm^2 at 20 K in zero field. It was observed that J_c and the irreversibility field increase with an increasing sintering temperature up to 900 ºC. Furthermore, nano-SiC addition has significantly improved the irreversibility field compared to undoped MgB_2 films.

Fabrication, microstructure and critical current density of pure and Cu doped MgB_2 thick films on Cu, Ni and stainless steel substrates by short-time in-situ reaction, *Q.W. Yao, X.L. Wang, S. Soltanian, A.H. Li, J. Horvat, S.X. Dou,* Ceramics International 30 (2004) 1603.

Pure and Cu doped MgB_2 thick films have been prepared on Cu, Ni and stainless steel substrates using a short-time sintering method. Results showed that single MgB_2 phase films can be easily formed in a short period of time (3 min) at temperatures above 700 degreesC. Un-doped MgB_2 films were found to be loosely attached to the Ni and stainless steel substrates. However, the MgB_2 with Cu powder addition adhered well to the substrates without serious degradation of T_c and flux pinning. The J_c increased one order of magnitude and irreversibility field determined from M-H loops also increased when sintering temperature increased from 745 to 900 ºC. J_c values in the range of 1-9 x 10(5) A/cm^2 at 15 K have been achieved for both doped and un-doped films sintered at 900 ºC for 3 min.

Strong pinning and high critical current density in carbon nanotube doped MgB_2, *W.K. Yeoh, J. Horvat, S.X. Dou, V. Keast,* Supercond. Sci. Technol. 17 (2004) S572.

Polycrystalline samples of multi-walled carbon nanotube (CNT) doped MgB_2 superconductors were synthesized by solid state reaction. The carbon nanotube substitution results in a small decrease in lattice parameter and T_c as compared to ordinary carbon substitution. Enhancement of H_{c2} and H_{irr} shown by CNT doped samples show that the effect of CNT doping is two-fold. For sintering temperatures higher than 900ºC, the CNTs partially decompose, allowing substitution of boron for carbon. This results in an increased H_{c2}. However, remains of the CNTs are incorporated into the crystal matrix of MgB_2, and they act as pinning centres. For lower sintering temperatures, there is little substitution of boron for carbon, and CNTs are incorporated into the crystal matrix as a whole, acting as pinning centres without affecting H_{c2}.

Optical losses in dielectric apertured terahertz VCSEL, *Y.H. Yu, S.C. Lee, D.C. Kim, C. Zhang, P. Harrison,* Optics and Laser Technology 36 (2004) 575.

The resonant wavelength and mode radius of the fundamental modes supported by an oxide apertured terahertz vertical surface emitting laser are determined from Gaussian resonant theory and scalar variational method. The reflectivity of the Bragg mirror is calculated for the lowest modes and it decreases as the aperture size decreases. The aperture radius, thickness, and axial position in the cavity are shown to be an important factor for high efficiency vertical cavity surface emitting lasers and single mode operation. When the aperture size is much larger than the emitting wavelength, the optical loss is negligible. However, the optical loss strongly depends on the aperture size and thickness when aperture size is similar to or smaller than emitting wavelength.

Calculation of the nonlinear free-carrier absorption of terahertz radiation in semiconductor heterostructures*, C. Zhang, J.C. Cao,* Phys. Rev. B 7019 (2004) 3311.

Nonlinear absorption of terahertz waves by electrons in a semiconductor heterostructure is calculated. We solve the quantum transport equation for electrons strongly coupled to terahertz photons. The electrical field of the laser radiation is included exactly, and the electron-impurity interaction is included up to the second order. It is found that Joule heating of the electronic system due to impurity scattering decreases rapidly due to the strong electron-photon interaction. Our result is the dynamic equivalence of electron localization in a strong field. In the limit of weak radiation field, the current is linear in the field strength.

Nonlinear free-carrier absorption in semiconductor heterostructures in terahertz regime, *C. Zhang, S.H. Pilehrood,* SPIE 5277 (2004) 284.

Absorption of electromagnetic waves in electronic systems coupled to intense terahertz waves is calculated. We formulate a theoretical framework suitable for calculating the frequency-dependent electrical current under an intense THz radiation. This first principle method is based on the time-evolution of electron density

matrix and it includes electron-photon coupling to all orders. We first obtained the time-dependent electronic states as a function of terahertz field and frequency. The electron-impurity scattering is included to the second order. The absorption of electromagnetic waves of a probing field via various electron-terahertz-photon coupling is then obtained in terms of frequency-dependent dielectric functions.

Comparative study of in situ and ex situ MgB_2 films prepared by pulsed laser deposition, *Y. Zhao, M. Ionescu, J. Horvat, S.X. Dou,* Supercond. Sci. Technol. 17 (2004) S482.

Two types of MgB_2 film were prepared by pulsed laser deposition with *in situ* and *ex situ* annealing processes, respectively. Significant differences in properties between the two types of films were examined. The *ex situ* annealed MgB_2 film has a T_c of 38.1 K, while the *in situ* film has a suppressed T_c of 34.5 K. The resistivity at 40 K for the in situ film is larger than that of the *ex situ* film by a factor of 6. The residual resistivity ratios are 1.1 and 2.1 for the *in situ* and *ex situ* films, respectively. A large slope of the H_{c2}-T curve was achieved in the *in situ* annealed film. The J_c (H) curves of the *in situ* film show a much weaker field dependence than those of the *ex situ* film, attributable to stronger flux pinning in the *in situ* film. The small-grain (< 100 nm) feature and high oxygen level detected in the *in situ* annealed MgB_2 film may be decisive for the significant improvement of $J_c$and H_{c2}.

Si addition in in situ annealed MgB_2 thin films by pulsed laser deposition, *Y. Zhao, M. Ionescu, J. Horvat, A.H. Li, S.X. Dou,* Supercond. Sci. Technol. 17 (2004) 1247.
Various amounts of Si up to a level of 18 wt% were added into MgB_2 thin films fabricated by pulsed laser deposition (PLD). Si was introduced into the PLD MgB_2 films by sequential ablation of a stoichiometric MgB_2 target and a Si target. The precursor films were annealed *in situ* at 685ºC for 1 min. Up to an Si level of ~11 wt%, the superconducting transition temperature (T_c) of the film does not change significantly, as compared to the undoped film. The magnetic critical current density (J_c) of the film at 5 K was increased by 50% with ~3.5 wt% Si addition, as compared to the undoped film. The slope of H_{irr} (T) and H_{c2} (T) curves of the 3.5 wt% Si added MgB_2 film is slightly higher than that for the undoped film.

In-situ fabrication of nanostructured cobalt oxide powders by spray pyrolysis technique, *Z.W. Zhao, K. Konstantinov, H.K. Liu, S.X. Dou,* J. Nanoscience and Nanotechnology 4 (2004) 861.

Nano-crystalline Co_3O_4 and CoO powders have been prepared by a spray pyrolysis approach. The effects of the reaction temperature and initial salts on the crystallinity and phase composition have been studied. Based on the TEM and XRD results, the crystal sizes were in the range of 1-10 nm. SEM and TEM observations also reveal that the nano-powders easily create micron-scale spherical agglomerates. The Co_3O_4 powders obtained by spraying nitrate solution at 500 ºC show high specific surface area, which according to the BET method is 82.37 m^2/g. The time/temperature phase diagram of cobalt oxides developed from XRD and DTA/TGA analyses shows the existence of a CoO phase at low and high temperature ranges when some specific preparation conditions are applied.

Effects of precursor powders and sintering processes on the superconducting properties of MgB_2, *S.H. Zhou, A.V. Pan, J. Horvat, M.J. Qin, H.K. Liu,* Supercond. Sci. Technol. 17 (2004) S528.

Different precursor powders and procedures were used to fabricate MgB_2 superconductor. It was found that the purity of the B powder had strong effects on the T_c and J_c of MgB_2. The J_c of the sample made from 90% B powder decreased 40 times at 3 T and 20 K compared with the 99% B powder samples. The impurity phases might be the reason for the suppression of the T_c and the J_c. Variation of the Mg:B ratio also influenced the MgB_2 properties. J_c decreased with fluctuations from the normal rate (Mg:B = 1:2). It was found that the effects of the oxidization of the Mg powder on J_c were not strong when the Mg powder was only slightly oxidized. However, when the Mg powder was severely oxidized, the J_c decreased significantly. A two-step sintering process was adopted to make MgB_2. In this process, the first sintering stage was at a lower temperature. It was found that this pre-sintering did not have a good effect on the properties, despite

the fact that the mass density was improved. The phase composition and microstructure were analysed to explain the different effects.

Effects of Si and C Doping on the Superconducting Properties of MgB_2, *S.H. Zhou, A.V. Pan, M.J. Qin, X.L. Wang, H.K. Liu, S.X. Dou,* in Advances in Cryogenic Engineering: Transactions of the International Cryogenic Materials Conference - ICMC, Vol. 50. Edited by U. Balachandran. AIP Conf. Proc. 711 (2004) 554.

C and Si powders of different sizes were doped into MgB_2 separately or together. Samples were made by a solid-state reaction method. It was found that the C doping had a strong negative effect on critical temperature (T_c) while the Si doping did not significantly depress T_c. All of these doping materials increased J_c at higher fields when the doping particles were of nanometer sizes. At 20 K and 4 T, J_c of the sample doped with nano-Si achieved $10^4 A/cm^2$, which is 2 orders of magnitude higher than that of coarse Si doped MgB_2. J_c of the sample doped with nano-carbon is one order of magnitude higher than for the sample doped with coarse carbon particles.

Current & Ongoing Research Projects

Funded ARC Projects in 2004 round at ISEM

ARC Centre of Excellence

Nano-materials for energy storage

Years funded:	2004	2005	2006	2007
Amount funded:	$198,174	$198,174	$198,174	$198,174
Chief Investigator:	H.K.Liu			
Research Fellow:	G.X. Wang			
Postgrad Students:	S.H. Ng, M. Park			

ARC Large/Discovery Grants Scheme

First Principles for Development of High Temperature Superconducting Wires

Years Funded:	2002	2003	2004	2005	2006
	$222,295	$233,899	$217,899	$203,899	$209,899
Total Funding:	$1,087.891				
Project ID:	DP0211240				
Chief Investigator:	SX Dou, J Horvat				
Assoc. Investigator:	H Weber, E Collings, J Habermeier				
Postgrad Student:	S. Keshavarzi, M. Roussel				

Significant advances in research of high temperature superconductors (HTS) have been made in the past decade. However, the full commercialisation of HTS devices has not yet been achieved because the levels of electrical performance remain just below those required for technical and commercial success. In order to secure the future of HTS it will be essential to increase the critical current density, reduce the AC losses and lower the cost. The objective of the proposed cluster of projects is to provide new insights into fundamental HTS materials properties such as critical current density, flux pinning, flux dynamics and AC losses by focussing on the complex interplay between physics, fabrication and materials issues. The knowledge gained will make possible improvements in the development of HTS conductors.

Enhancement and elucidation of flux pinning in doped Bi-Sr-Ca-Cu-O high temperature superconducting single crystals

Funded:	2002	2003	2004
Amount Funded:	$61,184	$62,967	$62,967
Total Funding:	**$187,118**		
Project ID:	DP0211328		
Chief Investigator:	X.L. Wang		
APD:	X.L. Wang		

The proposed project aims to study the effects of elevated doping on the intrinsic electromagnetic properties of Bi-Sr-Ca-Cu-O high temperature superconducting (HTS) single crystals grown by two-dimensional and spiral-growth mechanisms with a particular focus on structure, conductivity and thermal neutron irradiation. Studies of the relationship between microstructures, anisotropy and flux pinning will lead to a better understanding of the pinning behaviour of Bi-based HTSC. The outcome will be better methods for introducing suitable pinning centres into Bi-based high temperature superconductors.

Analysis, simulation, fabrication and characterization of reliable, robust and scalable compact cooling elements based on semiconductor nanostructures

Funded:	2003	2004	2005
Amount Funded:	$75,000	$80,000	$40,000
Total Funding:	**$195,000**		
Project ID:	DP0343516		
Chief Investigator:	C. Zhang, R.A. Lewis		
Postgraduate students:	B.C. Lough, Z. Dou, S.P. Lee		

Project Summary: Modern electronic, microelectronic and optoelectronic devices generally work better when they are cooler. We aim to develop a semiconductor nanostructure cooling element which directly integrates into existing devices. The solid-state cooling element will be reliable, robust, scalable and operate in any orientation. The basis of operation is thermionic emission - electrons are the working fluid.

Our project combines (1) analysis and simulation, (2) fabrication of nanostructures and (3) experimental test-benching using optical and electrical methods. The outcome of this research has the potential to revolutionize cooling of modern electronic and photonic systems, from computer motherboards to mobile phones.

Fabrication, Charge and Spin Ordering, Magnetoresistance, and polaron effects in nano-size and single crystals of novel transition metal perovskite oxide

Funded:	2003	2004	2005
Amount Funded:	$90,000	$77,000	$78,000
Total Funding:	**$245,000**		
Project ID:	DP0345012		
Chief Investigator:	X.L. Wang, M. Ionescu, Z.X. Cheng		
Partner Investigator:	Dr.M James, Prof. R.S. Liu, Prof. W. Lang		
Postgraduate students:	M. Farhoudi, G. Peleckis		

The aim of the project is to synthesize a systematic series of novel colossal magnetoresistance manganese, cobalt and iron based transition metal perovskite oxides in the forms of nano-structures, nano-structured composites and single crystals using advanced nano-technology and crystal growth techniques. Extensive fundamental studies on magnetoresistance, spin and change ordering, and nano-scale behaviours will be carried out by neutron diffraction, synchrotron radiation, transport and magnetic measurements over a wide temperature range and magnetic fields. The outcomes of this project are likely to lead to a better understanding of the colossal magnetoresistance mechanisms, the discovery of fascinating new physical phenomena and suitable magnetoresistance materials for superior magnetic recording, sensing and switch devices.

Control of Nano-Structure for Enhancing the Performance of Magnesium Diboride Superconductor by Chemical Doping

Funded:	2004	2005	2006
Amount Funded:	$100,000	$100,000	$105,000
Total Funding:	**$305,000**		
Project ID:	DP0449629		
Chief Investigator:	S.X. Dou, M.J. Qin,		
Partner Investigator:	D.C. Larbalestier, R.L. Flukiger, L.F. Cohen		
Postgraduate students:	W.K. Yeoh, O. Shcherbakova, Y. Zhang		

Superconductor technology will play a significant role in a wide range of industry sectors and environments in the twenty first century. Widespread applications now depend significantly on cost-effective resolution of fundamental materials and fabrication issues. The aim of the proposed program is to bring together international experts from four leading groups to tailor the microstructure at nanoscale to improve flux pinning and the critical current density of the newly discovered magnesium diboride superconductors

through readily available chemical doping. The expected outcome is the capability to produce a new generation of superconductors having high performance at low cost.

Hydrogen storage materials for energy conversion applications

Funded:	2004	2005	2006
Amount Funded:	$85,000	$85,000	$85,000
Total Funding:	**$255,000**		
Project ID:	DP0449660		
Chief Investigator:	H.K. Liu, Z.P. Guo		
Partner Investigator:	J. Lee, A. Zuettel, P.H. Notten		
APD:	Mrs ZP Guo		
Postgraduate students:	Z.G. Huang		

For a clean environment, the ideal synthetic fuel is hydrogen because it is lightweight, highly abundant and its oxidation product (water) is environmentally benign. However, the effective storage of hydrogen remains a scientific challenge. This project aims to develop innovative materials with high hydrogen storage capacity and long cycle life, including new composite hydrides, catalysed metal hydrides and various nanotubes. The expected outcome is the achievement of high reversible hydrogen storage capacity to meet all the demands required for energy conversion applications, in particular, for hydrogen storage/fuel-cell vehicular applications.

Development of high-temperature superconducting coated conductors by pulsed-laser deposition technique for future long-length applications

Funded:	2004	2005	2006
Amount Funded:	$70,000	$70,000	$70,000
Total Funding:	**$210,000**		
Project ID:	DP0451267		
Chief Investigator:	A.V. Pan, M. Ionescu		
APD:	A.V. Pan		

The aim of the project is to develop a novel technology for manufacturing flexible coated conductors with the help of a pulsed laser deposition technique, in order to enhance the current-carrying ability of high-temperature superconducting coatings (including multi-layered coatings) for future long-length high power applications. To achieve desirable electromagnetic properties governed by the nano-structures of the coatings, a well-balanced combination of world-class "global" and "local" electromagnetic property measurements with advanced structural characterisations is suggested. It is expected that a controlled network of nano-scale pinning centres will allow the development of high performance coated conductors.

Non-linear dynamics in electronic systems and devices under intense terahertz radiation

Funded:	2004	2005	2006
Amount Funded:	$120,000	$140,000	$170,000
Total Funding:	**$430,000**		
Project ID:	DP0452713		
Chief Investigator:	C. Zhang R.A. Lewis X. Zhang R.E. Vickers		

Non-linear interactions allow for a detailed and intricate probing of materials. Sufficiently high-power light directed at a subject can yield spectroscopic data about multiple material parameters, providing a unique diagnostic tool for many applications. We propose to study the non-linear dynamic properties of electronic systems and devices under various external conditions. A thorough understanding of non-linear properties will accelerate development of new optoelectronic device in the terahertz frequency regime. Examples of these devices are oscillators and sensors.

ARC Research Fellowships

Strategic Partnerships with Industry - (SPIRT) Scheme - Linkage Projects & Linkage APAI

Developing New Cathode Materials for Lithium-ion Batteries Using Australian Mineral Resources

Years funded:	2002	2003	2004
Amount funded:	$83,000	$84,000	$84,000
Total funding:	$251,000		
Project ID:	LP0214179		
Chief Investigator:	Prof Shi Xue Dou, Dr G Wang		
Partner Investigators:	Prof J Lee		
Research Fellow:	K. Konstantinov		
APA(I) Award(s):	S. Bewlay		
Industry Partner(s):	Sons of Gwalia Ltd. OM Group		
Postgraduate students:	Y. Chen		

This project will bring together expertise in electrochmistry, materials science and structure characterisation to conduct collaborative research with Australian industry partners, Queensland Nickel Technology Pty Ltd and Sons of Gwalia Ltd. The aims of this project will be to investigate a series of cathode materials for use in lithium-ion batteries. The significance of this research is that the technology for preparing a series of new electrode materials for lithium-ion batteries will be developed by taking advantage of abundant Australian minerals resourecs. The expected outcomes will be to identify several new cathode materials with high energy density, long cycle life, low toxity and low cost.

Fabrication and Characterisation of Magnesium Diboride Superconducting Wires

Years funded:	2002	2003	2004
Amount funded:	$110,000	$100,000	$100,000
Total funding:	$310,000		
Project ID:	LP0219629		
Chief Investigator:	Prof Shi Xue Dou, Dr XL Wang, Dr M Ionescu		
Partner Investigators:	Dr MD Sumption		
APA(I) Award(s):	Yue Zhao, S. Soltanian		
Industry Partner(s):	Alphatech International, The Hyper Tech Research Inc.		

The newly discovered superconductivity at 40K in magnesium diboride ($_{MgB2}$) opens a technical window to a range of electric power applications, previously thought accessible only with high temperature superconductors. The aim of the proposed project is to investigate the fabricability and properties of $_{MgB2}$ superconducting wires using a number of processing techniques established in previous low temperature and high temperature superconductors. The expected outcome is to have a $_{MgB2}$ conductor that has a higher performance in a field than niobium-titanium (NbTi) alloy, a higher operating temperature (up to 20K), but at a cost less than currently commercial NbTi wire.

Investigation of Nano-materials for use in Lithium Rechargeable Batteries

Years funded:	2002	2003	2004
Amount funded:	$67,000	$60,000	$60,000
Total funding:	**$187,000**		
Project ID:	LP0219309		
Chief Investigator:	Prof Hua Kun Liu, Dr S Zhong		
Partner Investigators:	A/Prof J Ahn		
APA(I) Award(s):	L. Yuan		
Industry Partner(s):	Sons of Gwalia Ltd, OM Group, Lexel Battery Ltd		
Postgraduate student:	Z.W. Zhao, M. Lindsay		

Lithium ion batteries are emerging as a new generation of rechargeable batteries for power sources of portable electronics. The aim of this project is to explore potential applications of novel nano-materials such as intermetallic alloys, transition-metal oxides, and carbon nanotubes as anode materials in lithium-ion rechargeable batteries. Significance and expected outcomes will be the development of alternative anode materials with improved performance in energy capacity and cycle life over existing anode materials. This could open opportunities for Australian mineral companies to take advantage of the developments to produce value-added new products.

Fabrication of Magnesium Diboride (MgB_2) thick films

Years funded:	2002	2003	2004
Amount funded:	$22,545	$22,545	$22,545
Total funding:	**$67,635**		
Project ID:	LP0228370		
Chief Investigator:	Dr X L Wang		
APA(I) Award(s):	Q.W. Yao		
Industry Partner(s):	SFC Enterprises Pty Ltd		

The recent discovery of superconductivity at 39 K in $_{MgB2}$ has stimulated considerable interest in terms of both fundamental research and applications. The purpose of the proposed project is to conduct fundamental studies on the synthesis, structures and microstructures, and physical properties of doped and undoped $_{MgB2}$ thick films. The ultimate goal of this study is to fabricate high quality $_{MgB2}$ thick films on different substrates and to gain a better understanding of their various properties with a view to device application.

Lithium/Sulfur rechargeable battery for power applications

Years funded:	2004	2005	2006
Amount funded:	$75,000	$75,000	$75,000
Total funding:	**$225,000**		
Project ID:	LP0453698		
Chief Investigator:	H.K. Liu, J. Wang, G. Wang		
APD Award(s):	J. Wang		
Industry Partner(s):	Guangzhuo Delong Energy Technology		

The Lithium/Sulphur battery system is very promising for large-scale power applications as it has the highest energy density and lowest cost among various types of rechargeable batteries. However, the degradation of the capacity and short cycle life of Li/S battery have been problematic for commercial development. The aim of this project is to study the mechanisms of capacity fading and to develop effective means such as use of carbon nanotubes and nanosize composite absorbents to improve the cycle life of Li/S batteries. The expected outcomes are the development of sulphur-containing cathode materials and polymer electrolytes, enabling electric vehicles to be a technically competitive and environmentally superior transportation option.

Large-scale rechargeable lithium battery for power storage and electric vehicle applications

Years funded:	2004	2005	2006
Amount funded:	$110,000	$110,000	$110,000
Total funding:	**$330,000**		
Project ID:	LP0453766		
Chief Investigator:	G. Wang, H.K Liu, K. Konstantinov, J. Ahn, B. Ammundsen		
APA(I) Award(s):	J. Yao		
Industry Partner(s):	Pacific Lithium New Zealand Limited, Sopo Battery Energy Co., Ltd		
Postgraduate student:	S. Needham		

This project aims to develop large-scale rechargeable lithium batteries for power storage and electric vehicles. In order to achieve this target, the related cathode materials, anode materials and electrolyte systems will be developed. The design of battery modules and assembly of prototype lithium ion batteries will be performed. The success of the research will encourage the production of electrode materials and manufacture of rechargeable lithium batteries in Australia. The utilisation of advanced rechargeable lithium batteries in electric vehicles will provide sustainable energy for transportation and greatly reduce green-house emissions in Australian urban areas.

Enhancing the Understanding and Performance of Passivating TiO2 Coatings for Photovoltaic Devices

Years funded:	2004	2005	2006	2007
Amount funded:	$75,000	$127,500	$105,000	$52,500
Total funding:	**$360,000**			
Project ID:	LP0455328			
Chief Investigator:	BS Richards, M Ionescu			
Partner Investigators:	KR McIntosh, KM Provancha, R Swanson			
APA(I) Award(s):	1			
APDI :	BS Richards			
Industry Partner(s):	Kieth McIntosh Consulting, SierraTherm Production Furnaces, Inc. SunPower Corporation			

Titanium dioxide (TiO2) has been widely used as an antireflection coating in the silicon (Si) photovoltaics industry as it exhibits excellent optical properties and low deposition cost. However, recently manufacturers have been turning to alternatives such as hydrogenated silicon nitride coatings that exhibit greatly improved electronic properties, but cost 4 - 10 times more to deposit.

This project seeks to understand the fundamental limitations behind the poor surface passivation afforded by TiO2 to a Si wafer, and subsequently develop a passivating TiO2 coating that can reduce the cost of electricity generated by Si solar cells.

ARC linkage-infrastructure

T-ray factory: a new Australian source of strong, pulsed, broadband, terahertz radiation

Years funded:	2004
Amount funded:	$113,190
Project ID:	LE0453974
Chief Investigator:	R.A. Lewis, C. Zhang, H.H. Tan, A.M. Sanagavarapu, A.R. Hamilton
Partner Institution(s):	University of Wollongong The Australian National University University of Technology, Sydney The University of New South Wales

Australian scientists and engineers require immediate access to frontier T-ray (terahertz radiation) technology to solve pressing current problems in semiconductor nanostructures and emerging problems in fields as diverse as biophysics and national security. Recent innovations now make practical the production of bursts of terahertz radiation by applying ultrafast optical pulses to photoconductive or electro-optic media, facilitating unparalleled time-resolved spectroscopy and imaging. The state-of-the-art equipment to be purchased and installed at Wollongong will enhance the existing excellent terahertz infrastructure (unique spectrometers, optically-pumped molecular laser) and efficiently service researchers in the dynamic Sydney (UTS, UNSW) - Wollongong (UoW) - Canberra (ANU) corridor

Linkage International Awards

Investigation of a series of metallic substrate materials suitable for developing long Y-Ba-Cu-O superconductors

Years funded:	2002	2003	2004
Amount funded:	$19,396	$17,596	$17,596
Total funding:	$54,588		
Project ID:	LX0211084		
Chief Investigator:	Prof Hua Kun Liu - University of Wollongong		
	Prof D Shi - University of Cincinnati		
Postgraduate students:	A.H. Li		

Researchers from Institute for Superconducting and Electronic Materials, the University of Wollongong (UoW) & the Dept. Mat. Sci & Eng., University of Cincinnati (UC) in USA will build strong collaborations through joint research on a series of metallic substrate materials. Significance: The research work will contribute to the development of the second generation of high temperature superconducting wire technology. Expected outcomes: strengthen international research experience for junior researchers and develop new collaborations between senior researchers from UoW in Australia and UC in USA.

Simulation and characterisation of opto-thermionic cooling devices

Years funded:	2003	2004	2005
Amount funded:	$15,700	$18,700	$18,700
Total funding:	$53,100		
Project ID:	LX0348004		
Chief Investigator:	A/Professor C. Zhang, A/Professor R.A. Lewis		
	CI Prof KA Chao Lund University, Sweden		

The aim of the project is to study and develop a solid state cooling device by combining two mechanisms, thermionic emission and optical recombination. The first stage of the research is to develop theoretical models and numerical methods which will allow us to obtain an optimal condition of power and efficiency. Under this ARC LX grant, mutual visits for the Australian CIs and the international OI have been arranged.

In August 2003, the international OI, K A Chao visited our group in Wollongong. During his visit, we discussed the theoretical and numerical part of the project and analysized different structures with different material parameters. A model for limiting the heat back flow in an operational device was investigated in detail and we are now performing computations on the energy flow in various devices. The Australian CI, C Zhang is scheduled to visit Lund University in April 2004. Other visits and collaborative activities have also been planned for the second half of 2004 and will be reported in the next progress report.

Magneto-optical imaging of super-current flow in superconducting tapes and wires

Years funded:	2004	2005	2006	
Amount funded:	$14,140	$10,960	$11,160	
Total funding:	$36,260			
Project ID:	**LX0453582**			
Chief Investigator:	1	CI	Prof SX Dou	University of Wollongong
	2	CI	Dr AV Pan	University of Wollongong
	3	OI	Prof TH Johansen	University of Oslo
Collaborative Countries:	Norway			

This project is aimed at establishing the connections between local and global superconducting current-carrying abilities in magnesium diboride and high temperature superconducting tapes and wires. Local high-resolution magneto-optical imaging combined with transport current techniques will be employed. Super-current stream-lines and critical current density distributions will be quantitatively obtained from local magnetic flux behaviour. Pinpointing the connections is expected not only to promote production technology, but also to elucidate factors influencing the current-carrying ability in the tapes and wires.

Systemic Infrastructure Initiative Grants
Department of Education, Training and Youth Affairs

Nanofabrication facilities for processing of novel multilayer materials

Years funded:	2004
Amount funded:	$487,500
Institutions contribution:	$192,500
Total funding:	$680,000
Chief Investigators:	Prof SX Dou, M. Ionescu, X.L. Wang, H.K. Liu, G.X. Wang T. Silver, R.A. Lewis – University of Wollongong A/Prof S. Ringer – University of Sydney Prof GQM Lu – University of Queensland Prof EM Goldys – Macquaire University Prof M. M Wilson – UTS A/Prof DN Jamieson, University of Melbourne A/Prof J. Mazierska - James Cook University Dr. J. Low - Curtin University of Technology Dr. R. Ramer – UNSW Prof. G. Smith – UTS Prof. M. Skyllas-Kazacos - UNSW

The proposal seeks to obtain nanofabrication facilities including a modified metallorganic chemical deposition (MOCVD), electron beam evaporation (EBE) and lithography facilities for the processing of novel multilayer materials and devices. These facilities will significantly enhance the national capacity in nanofabrication for a wide range of novel materials and devices.

ARC Small & Near Miss Grants

Current transport in MgBZ superconductor

Amount funded: **Chief Investigator:**

$10,350 J. Horvat

Diluted Magnetic Semiconductor (DMS) materials for Spintronics

Amount funded: **Chief Investigator:**

$8,000 M J Qin

An investigation of transition metal diboride nanotubes for hydrogen and lithium storage

Amount funded: **Chief Investigator:**

$9,000 G X Wang

Novel lithium phosphor-olivines for lithium storage electrodes

Amount funded: **Chief Investigator:**

$10,000 G X Wang

University of Wollongong

University Research Council, ISEM Performance Indicator & Management

Year funded: 2003 **Amount funded:** $125,000

2004 International Cryogenic Materials Conference (ICMC) Topical Workshop, 10th-16th February 2004, Wollongong, Australia

Effect of progressive substitution of La^{3+} by Bi^{3+} on the structure, magnetic and transport properties of $La_{0.67}Sr_{0.33}MnO_3$, *Z.X. Cheng, X.L. Wang.*

Polycrystalline $La_{0.67-x}Bi_xSr_{0.33}MnO_3$ (x=0.1, 0.2, 0.3 and 0.67) was prepared by solid state reaction. The effects of La substitution by Bi with typical polarized lone pair electron character on structure, magnetic and transport properties are presented. Results show that these properties anre dramatically affected by the polarized lone pair $6s^2$ electrons though Bi^{3+} and La^{3+} have nearly the same radii. Structure refinement by the Rietveld method shows that the substitution changes the structure from the rhombohedral to the tetratogonal. At the same time, the angle of the Mn-O-Mn chain decreases, which weakens the double exchange between adjacent Mn^{3+} and Mn^{4+} ions via the bridging O. As a consequence, the ferromagnetic coupling temperature decreases from 370 K down to 330 K as x increases from 0 to 0.3, and down to 270 K when La is totally substituted by Bi. With increasing substitution level, μ_{eff} decreases from the near theory value of 4.2 μ_B down to 2.5 μ_B for x= 0.3 and 0.08 μ_B for the fully substituted sample. The sample with x=0.67 shows a very weak ferromagnetic property. However, μ_{eff} should not change as much as this if only the unchanged Mn^{3+}/Mn^{4+} ratio were considered in the $La_{0.67-x}Bi_xSr_{0.33}MnO_3$ system. The decrease of μ_B can only be explained by the enhanced antiferromagnetic coupling that occurs as the ferromagnetic coupling is weakened by the Bi. With increasing Bi content, the resistivity increases, and the temperature of the semiconductor to metal transition rises. Eventually the totally substituted sample becomes an insulator.

Enhancement of critical current density in Cu sheathed MgB_2 wires and tapes by nano-Si dopeing and short-time in-situ reaction, *M. Delfany, X.L. Wang, I. Kusevic, E. Babic, O. Husnjak, M.J. Qin, S. Soltanian, S.X. Dou.*

MgB_2/Cu wires and tapes have been prepared using the powder-in-tube and reaction in-situ techniques. The effects of sintering conditions and 5 wt% of nano-Si doping on the phase formation, superconductivity and critical current density were investigated. Samples were characterized by using XRD, SEM, TEM, transport, and magnetic measurements. Results showed that long sintering at high sintering temperatures led to severe reaction between the magnesium and Cu, forming a thicker layer of $MgCu_2$ at the interface and causing magnesium deficiency in the superconducting core and deterioration of the superconducting properties. It was found that the thickness of the reacted layer could be reduced from 50–100 μm to less than 10 μm by lowering sintering temperatures and shortening sintering times. The J_c values were considerably improved. In addition, nano-Si powders reacted with the MgB_2 during heat treatment and formed Mg_2Si as an impurity phase. TEM examination confirms the presence of nanometer size impurities uniformly distributed in the superconducting matrix. The impurity increases the resistivity values by a factor of 1.35 at both room temperature and 40 K in the sample with 5 wt% Si doping compared to the undoped sample. An enhancement in the J_c field dependence accompanied by a little decrease in the T_c of less than 2 K was found by both transport and magnetic measurements due to the nano-particle Si doping. The J_c values are improved by a factor of 5 at 5 T and 5 K and by more than one order of magnitude at 3.5 T and 20 K in the tape samples doped with 5 wt% nano-sized Si compared to the undoped sample.

Enhancement of H_{c2} and flux pinning in MgB_2 superconductor by nano-particle doping, *S.X. Dou.*

Pure MgB_2 has very low H_{c2} which sets a limit on $J_c(H)$ performance in most applications. Extensive studies on the improvement of $J_c(H)$ showed that there were two distinguishable but closely related mechanisms that control the performance of $J_c(H)$ in these samples: increase of H_{c2} and improvement of flux pinning. Because of the large coherence length of MgB_2, chemical doping has been found to be effective to improve flux pinning. However, most of the dopants used so far are only effective at low temperatures. Nano SiC particle doping, on the other hand, introduced many nano-scale precipitates and disorder at B and Mg sites,

leading to a significant enhancement of both H_{c2} and $J_c(H)$ over a wide range of temperatures, with only a minor effect on T_c as a consequence of the unique two-gap superconductivity of MgB_2. EELS and TEM analysis revealed impurity phases: Mg_2Si, MgO, MgB_4, BO_x, $Si_xB_yO_z$, and BC at a scale below 10nm and an extensive domain structure of 2-4nm domains in the doped sample, which serve as strong pinning centers. J_c for the 10% nano-SiC doped sample increased by more than an order of magnitude at high fields and all temperatures compared to the undoped samples. A record high $H_{c2}(0)$ value of 37T for bulkMgB_2 was achieved by transport measurements for the 10% nano-SiC doped sample. The strong up-turn of $H_{cs}(T)$ at low temperatures indicates an impurity scattering on the Mg sites. The unique feature of nano-SiC doping is the enhancement of H_{c2} and $J_c(H)$ by impurity scanning and collective pinning, respectively.

Improvement of field dependence of J_c of MgB_2/Fe wires by interaction of superconducting core with iron sheath, *J. Horvat, S. Soltanian, S.X. Dou.*

The field dependence of transport J_c for MgB_2/Fe wires is strongly improved by the iron sheath. The improvement goes far beyond the effect of simple magnetic shielding by iron. While the magnetic properties of iron are almost unchanged with temperature between 10 and 30 K, the field dependence of J_c undergoes a major change. For the field perpendicular to the wire, there is an initial decrease and then a plateau in the the field dependence of J_c for T > 30 K, which gradually grows into a peak in $J_c(H)$ at lower temperatures. The field of the peak is strongly temperature dependent, ranging from less than 1 T at 30 K, to almost 4 T at 10 K. For the field parallel to the wire, the peak in $J_c(H)$ appears at T > 30 K and the plateau appears at lower temperatures. However, for the parallel field, there is no initial decrease of J_c in small fields. The field of the peak and the field of the end of the plateau depend on the temperature in a similar way to the field of the peak for the perpendicular field. At the same time, the iron sheath shields only 0.2-0.3 T of the external field, which is independent of temperature in this temperature range. Therefore, the appearance of the plateau and the peak effect in $J_c(H)$ should be explained in terms of the interaction between the ferromagnetic sheath and the superconductor.

The influence of vortex pinning on superconducting screening on different length-scales for bulk MgB_2 superconductor, *J. Horvat, S. Soltanian, A.V. Pan, X.L. Wang, S.X. Dou.*

Superconducting screening in bulk MgB_2 occurs at different length scales, and each of the screenings gives a different contribution to the irreversible moment Δm. This is why erroneous values are obtained for J_c and its field dependence when calculating J_c from Δm by simply applying the critical state model. The field dependence of the screening current on each of the length scales is a different stretched exponential function. This leads to a dominant contribution from each of the screenings to Δm in a particular range of field. The value and field dependence of the thus obtained J_c artificially depends on the sample size. The influence of the change of the vortex pinning on each of the stretched exponential functions will be presented, together with the implications for accuracy of magnetically measured J_c.

Enhancement of critical current density in $Yba_2Cu_3O_{7-\delta}$ thin films grown by PLD on YSZ (100) surface modified with Ag nano-dots, *M. Ionescu, A.H. Li, Y. Zhao, H.K. Liu, A. Crisan*

Y123 thin films were grown by pulsed laser deposition (PLD) on YSZ (100) substrate. Prior to the film deposition, a discontinuous layer of Ag was deposited on the substrate, using also PLD, Atomic force microscopy (AFM) investigation of the interface Ag layer showed that its morphology consisted of self-assembled islands of nanometer size, randomly distributed on the surface of the substrate. The Y123 superconducting films grown on such a substrate were characterized by AFM, X-ray diffraction (XRD), secondary electron microscopy (SEM) and DC magnetization. The results show that there are no significant differences in suface morphology, crystallographic orientation, phase composition or superconducting transition temperature between the Y123 films grown on YSZ (100) with an Ag nano-dot layer and a control Y123 film grown on a virgin YSZ (100) surface. On the other hand, at 77K, the magnetic critical current density (J_c^m) was three times higher for the Y123 film grown on theYSZ with the modified (100) surface than for the film grown on YSZ with the virgin (100) surface. At 5K the enhancement of J_c^m was approximately seven times, at both low and high fields. This suggests an increase in pinning, caused presumably by point defects formed in the YSZ film above the Ag islands.

Increased pinning in melt-textured Bi2212 by uranium oxide addition, *M. Ionescu, B. Winton, T. Silver, S.X. Dou.*

Uranium oxide containing 9wt% ^{235}U was added into Bi2212 powder prior to melt texturing, in a composition range between 0.1wt% and 3wt%, followed by neutron irradiation at a fluence of $5 \times 10^{15}/cm^2$. We distinguished two types of pinning mechanisms. The first mechanism results from the addition of UO_2 and partial decomposition of Bi2212 phase in the proximity of UO_2 particles, where some Ca, Sr and Cu atoms are extracted from the Bi2212 structure, resulting in a Sr-, Ca- and Cu-depleted Bi2212 phase. The released Ca and Sr oxides, together with UO_2, form a new compound, USr CaO_5, whilst CuO remains as a separate phase. The second mechanism results from the splayed fission tracks following the neutron irradiation and fission of ^{235}U atoms. A quantitative assessment of these two pinning effects was carried out by AC susceptibility and DC magnetization measurements at a temperature of 5K. It was found that in the presence of UO_2, Bi2212 shows a strong increase in flux pinning as compared to a control sample containing no UO_2 additions.

Cryogenic magnetic sensor based on the magneto-resistive effect in bulk Bi2212 doped with $USr_{1.5}Ca_{1.5}O_6$, *M. Ionescu, B. Winton, T. Silver, S.X. Dou, R. Ramer.*

The measurement of magnetic fields at cryogenic temperatures is usually performed with sensors based on the Hall effect. Here we propose a much cheaper alternative, based on the large magneto-resistive (MR) effect observed in bulk Bi2212. Melt-textured Bi2212 bulk was doped with various amounts of $USr_{1.5}Ca_{1.5}O_6$ up to a level of 6wt%. The dependence of resistance on the applied DC field was measured between room temperature and 5K in applied DC fields up to 9T. This dependence shows a strong MR effect around the doping level of 6wt% at low applied fields. The temperature range where the MR effect is large enough to be considered useful for applications is situated between 45K and 85K, with a maximum around 77K. This effect could be used for constructing low-cost magnetic sensors for cryogenic applications, as opposed to higher-cost sensors based on the Hall effect.

Flux pinning and vortex dynamics in Pb and Gd co-doped Bi2212 single crystals, *S. Keshavarzi, J. Horvat, M.J. Qin, X.L. Wang, S.X. Dou.*

The flux pinning and vortex dynamics of $Bi_{2-x}Pb_xSr_2Ca_{1-y}Gd_yCu_2O_{8+z}$ (x=0, 0.34; y=0, 0.12) single crystals have been studied by magnetic hysteresis loop and relaxation measurements. Results showed that the solely Gd-doped samples had reduced flux pinning compared with undoped crystals and the secondary peak effect was absent. Crystals co-doped with Pb and Gd revealed enhancement of flux pinning at low fields with a slow relaxation rate. However, the pinning is weaker and the relaxation rate faster in higher fields fompared to solely Gd-doped samples. Evolution of the dimensionality of the vortex system under the application of different magnetic fields is discussed.

Vortex pinning by correlated disorder in nanoparticle doped MgB_2, *I. Kusevic, E. Babic, O. Husnjak, S. Soltanian, X.L. Wang, S.X. Dou.*

The magnetoresistivity and critical current density of well-characterized Si-nanoparticle doped and undoped Cu-sheathed MgB_2 tapes have been measured for temperatures $T \geq 28$ K in magnetic fields $B \leq 0.9$ T. The irreversibility lines $B_{irr}(T)$ for doped tapes show a step-wise variation with a crossover field depending on the Si-content. Such $B_{irr}(T)$ variation is typical for high temperature superconductors (HTS) containing columnar defects (with a crossover occurring near the matching field B_ϕ) and is very different from the smooth $B_{irr}(T)$ variation in undoped MgB_2 samples. However, in nanoparticle doped MgB_2, the enhancement of B_{irr} with respect to that of undoped MgB_2 persists at all field scales (including $B >> B_\phi$), which is not the case in HTS containing columnar defects. The microstructure studies of nanoparticle doped MgB_2 samples show uniformly dispersed Mg_2Si nanoprecipitates, which probably act as a correlated disorder. The observed difference between the field variation of the critical current density and the pinning force density of the doped and undoped tape supports the above findings. The impact of these results for a further enhancement of flux pinning and critical currents in MgB_2 is briefly discussed.

Microstructures and phase evolution in $Yba_2Cu_3O_y$ films grown on various substrates fabricated via a non-fluorine sol-gel route, *A.H. Li, M. Ionescu, H.K. Liu, S.X. Dou, D.L. Shi.*

$Yba_2Cu_3O_y$ films were grown on polycrystalline Ag and single crystalline YSZ (100), $SrTiO_3$ (100) and MgO (100) substrates, using a non-fluorine sol-gel method and a spin coating technique. The effects of heat-treatment conditions on the Y123 phase formation, phase evolution, crystallographic orientation and microstructure were investigated using differential thermal analysis (DTA), differential scanning calorimetry (DSC), X-ray diffraction (XRD), atomic force microscopy (AFM), optical microscopy, secondary electron microscopy (SEM) and transmission electron microscopy (TEM). For Ag substrates, Y123 phase started to form at 750°C and higher temperatures improved the degree of *(001)* texture. Mirror-like surfaces without cracks were achieved by sintering at 750-900°C. However, voids were observed for films grown on the Ag at temperatures higher than 810°C, and their number and size increased as the sintering temperature was increased. A large number of microcracks were observed for films grown on single crystal substrates. However, after the optimized conditions were established, epitaxial film free of cracks was obtained. A possible mechanism for the formation of cracks is discussed.

Microstructure observations of Ag and Ag-alloy sheathed Bi2223 tapes, *H.K. Liu, Z.M. Zhang, R. Zeng, M. Apperley.*

37-filament Bi-2223 tapes with different configurations of Ag, AgAu7wt%, AgSb0.6wt% and AgMg0.2wt% as the precursor and restack sheaths were fabricated using commercial Bi-2223 precursor material and powder-in-tube techniques. Short length samples were heat treated at a temperature in the range of 832^{o}C to 846^{o}C for the first stage (HT 1), followed by a second stage (HT 2) at 825^{o}C for 40 h and slow cooled to 785^{o}C. An intermediate roll pass was performed between the heat treatment stages. The critical current (I_c) of the tapes was measured at 77 K in self-field and in fields up to 1T. The microstructure of the alloy sheaths was examined using optical microscopy, and the Bi-2223 filaments after HT 1 and HT 2 were examined using scanning electron microscopy (SEM). It was observed that the sequence of hardness, tensile strength, and critical bend strains from higher to lower levels is very much related to the grain sizes in the restack sheath. I_c of the tapes in zero field and in applied field was influenced by the phase composition, core density, grain connectivity, grain alignment and the interface between the Bi2223 filament and sheath.

Long-range coupling of surface vortices in Nb films, *A.V. Pan.*

If a magnetic field is applied almost parallel to the main surfaces of Nb films, a magnetically anisotropic medium is formed in the applied field range $B_{c2} \leq B_a \leq B_{c3}$. It consists of a surface superconducting sheath on both films surfaces separated by the normal interior. If the magnetic field is slightly misaligned from the parallel orientation, then the perpendicular component of the field enters the film in the form of quantised flux: 2D-like Kulik or surface vortices. With the help of mechano-magnetic measurements of the oscillating superconductor in a magnetic field, it has been shown that these vortices can be coupled in coherent pairs over the normal interior of the film. The thickness of the normal region is comparable to the film thickness. The thickest film investigated is about 10λ thick, where λ is the magnetic field penetration depth. The coupling is also shown to exist below B_{c2}, presumably due to a large density of Abrikosov vortices parallel to the film surfaces, which suppress the superconducting order parameter in the interior of the films and hence create a magnetic anisotropy below B_{c2} as well.

Critical current density enhancement in MgB_2 wires by iron sheath, *A.V. Pan, S.X. Dou.*

The magneto-optical imaging technique combined with transport current measurements has shown that the transport super-current distribution within the MgB_2 core of the wires sheathed by ferromagnetic iron is significantly modified if the wires are cooled through the transition temperature in an external magnetic field. The super-currents are flowing in the middle of the bulk superconducting core, starting from very low applied fields, which are much lower than the full penetration field. In contrast, other magnetic states investigated in the iron-sheathed wires have exhibited a conventional current flow near the surface of the superconductor. Global magnetization measurements have shown that the magnetization of the sheathed wire composite in the field applied perpendicular to the wire axis depends much more strongly on magnetic history than for superconducting wires without the iron sheath. The critical current density in the sheathed round and flat wires is about one order of magnitude higher than in the same wires without the iron sheath.

The results obtained are described in terms of the overcritical state enabled by the interaction between the superconducting core and the soft magnetic sheath environment.

Low field vortex behaviour in various superconductors, *A.V. Pan, S.X. Dou, V.M. Pan.*

Different types of superconductors, possessing high values of critical current density (J_c), have been investigated at small magnetic fields (B_a) over a wide temperature range. It has been shown that the temperature dependence of the characteristic field (B*), separating the B_a-independent J_c plateau (single vortex pinning regime) and the region with $J_c(B_a)$ (collective pinning), can be attributed wither to the temperature dependence of the magnetic penetration depth for Nb films and MgB_2 bulk superconductors, or to thermally activated processes for Bi-based superconductors and $Yba_2Cu_3O_7$ superconducting films. In both cases the vortex pinning influence has appeared to have a secondary role. An exception in such B*(T) behaviour is considered for Nb films when the magnetic field has its main component applied perpendicular to the main surface of the film.

Nano-structure and high critical current density of HTS $Yba_2Cu_3O_{7-\delta}$ films (Invited Talk)**,** *V.M. Pan, V.A. Komashko, V.L. Svetchnikov, C.G. Tretiatchenko, Yu.V. Cherpak, A.V. Pan, S.X. Dou, E.A. Pashitskii, S.M. Ryabchenko, A.V. Semenov, Yu.V. Fedotov.*

With the help of HREM, EBSD and XRD techniques we have shown that a nano-dimensional network of low-angle domain boundaries (LABs), consisting of natural linear defects (out-of-plane edge dislocations) is formed in high-quality YBCO films epitaxially-grown by an off-axis dc magnetron sputtering technique. The domains are 30-300 nm in size and misoriented by about one degree. The average in-plane density of the dislocation lines is shown to be up to 10^{11} cm^{-2}. The LABs are ordered rows of parallel dislocations with non-superconducting cores where T_c is locally suppressed. The variation of superconducting and normal intervals forms a "fence" network. Dislocation cores provide strong pinning. Spaces between dislocations are transparent for supercurrent flow across the LABs. The supercurrent density, limited by the transparency, is considered as the effective depairing current density in the case where the vortices are firmly pinned. Variations of linear defect density and spatial distribution result in a certain J_c limitation mechanism. Magnetic field, angular and temperature dependencies of $J_c(T,H)$ have been measured by SQUID magnetrometry, ac magnetic susceptibility, and dc transport current techniques in YBCO films with $H_c(77\ K) \geq 2 \times 10^6$ A/cm^2. Two mechanisms of J_c limitation are proposed: depairing/transparency and vortex depinning. The vortex depinning mechanism from linear defects is shown to quantitatively describe the $J_c(T,H)$ dependences measured. This model takes into account the statistical distribution of dislocation domain sizes and inter-dislocation spacing within boundaries.

High-pressure synthesized MgB_2 with high critical currents: peculiarities of structure formation, influence of Ta, Ti, SiC and Zr additions, *T.A. Prikhna, W. Gawalek, Ya.M. Savchuk, N.V. Sergienko, J.-L. Soubeyroux, S.X. Dou, V.E. Moschil, M. Wendt, F. Odier, T. Habisreuther, Ch. Schmidt, J. Dellith, V.S. Melnikov, S. Lefloch, X. Chaud, S. Pairis, C. Brachet, P.A. Nagorny.*

High-pressure synthesized magnesium diboride-based material demonstrated at 20 K a critical current density (J_c) higher than 100 kA/cm^2 up to 3 T and higher than 10 kA/cm^2 in fields up to 5 T. In the magnetic fields up to 2 T high-pressure synthesized MgB_2 (with 10% of Ti) at 20 K has a critical current density comparable to that of Nb_3Sn at 4.2 K. The structure of samples high-pressure synthesized from Mg and B and determined by XRD analysis to contain mainly well-crystallized MgB_2 phase turned out to be more complicated, as SEM and microprobe analysis showed. In parallel with Mg and B the nanostructure of the main "matrix" phase of the samples contained oxygen and in the "matrix" there were distributed Mg-B (or more likely MgB_2) inclusions from nanometers up to 10μm in size. We found a correlation between increased J_c and irreversibility field (H_{irr}) in in the 10-30 K temperature interval and a higher amount of Mg-B inclusions distributed in the sample "matrix". The influence of Ta, Ti, SiC and Zr additions on J_c, H_{irr}, and the structure of high-pressure synthesized MgB_2 is under discussion.

Optimization of the second heat treatment process for the enhanced performance of Bi-2223 multifilamentary tapes, *M. Roussel, A.V. Pan, R. Zeng, H.K. Liu, S.X. Dou.*

Ag-sheathed Bi-2223 ($Bi_{1.72}Pb_{0.34}Sr_{1.85}Ca_{1.99}Cu_3O_x$) tapes were produced using the powder-in-tube technique and two heat treatments, with an intermediate mechanical deformation. The second heat treatment is considered to be responsible for reducing the amount of secondary phases, such as Bi-2212 and Bi-2201, as well as for healing the deformation-induced defects, such as cracks, that compromise the structural integrity and the current-carrying ability of the tapes. In the present work, the second heat treatment consisted of a two-step annealing process with the first step at 825°C followed by the second one at a lower temperature. The second-step temperature of the second heat treatment was varied. The annealing conditions of the final step have been shown to have considerable influence on the current-carrying ability of the tapes. This influence has been investigated in terms of the interplay between structural integrity, secondary phase formation, transport properties and magnetic flux penetration. "Local" (magneto-optical imaging) and "global" (X-ray diffraction, magnetization and transport measurement) techniques have been employed. The optimal second sintering stage conditions among the tapes investigated have been found for the slow-cooled (1°C/min) sample from 825°C (no second step sintering) and for the sample annealed at 750°C for 30 hours during the second step. For these samples the highest transport currents, high magnetic critical current densities, the least amount of cracks and low amounts of secondary phases have been found.

Interplay between microstructure and thermo-magnetic instabilities in MgB_2 films produced by pulsed-laser deposition, *M. Roussel, A.V. Pan, Y. Zhao, S.X. Dou, T.H. Johansen.*

Flux jumps in MgB_2 thin films have been studied using magneto-optical imaging (MOI) and magnetization measurement. Two films produced by pulsed laser deposition (PLD) are comparatively studied. One was annealed *in-situ,* that is, in the deposition chamber at 685ºC for 12 minutes while the other was annealed *ex-situ* i.e. in a furnace at 900ºC for 30 minutes. Both films show dendritic instabilities on MOI when subject to a slowly increasing perpendicular magnetic field. Those thermo-magnetic instabilities are also noticeable in the magnetization loops. However, the dendritic structures exhibit different shapes from one film to another as well as different temperature thresholds. The field dependence of the critical current density J_c is also very different with significantly stronger pinning force in the *in-situ* film. Furthermore, microstructural studies (scanning electron microscopy and atomic force microscopy) reveal that the *in-situ* film is poorly crystallized compare to the *ex-situ*, which exhibits a typical crystallized surface with random orientation. The influence of the microstructure on flux jumps and pinning properties of the MgB_2 films is discussed.

Synthesis and characterization of epitaxial YBCO thin films prepared by a fluorine-free sol-gel method for coated conductors, *D. Shi, Y. Xu, A. Li, H.K. Liu, H. Yao, Z. Han.*

In our recent studies, using a fluorine-free sol gel approach involving a trimethylacetate salt and proponic acid (TMAP) precursor solution, well textured, epitaxial YBCO thin films were synthesized. The transport critical current density was found to steadily increase as the microstructure was improved in the YBCO thin film prepared by the fluorine-free sol gel TMAP method. Hence, a high transport J_c was recently obtained on the order of 1 MA/cm^2 at 77K. Although the detailed mechanism of the carbon removal process has not yet been clearly established for the fluorine-free sol gel synthesis, it provides an effective alternative method for making long-length conductors for large-scale applications. In the recent studies, we have found that the TMAP approach presents several unique advantages including:

1. No HF formed during the process, which is difficult to remove in the TFA method
2. Stable precursor solution having a long shelf time of several months
3. Much denser microstructure compared to TFA films
4. No extra phase (such as BaF_2 in TFA approach) in addition to YBCO

With these advantages, our current experimental results have clearly shown that high-quality YBCO thin films can be synthesized by the newly developed, fluorine-free TMAP method for coated conductor development. The transport J_c is expected to improve upon optimization of processing parameters and enhancement of microstructures. Current experimental data on the synthesis and characterization of TMAP YBCO films will be presented in this talk.

The effect of Al and nano-particle SiC doping on the superconducting properties of MgB_2 superconductor, *S. Soltanian, X.L. Wang, J. Horvat, M. Ionescu, H.K. Liu, S.X. Dou.*

The effect of co-doping with Al and nano-particle SiC on the superconducting properties of MgB_2 has been investigated. Polycrystalline pellets of $Mg_{1-x}Al_xB_{2-x}SiC_x$ samples with the nominal composition x= 0.025, 0.05, 0.1, 0.2, 0.3 Al and nano-particle SiC powder were prepared using an *in-situ* reaction method. For all samples the phases, lattice parameters, microstructures, superconductivity, and critical current density were characterized by XRD, SEM and magnetic measurements. Results show that the powders severely react with the MgB_2 during the heat treatment, resulting in the loss of superconductivity. It was found that both the *a*- and *c*-lattice parameters, as well as the T_c, J_c and H_{irr} considerably decreased with an increasing doping level. For the sample doped with the highest nominal composition of x=0.3 the T_c dropped more than 18 K compared to the pure sample. In contrast to the SiC doped sample, the negative effect of Al doping is dominant, and no improvement in J_c and H_{irr} was found compared to the undoped sample.

Effect of nano-particle SiC doping on the superconductivity and critical current density of MgB_2, *S. Soltanian, X.L. Wang, J. Horvat, M.J. Qin, H.K. Liu, S.X. Dou.*

Chemical doping is found to be an effective way to enhance the critical current density (J_c) at high magnetic fields in MgB_2 superconductor. In this paper, we present the effect of nano-particle SiC doping on the superconductivity, upper critical field and critical current density of this superconductor. Wire and pellet samples were prepared using the reaction in situ technique. All the samples were sintered at 800°C for 1h in Ar. Samples were characterized by X-ray diffraction (XRD), scanning electron microscopy (SEM), transmission electron microscopy (TEM), and transport and magnetic measurements. Results show that the SiC reacts with MgB_2 and forms Mg_2Si, MgO, MgB_4, BC, and BO_x as impurity phases at sizes of less than 10 nm and uniformly distributed in the samples with grain sizes of about 100 nm. Transport and magnetic measurement results show that the critical temperature decreases slightly by 10 wt% SiC doping, however, the upper critical field (H_{c2}), J_c at high magnetic fields, and the irreversibility field (H_{irr}) are significantly enhanced as a result of this doping. The SiC doped sample also shows a remarkably lower sample size effect than the pure sample.

Significant improvement of critical current density in MgB_2/Cu short tapes through nano-SiC doping and sort-time in-situ reaction, *X.L. Wang, Q.W. Yao, J. Horvat and S.X. Dou.*

Pure and 10 wt% nano-SiC doped MgB_2/Cu short tapes were fabricated using a coating and pressing method. Samples were sintered by an in-situ reaction process at 667°C - 700°C for just 6 min. It was observed that the nano-SiC doped tapes significantly react with the Cu sheath at 700°C, while pure samples have less reaction with Cu. However, when sintering at 667°C, the reaction with Cu is significantly reduced for the nano-SiC doped samples, leading to very high critical current densities of more than 1 MA/cm^2 in zero field at T ≤ 10 K. The J_c values exceeded 10^5 A/cm^2 at 30 K in zero field, 20 K in 2 T, and T ≤ 10 K in 4 T. These J_c values are one to two orders of magnitude higher than for pure MgB_2/Cu short tapes sintered at 700°C for 6 minutes, or the best reported J_c data in Cu sheathed wires and tapes. They are comparable to the J_c values reported for MgB_2/Fe tapes. These nano-SiC doped MgB_2/Cu tapes also exhibited very little flux jumping at 5 K, indicating high thermal stability. X-ray diffraction results indicate that no Mg_2Si formed in the nano-SiC doped tapes. It is proposed that the nano-SiC addition resulted in a low formation temperature for the MgB_2 phase compared with pure MgB_2/Cu.

Study of the U/n method in $Bi_2Sr_2Ca_2Cu_2O_{8+\delta}$ bulk using USr_2CaO_6, *B. Winton, T. Silver, M. Ionescu, S.X. Dou.*

Previous experience in using the U/n method to increase J_c of Bi-2212 has been limited by the negative effects of large amounts of uranium oxide addition on Bi-2212. The use of UO_2 as a medium causes increasing J_c after irradiation for additions of up to 0.4wt% U but J_c decreases with further additions. The use of USr_2CaO_6 as an alternative to UO_2 showed much greater promise for U/n doping with increases in J_c demonstrated for up to 1.5wt%U even before irradiation. Measurements of the melting point, T_c and J_c are reported for additions of various concentrations of USr_2CaO_6 between 1.1 wt% - 6.6 wt% (0.5wt%U – 3wt%U) to melt textured Bi-2212 bulk. DTA demonstrates decreases in melting point of 0.165% with

addition of 1wt%U, increasing with further additions such that the melting point of 3wt%U matches that of pure Bi-2212. Magnetic measurements show an increase in T_c of up to 3.2% with increasing compound concentrations while J_c is also increased with the addition of Uranium compound.

Effect of carbon nanotube and titanium carbide nano-particle doping in magnesium diboride, *W.K. Yeoh, J. Horvat, S.X. Dou.*

The effect of carbon nanotube (CNT) and nano-particle TiC on MgB_2 has been studied by varying the doping level, period of sintering and the sintering temperature. For the carbon nanotube doping, there is little substitution at sintering temperatures below 800°C for all the doping levels. The level of carbon substitution for B increased with sintering temperature. Partial C substitution for B was found to enhance J_c in magnetic fields but slightly depress T_c. For 10% CNT doped samples sintered at 900°C, the J_c increased by a factor of 45 at 5K in a field of 8T, and at 20K in a field of 5T, as compared to the undoped sample. For TiC doping, the TiC remained unreacted until 800°C. The extent of TiC reaction with B increased with increasing sintering temperature, while T_c and the a-axis lattice parameter decreased, indicating carbon substitution for B. J_c(B) at 5K showed a modest improvement for the 10% TiC doped sample treated at 900°C. J_c for higher doping levels and treated at higher temperatures was degraded due to the depression of T_c.

Process optimization and characterization of Ag/AgMg sheathed multifilament Bi-2223 composite tapes, *R. Zeng, M.H. Apperley, H.K. Liu, S.X. Dou.*

The fabrication process for multifilament Ag/Ag-alloy sheathed Bi-2223 tapes has been continuously investigated and optimized to improve the properties of the tapes. It has been found that increasing the filling factor of Bi-2223, optimizing the thermo-mechanical cycles and optimizing the cooling rate of the final heat treatment have a significant effect on the tape properties. The performance of AgMg sheathed Bi-2223 tapes has been significantly improved such that engineering critical current density (J_e) greater than 8000 A/cn^2 at 77K in 200m long PIT tapes has been achieved. Further improvement in the processing of short lengths of tape resulted in critical currents (I_c) exceeding 100A at 77K in self-field. AgMg sheathed Bi-2223 multifilament tapes were characterized using the standard four-probe transport technique and non-contract Hall magnetometry. Defects and current flow distribution in tapes were observed by 2D mapping of the measurement data.

Pulsed laser deposition of MgB_2 film with high surface smoothness, *Y. Zhao, M. Ionescu, S.X. Dou.*

High surface smoothness of superconducting MgB_2 film was obtained by pulsed laser deposition followed by *in situ* annealing. The high surface smoothness is essential for industrial manufacturing of superconducting junctions and electronics. However, *in situ* MgB_2 films prepared by pulsed laser deposition (PLD) generally has particulates with a variety of sizes on its surface, which hinder the application of PLD MgB_2 films. By the "off-axis" deposition technique, we deposited MgB_2 films with the normal of the film plane perpendicular to the plume axis and effectively avoided the presence of particulates on the thin film. The films were annealed *in situ* at 685℃ for 1 min. Due to the big difference in volatility and atomic weight between Mg and B, the very smooth and homogeneous surface of MgB_2 thin film together with good T_c was only obtained by a suitable match of laser pulse repetition, laser energy and background Ar gas pressure. The mean square root roughness (R_{ms}) detected by atomic force microscopy (AFM) is 3-4 nm within a 5x5 μm^2 area, while the R_{ms} of "normal" deposited MgB_2 film is more than 60nm. The T_c value determined by dc magnetization is 27K, only slightly lower than for the "normal" deposited film.

Si addition in MgB_2 thin films by pulsed laser deposition, *Y. Zhao, M. Ionescu, J. Horvat, A.H. Li, S.X. Dou.*

A series of MgB_2 thin films were fabricated by pulsed laser deposition (PLD) on Al_2O_3-R substrate, and doped with various amounts of Si, up to a level of 18wt%. Si was introduced into the PLD MgB_2 films by sequential ablation of a stoichiometric MgB_2 target and a Si target. The precursor films were deposted at 250°C and annealed in situ at 685°C for 1min. Up to a Si doping level of ~11wt%, the superconducting transition temperarure of the film only changes marginally, as compared to the control, undoped film, for which the T_c was 27K. The magnetic critical current density (J_c) of the film at 5K was increased by 50% at a

Si doping level of ~3.5wt%, as compared to the control film. Also, the irreversibility field of the Si-doped MgB_2 films (H_{irr}) at low temperature is higher than for the undoped film.

Effect of precursor powder on superconducting properties of MgB_2 superconductor, *S. Zhou, A.V. Pan, J. Horvat, N.J. Qin, S.X. Dou.*

Different precursor powders and procedures were used to fabricate MgB_2 superconductor. It was found that the purity of the B powder has strong effects on the T_c and J_c of MgB_2. The J_c of the sample made from 90% B powder decreased 40 times at 3 T and 20 K compared with the 99% B powder samples. The impurity phases might be responsible for the suppression of T_c and J_c. Variation of the Mg:B ratio has an influence on the MgB_2 properties, with J_c decreasing with fluctuation from the normal ratio (Mg:B = 1:2). The effect of Mg powder oxidation was studied. It was found that effects from the oxidation of the Mg powder were not strong when the oxidation was mild. However, when the Mg was oxidized severely, the J_c decreased quickly. A two-step sintering process was adopted to make MgB_2. This process involved an initial lower temperature sintering followed by one at a higher temperature. It was found that the first sintering did not have good effects on the properties, despite the fact that the mass density was improved. Phase composition and microstructure were analysed to explain the effects of the different factors.

Advanced Materials for Energy Conversion II, TMS (The Minerals, Metals & Materials Society) Annual Meeting, 14th-18th March 2004, Charlotte, USA

In-situ production of nano-structured ceramics by spray solution technique, *K. Konstantinov, Z.W. Zhao,L. Yuan, H.K. Liu, S.X. Dou.*

Various nano-structured M_xO_y ceramics, e.g. CoO, Co_3O_4, SnO_2, and NiO, have been prepared in-situ by a spray pyrolysis method. The effects of the temperature and sintering time on nano-crystallinity, phase composition, and other physical or electrochemical parameters have been studied in detail. Different methods, including X-ray diffraction, gas sorption analysis (for estimation of BET surface area), and TEM and SEM techniques, combined with EDX analysis and standard battery testing methods, have been used to characterized the powders obtained. We have demonstrated that the method used is flexible and universal, and it permits good control of the crystal size and phase product, allowing in-situ production of simple or complex ceramics possessing specific surface areas that are generally larger than for the corresponding materials obtained via conventional technology. The obtained materials have promising potential applications as anode battery materials, catalysts or capacitors. (Published in Proceedings, Advanced Materials for Energy Conversion II, TMS Annual Meeting, March 14-18 2004 Charlotte USA, page 331-338.)

2nd International Symposium on Ultrafast Phenomena and Terahertz Waves, 11th-13th May 2004, Shanghai, China

Radiation induced magneto-plasmon sound wave in semiconductor nanostructures, *C. Zhang* (Keynote Speaker).

By employing the exact time dependent wavefunctions for an electron gas under a quantizing magnetic field and a laser radiation, we study the dielectric properties of a system when the laser frequency equals to the cyclotron frequency. This resonant condition leads to a new magneto-photon-plasmon (magnetopolariton) mode. Unlike the ordinary magnetoplasmon, the energy of the new mode increases rapidly with decreasing magnetic field in the low field regime. As the wave number increases, this new mode behaves like a sound wave.

9th International Workshop on Similarity in Diversity, 17th-19th June 2004, Daejeon, Korea

A new magnetopolariton mode in a two dimensional electron gas under electromagnetic radiation (Invited Talk), *C. Zhang.*

We study the properties density response function of a semiconductor heterostructure under a quantising magnetic field and laser radiation. Under the resonant condition where the photon sideband gap equals the Landau level separation, a new intra-level plasmon mode occurs. The new mode increases rapidly with the decreasing magnetic field in the low field regime and behaves like a sound wave in the large wavevector regime.

12th International Meeting on Lithium Batteries, 27th June – 2nd July 2004, Nara, Japan

Nanostructured Si/TiC composite anodes for Li-ion batteries, *Z.P. Guo, Z.W. Zhao, H.K. Liu, S.X. Dou.*

Silicon and titanium carbide (TiC) nanocomposites were synthesized using a high-energy ball milling technique. X-ray diffraction analyses show that the nanocomposite consists of amorphous silicon and nanocrystalline titanium carbide. The electrochemically inactive TiC working as a buffer matrix successfully prevents Si from cracking/crumbling during the charging/discharging process. The nanocomposite containing 40 mol % silicon obtained after milling for 4 h exhibits a stable capacity of ~380 mAh/g, suggesting its promising nature in anode materials for the lithium ion battery.

Study of polypyrrole/ silicon composites as anode materials for Li-ion batteries, *Z.P. Guo, J. Wang, H.K. Liu, S.X. Dou.*

Silicon and polypyrrole composites were synthesized using high-energy mechanical milling. The polypyrrole acts as a matrix to hold the active silicon grains as they repeatedly alloy with lithium during the operation of a lithium battery. Polypyrrole decreases the initial irreversible capacity loss of the silicon anode due to the reduction in the thickness of the solid electrolyte interface (SEI) layer formed. The composite containing 50 wt % silicon obtained after milling for 4 h exhibits a good reversibility, higher coulombic efficiency and better cycle life than the bare silicon.

Synthesis of nanocrystalline transition metal and oxides for lithium storage, *G.X. Wang, Y. Chen, L. Yang, J. Yao, S. Needham, H.K. Liu, J.H. Ahn.*

Nanosize silver and tin dioxide powders were synthesised by a novel reverse-micelle technique. The reverse-micelles were formed by micro-emulsion of organic solvents, water based salts and surfactants. The spherical nanosize Ag powders were formed via in-situ reduction. Tin hydroxide precipitation took place in reverse micelles and converted to tin dioxide nanopowders after heat treatment. The Ag and SnO_2 powders have a particle size in the range of 20 – 50 nm. The as-prepared nanosize Ag and SnO_2 nanopowders were used in lithium-ion cells for lithium storage.

Electrochemical properties of carbon-coated $LiFePO_4$ cathode materials, *G.X. Wang, L. Yang, S.L. Bewlay, Y. Chen, H.K. Liu, J.H. Ahn.*

Carbon coated lithium iron phosphates were prepared by a carbon aerogel synthesis process, through which $LiFePO_4$ particles were embedded in amorphous carbon. The carbon coating effect can significantly enhance the electronic conductivity of $LiFePO_4$. The electrochemical properties of the as-prepared $LiFePO_4$ cathode materials were systematically characterised. The carbon coated $LiFePO_4$ cathode demonstrated a high capacity and stable cyclability.

Applied Superconductivity Conference (ASC04), 4th-8th October 2004, Jacksonville FL, USA

Enhancement of upper critical field and flux pinning in magnesium diboride superconductor by nano-particle doping, *S.X. Dou.*

A systematic study of the effect of nano particle SiC and nano carbon tubes (CNT) on the field performance of the critical current density of magnesium diboride has been carried out. The results showed that these dopants have two distinguishable contributions to the significant enhancement of field performance: increase of upper critical field and improvement of flux pinning. On the one hand, nano SiC particle and CNT doping causes C substitution for B, resulting in intrinsic scattering at B and Mg sites, leading to significant enhancement of upper critical field with only a minor effect on T_c as a consequence of the unique two-gap superconductivity. On the other hand these dopants introduced many precipitates at a scale below 10nm and an extensive domain structure of 2-4nm domains, which serve as strong pinning centers. Critical current density for the nano doped samples increased by more than an order of magnitude at high fields and all temperatures compared to the undoped samples. A record high upper critical field value for bulk MgB_2 was achieved by transport measurements for the nano doped sample. The strong up turn of the upper critical field at low temperatures indicates an impurity scattering on the Mg sites. The unique feature of nano-SiC and CNT doping is the enhancement of both upper critical field and flux pinning, compared with other doping, giving it a great potential for many applications.

Effect of carbon nanotube size on superconductivity properties of MgB_2, *W.K. Yeoh, J. Horvat, S.X. Dou and P. Munroe.*

Experimental results are presented for the incorporation of carbon nanotube in polycrystalline MgB_2 superconductor based on X-ray diffraction and transmission electron microscopy measurements. Electron microscopy studies show that nanotubes are embedded in the MgB_2 matrix with a fraction of the nanotubes found to be unreacted and entangled. In contrast, magnetization measurements indicate a change in the critical current density with the length of nanotubes and not with their outside diameter. This implies that longer nanotubes tend to entangle, preventing their homogenous mixing with MgB_2 and dispersion. Overall, carbon nanotube doping of MgB_2 enhanced the critical density and depressed the critical temperature.

Superconducting and Microstructural Properties of Two Types of MgB_2 Films Prepared by Pulsed Laser Deposition, *Y. Zhao, M. Ionescu, M. Roussel, A. V. Pan, J. Horvat, S. X. Dou.*

Significant differences in superconducting and microstructural properties between two types of MgB_2 films prepared by pulsed laser deposition were determined. A very high H_{c2}-T slope of 1.1 T/K was achieved in the *in situ* film. The J_c-H curves of the *in situ* film also show a much weaker field dependence than that of the *ex situ* film. The magneto-optical (MO) images show that at 4 K the flux penetrates the *in situ* MgB_2 film through random paths, while for the *ex situ* film, the flux penetration pattern is mostly repeatable, indicating a defect-controlled flux penetration. Microstructural study (transmission electron microscopy and atomic force microscopy) revealed a relatively big grain size in the *ex situ* film. The correlation between the superconducting properties, microstructure and preparation conditions is discussed with regard to the two types of films.

European Micro and Nano Systems EMN 2004, 20th-21st October 2004, Paris

Nano-structured SnO_2 Anodes for lithium ion batteries, *L. Yuan, K. Konstantinov, G.X. Wang, H.K. Liu.*

A series of nano-crystalline SnO_2 and Carbon-SnO_2 nano-composites have been used as anode materials in Li-ion batteries. The initial powders were obtained *in situ* by spray pyrolysis technique. The process results in super fine nanocrystalline SnO_2, which is homogeneously distributed inside the amorphous carbon matrix. The SnO_2 was revealed as a structure of broken hollow spheres with porosity on both the inside and outside particle surfaces. This structure promises a highly developed specific surface area. XRD patterns and TEM images revealed the SnO_2 crystal size is about 5-15 nm. These composites show a reversible lithium storage capacity of about 590 mAh/g in the 1st cycle. The conductive carbon matrix with high surface area provides

a buffer layer to cushion the large volume change in the tin regions, which contributes to the reduced capacity fade compared to the SnO_2 without carbon. (Published in Proceedings, European Micro and Nano Systems EMN 2004, October 20-21 Paris France, page 257-260.)

49th Annual Conference on Magnetism & Magnetic Materials, 7th-11th November 2004, Jacksonville, Florida

Improvement of critical current density and thermally assisted individual vortex depinning in pulsed-laser-deposited $YBa_2Cu_3O_{7-\delta}$ thin films on $SrTiO_3$ 100 substrate with surface modification by Ag nanodots, *A.H. Li et al.*

$YBa_2Cu_3O_7$ films were fabricated by pulsed laser deposition on $SrTiO_3$ 100 single-crystal substrates whose surfaces were modified by the introduction of Ag nanodots. The critical current density sJcd was found to increase with the number of Ag shots. Zero-field magnetic J_{c0} at 77 K increased from 8×10^5 up to 3.5×10^6 A/cm^2 as the number of Ag shots increased from 0 to over 150 times. Microstructure investigations indicated that the crystallinity and the *ab* alignment gradually improved as the number of Ag nanodots increased. Thermally activated depinning of individual vortices is suggested to be responsible for the field-independent J_c plateau.

Thermally assisted flux flow and individual vortex pinning in $Bi_2Sr_2Ca_2Cu_3O_{10}$ single crystals grown by the traveling solvent floating zone technique, *X.L. Wang et al.*

Magnetoresisitivity and critical current density Jc as a function of temperature and field are studied for $Bi_2Sr_2Ca_2Cu_3O_{10}$ single crystals grown using the traveling solvent floating zone technique. Below a characteristic field Bp, Jc as a function of field exhibits a field-independent plateau associated with thermally activated pinning of individual vortices. Analysis of resistive transition broadening revealed that thermally activated flux flow is found to be responsible for the resistivity contribution in the vicinity of Tc. The activation energy U_0 is 800 K in low field, scales as $B^{-1/6}$ for $B < 2$ T and drops to 200 K with $B^{-1/2}$ for $B > 2$ T.

Synthesis, structures, and magnetic properties of novel Roddlesden–Popper homologous series $Sr_{n+1}Co_nO_{3n+1}$ (n=1,2,3,4, and infinite), *X.L. Wang et al.*

Roddlesden–Popper homologous series $Sr_{n+1}Co_nO_{3n+1}$ (n=1,2,3,4, and infinite) compounds were successfully synthesized by a high pressure and high temperature technique. Structure refinement revealed that these compounds crystallize in tetragonal structures, while the compound $n=\infty$ is cubic. These compounds are ferromagnetic with the Curie temperature decreasing from 255 K for n=1 to about 200 K for n=2–4 and down to 175 K for $SrCoO_3$. Co^{4+} ions are present in intermediate spin states for n=1–4, but in the low spin state in SrCoO3. Negative magnetoresistance was observed for Sr_2CoO_4 and found to be larger than that for $SrCoO_3$.

SPIE Photonics Asia Conference, 8th-12th November 2004, Beijing, China

Nonlinear electrical transport in quantum wells under intense radiation (Invited Talk), *C. Zhang* (Session Chairman: Nonlinear Phenomena).

The quantum transport equation for electrons under intense radiation was solved. The frequency-dependent electrical current driven directly by the radiation field is obtained. The electrical field of the laser radiation is included exactly and the electron-impurity interaction is included up to the second order. Our formalism rests on the solution of the density matrix for successive order of photon processes. It is found that as radiation intensity increases, the rate of multiphoton absorption and emission can exceed that of single photon processes. In the strong electron-photon coupling limit, rate of emission is comparable to that of absorption.

Invited Speaker Presentations / Seminars

12th National Meeting of Solid State Ionics, Soochow University, Soochow, Jiangsu, China, 24th-28th October 2004

S.X. Dou - *Development of nano-materials for electrode materials in Li ion batteries*

Institute of Materials, Northeastern University, Shenyang, China, 29th October 2004

S.X. Dou - *Nanomaterials and nanotechnology*

Institute of Materials Science, Shanghai University, 12th November 2004

S.X. Dou - *Control of nanostructure to enhance materials' performance*

Shanghai Institute of Microsystems and Information Technology, Chinese Academy of Sciences, Shanghai, 6th September 2004

Z.P. Guo - *Mg-based hydrogen storage materials*

Institute of Materials, Northeastern University, Shenyang, China, 29th October 2004

H.K. Liu - *Energy storage materials*

Institute of Materials Science, Shanghai University, 12th November 2004

H.K. Liu - *Electrode materials for advanced lithium-ion batteries*

National Synchroton Radiation Research Centre, Taiwan, 28th July 2004

G.X. Wang - *Electrode materials for advanced lithium-ion batteries*

2nd International Symposium on Ultrafast Phenomena and Terahertz Waves, 11th-13th May 2004, Shanghai, China

C. Zhang - *Radiation induced magneto-plasmon sound wave in semiconductor nanostructures*

9th International Workshop on Similarity in Diversity, 17th-19th June 2004, Daejeon, Korea

C. Zhang - *A new magnetopolariton mode in a two-dimensional electron gas under electromagnetic radiation*

SPIE Photonics Asia Conference, 8th-12th November 2004, Beijing, China

C. Zhang - *Nonlinear electrical transport in quantum wells under intense radiation*

Seminars by Visiting Scientists

Date	Name	Institute	*Title*
29th Jan 04	Prof Jai-Moo Yoo	National Research Lab Korea Institute of Machinery & Materials	Magnetic Texturing of Ni Substrates for YBCO Coated Conductor by Electrodepsoition and Research Activities of HTS Wire in KIMM
20th Jan 04	Prof J H Ahn	Department of Materials Engineering Andong National University, South Korea	Synthesis of nanopowders by reverse micelles Synthesis of carbon nanotubes by modified CVD Carbon nanotube dispersed PEO solid electrolytes
18th Feb 04	Dr T H Johansen	Department of Physics- University of Oslo, Norway	MOI of Individual Vortices Magneto-optical Imaging
19th Feb 04	Prof C T Lin	Max-Planck-Institut fur Festkorperforschung - Germany	Synthesis and Characterisation of HTS superconducting Single Crystals
20th Feb 04	Dr Giovanni Giunchi	EDISON SpA – R & D Division Milano, Italy	Grain Size Effects on the Superconducting Properties of High Density Bulk MgB_2
11th Mar 04	Prof S Y Ding	National Lab of Solid State Microscructures and Department of Physics Nangjing University	Pinning and Dynamics of Vortex Matter – Numerical study of HE, Me and PE by molecular – Dynamical approach
30th June 04	Dr Zdenek Janu	Instituet of Physics AS CR. Prague, Czech Republic	Normal State Transition in HTS and Conventional Superconductors
10th Aug 04	A/Prof Wei Jia Wen	Department of Physics, Hong Kong University of Science & Technology	Giant Electrorheological Effect of Nanoparticle Suspensions
17th Dec 04	Prof Miao Changyun A/Prof Pingjuan Niu	School of Information and Communications Tianjin Polytechnic University	RTD & HPT monolithic optoelectronic integration
20th Dec 04	Prof W Weber	Atomic Institute Vienna University of Technology, Vienna, Austia	MgB2: Mixed State Fundamentals
9th Sept 04	Cathy Foley	Applied Quantum Systems Group, CSIRO Industrial Physics, Lindfield	Superconducting Quantum Engineering at the CSIRO
5th Aug 04	Prof J Y Lee	Department of Materials Science & Engineering Korea Advanced Institute of Science and Technology	Hydrogen storage and production through $NaBH_4$ and development of direct Borohydride liquid fuel cell
3rd Aug 04	Prof J Y Lee	Department of Materials Science & Engineering Korea Advanced Institute of Science and Technology	A study on the electrochemical properties of Si-Cu-C composite for an anode material of Li-Ion batteries

Equipment and Facilities

ISEM facilities contain 9 laboratories with a floor space of approx 420m^2 comprising modern facilities for processing and characterization of HTS and energy storage materials; materials processing and a full range of materials characterization.

The majority of these facilities were founded through 6 ARC RIEF programs and the Metal Manufactures Ltd Consortium program over the past six years.

The following institutions and Chief Investigators have been involved with the ARC RIEF proposals:

Australian National University	Dr M. Das
Australian Nuclear Science & Technology Organisation	Dr E.R. Vance
CSIRO	Dr N Saviddes, Dr K Müller
Curtin University	Prof D.Y. Li and Dr I. Low
James Cook University	Prof J Mazierska
Macquarie University	A/Prof E Goldys
Monash University	Dr YB Cheng Dr. R. Krishanmurthy
University of Melbourne	A/Prof DN Jamieson
University of NSW	Prof M Skyllas-Kazacos, Dr R. Ramer
University of Queensland	Prof. M.G. Lu, Prof D.R. Mackinnon
University of Sydney	A/Prof S Ringer, Dr V Keast
University of Technology, Sydney	Prof J. Smith
Curtin University	A/Prof J. Low
University of West Sydney	Prof. M. Wilson

Materials Processing Facilities

- Freeze Drier, Lyph-Loch 4.5, 4.5l/24h
- Spray Drier, GA-32, ~100g/h
- Spray Drier OPD8 3l/hour
- Attrition Mill, 01-HD, 0-660rpm
- Planetary Mill, pulverisette 5, 0-300rpm agate
- Drawing Bench, 8m, fixed die, 11.5kW
- High energy ring mill
- Ultrasonic spray unit, 10-30μm droplets, 0.1-1 litre/hour
- Bull Block, 22cm diameter
- Rolling mill, 2 x 60mm flat & square rollers, 5cms
- Rolling mill, 2 x 55mm supported rollers, 5cm/s
- Swagging machine, 15-1mm diameter
- Hydraulic press, 10t-100t
- More than 30 various furnaces
- Controlled atmosphere gloveboxes
-

Thin Film Deposition and Structuring Facilities

- Excimer laser, ComPex301, 9W, 10Hz, 248nm
- Thin Films Pulsed-Laser Deposition (PLD) Chamber, 18" dia. With high vacuum system
- Ultra High Vacuum (UHV) PLD chamber equipped with ISD and IBAD (to be completed in 2005).
- UHV chamber (10^{-12} mBar) with multi-target rf magnetron sputtering and multi-pocket electron beam evaporation EBE techniques with direct HV connection to UHV analysis chamber.
- Electron Beam Lithography (EBL) system on the base of SEM (LaB6).
- Optical lithography.

Materials Characterisation

- DTA/TG, Setaram, 18-92, 1750°C
- XRD for Single Crystals
- TEM, J2000FX1, with EDS
- Gas absorption analyzer Nova 1000 for BET and pore size analyses
- XRD, M18XHFCu with HT 2000°C camera
- XPS, AES, ISS, UVPS in UHV analysis chamber connected to UHV thin film deposition chamber.
- SEM (LaB6 filament) JEOL, equipped with EDS
- SEM, Stereoscan 440, with EDS and EBSP
- AFM, Nanoscope IIIa
- Particle Size Analyser, Mastersizer S, 0.05-900μm
- XRD, PW1050, 3kW; XRD Texture, PW1078, 3kW
- DSC, TA300,-170°C+600°C

Physical Property Characterisation

- MPMS, 1.5-400K, 0-5T DC field
- PPMS, 4-400K, 0-9T DC field
- Horizontal field superconducting Magnet, 0-8T, 5-300K
- Lock-in Amplifier, SR510; Lock-in Amplifier, SR830DSP, 2 x PAR 5209 Lock-in Amplifier, PAR 124 Lock-in Amplifier
- Magneto Optical Imaging, 2K-300K, up to 0.2 T DC field
- Electromagnet, HSV-4H1, 2T, 100mm pole diameter
- Five power supplies (HP and Keithley) 0-900A
- Cryogenic Temperature Controller, ITC4, 0-500K
- SR560 low-noise preamplifier
- Pacific Power 3120 AMXoc current source, 12 kVA
- Spectrometers, Bomem DA3 - fast scan interferometer, Polytec FIR 25 (modified) - slow scan interferometer, Beckman FS 720 - slow scan interferometer, SPEX 1402 double grating 1 m instrument, SPEX 1704 single grating 1 m instrument, 2xSPEX 1870 single grating 0.5 m instruments
- Ballantine 1620 transconductance amplifier (up to 100A)
- Magnets, Oxford Instruments superconducting (0-7T), 2x4 inch iron-cored, Rawson-Lush gaussmeter
- Cantilever (torque force) magnetometer
- Various multimeters, HP and Keithley, including a nano-voltmeter
- VSM, Maglab, 2-400K, 0-12T DC field CTI 8001/8300 cryocooler
- Thermal conductivity measurement
- Function Generator, DSC340; Digital Oscilloscope, TDS320
- Digital Teslameter, DTM-132, with Hall Probe; Fluxmeter, 916
- 2 x He Recovery System, including liquefier – 40 litres/day
- Eddy current generator
- Electromagnet, 3473-70, 2T, 150mm pole diameter, Rawson-Lush Gaussmeter
- Lasers, Spectra Physics Model 2040 25 W Ar^+, Spectra Physics Model 165 6 W Ar^+, Spectra Physics Model 3900 Titanium-sapphire, Spectra Physics Model 380 Dye, Spectra Physics 15 mW HeNe
- Detectors, 4xInfrared Laboratories bolometers, Infrared Laboratories Ga-doped Ge photoconductor, N. Coast Scient. Corp Ge photoconductor, Photomultiplier with GaAs photo-cathode
- Cryostats, A number of L He with optical access, L N cryostats, 60 l L He storage, 30 l L He storage, 60 l L N storage, 50 l L N storage, 2x30 l L N storage, 25 l L N storage, A system for recovering and compressing He gas is in place
- Leak detector Vacuum system

Electro-Chemical Property Characterisation

- Cyclic Voltammograph, BAS CV-27
- Impedance Analyser, M6310
- Temperature Controlled Water Bath, F10-MF
- Four Channels Data Collection System, MacLab/4e

Electro-Chemical Property Characterisation (continued)

- ICP-OES, Vista MPX simultaneous axial spectrometer, 167-785nm range 0.009nm resolution 200nm
- Scanning Potentiostat, M326; Potentiostat, M363
- Power Supply, DCS 20-50, 0-20V, 0-50A
- Eight Channels Data Collection System, MacLab/8
- Controlled Atmosphere System (Glove Box), OP7
- Amplifiers, PAR 124A Lock-in, 2xPAR 5209 Lock-in, Stanford Research SR510
- CHI 660B Electrochemical Workstation
- Arbin MSTAT8000 Electrochemical Workstation
- Automatic PCT Measuring System

ICP-OES, Vista Simultaneous
Axial Spectrometer

Excimer Laser Ablation System for
Thin Film Deposition

Magnetic Property Measurement System
4K-300K, 0-5T

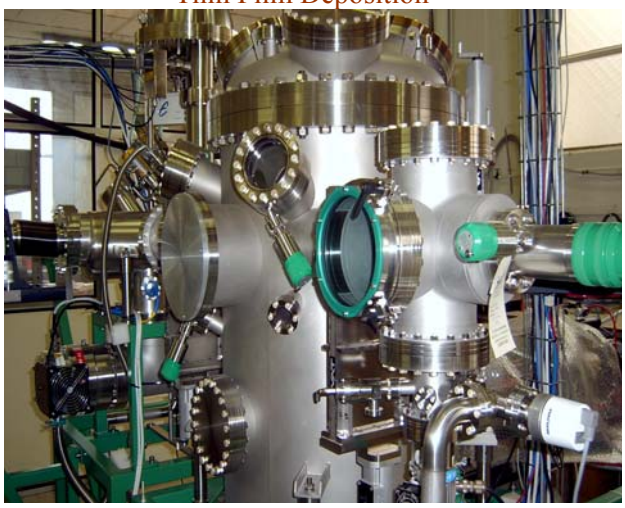

Electron Beam Evaporation Facility

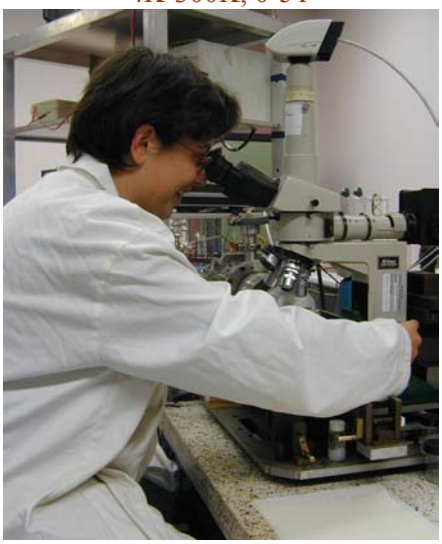

Magneto-Optical Imaging with
Cryocooler from 12K to 300K

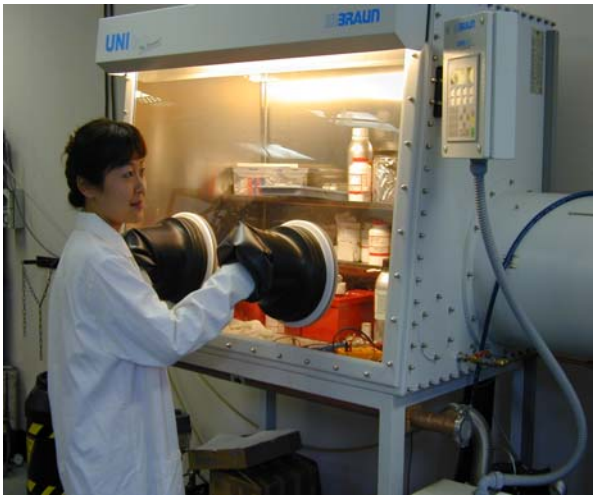

Glovebox for Creating Oxygen and
Moisture free Environment

Refereed Publications

Journal Articles

1. S.L. Bewlay, K. Konstantinov, G.X. Wang, S.X. Dou and H.K. Liu "Conductivity improvements to spray-produced $LiFePO_4$ by addition of a carbon source" *Materials Letters* **58,** 1788-1791 (2004)
2. F.S. Cai, G.Y. Zhang, J. Chen, X.L. Gou, H.K. Liu and S.X. Dou "$Ni(OH)_2$ tubes with mesoscale dimensions as positive-electrode materials of alkaline rechargeable batteries" *Angewandte Chemie International Edition* **43** 4212-4216 (2004)
3. Y Chen, G X Wang, J P Tian, K Konstantinov, H K Liu, " Preparation and properties of spherical $LiNi_{0.75}Co_{0.25}O_2$ as a cathode for lithium-ion batteries", Y Chen, G X Wang, J P Tian, k Konstantinov, H K Liu, Electrochimica Acta 50 435-441 (2004)
4. Z.X. Cheng, X.L. Wang, S. Keshavarzi, M.J. Qin, T.M. Silver, H.K. Liu, H. Kimura and S.X. Dou "The morphology, periodical modulation structure and effects of heat treatment on the superconductivity of (Tl,Pb)(Sr,Ba)-1223 single crystals" *Superconductor Science & Technology* **17** 696-700 (2004)
5. Z.X. Cheng, X.L. Wang, A.V. Pan, H.K. Liu, S.X. Dou**,** *Characterization and growth of magnesium diboride single crystals*, J. Crystal Growth 263 (2004) 218.
6. M. Delfany, X.L. Wang, S. Soltanian, J. Horvat, H.K. Liu and S.X. Dou "Nano-sized Al_2O_3 doping effects on the critical current density of MgB_2 superconductors" *Ceramics International* **30** 1581-1583 (2004)
7. S. X. Dou, V Braccini, S Soltanian, R Klie , Y Zhu, S Li, X L. Wang, D Larbalestier "Nanoscale-SiC doping for enhancing J_c and H_{c2} in superconducting MgB_2" Journal of Applied Physics **12** vol 96 7549 – 7555 Dec 2004
8. Yu.V. Fedotov, E.A. Pashitskii, S.M. Ryabchenko, A.V. Semenov, A.V. Pan, S.X. Dou, C.G. Tretiatchenko, V.A. Komashko, Yu.V. Cherpak and V.M. Pan, "Field behavior of the critical current in quasi-single-crystalline YBCO films" *Physica C* **401**, 316-319 (2004)
9. D.J. Goossens, K.F. Wilson, M. James, A.J. Studer and X.L. Wang "Structural and magnetic properties of $Y_{0.33}Sr_{0.67}CoO_{2.79}$" *Physical Review B* **69**, 134411-1 – 134411-6 (2004)
10. Z.P. Guo, J.H. Ahn, H.K. Liu and S.X. Dou "Characterization of Nanoparticles of $LiMn_2O_4$ synthesized by a one-step intermediate-temperature solid-state reaction" *Journal of Nanoscience and Nanotechnology* **4, No 1/2**, 162-166 2004)
11. J. Horvat "Nanopinning in high-temperature superconductors" *Encyclopedia of Nanoscience and Nanotechnology* **7** Ed: H.S. Nalwa, American Science Publishers, 207-218 (2004)
12. J. Horvat "Interaction of superconductor with magnetic sheath as a way for improvement of critical current in MgB_2/Fe superconductor" *Focus on Superconductivity*, Ed: Barry P Martins, Nova American Scientific Publishers, 175-190 (2004)
13. J. Horvat, S. Soltanian, A.V. Pan and X.L. Wang "Superconducting screening on different length scales in high-quality bulk MgB_2 superconductor" *Journal of Applied Physics* **96, 8**, 4342-4351 (2004)
14. J. Horvat, S. Soltanian, X.L. Wang and S.X. Dou "Effect of sample size on magnetic J_c for MgB_2 superconductor" *Applied Physics Letters* **84, 16**, 3109-3111 (2004)
15. M. Ionescu, A.H. Li, Y. Zhao, H.K. Liu and A. Crisan "Enhancement of critical current density in $Yba_2Cu_3O_{7-\square}$ thin films grown using PLD on YSZ (001) surface modified with Ag naono-dots" *Journal of Physics D: Applied Physics"* **37** 1834-1828 (2004)
16. M. Ionescu, B. Winton, T. Silver, S.X. Dou and R. Ramer "Cryogenic magnetic field sensor based on the magnetoresistive effect in bulk Bi2212+Usr_2CaO_6" *Applied Physics Letters* **84, 26,** 5335-5337 (2004)
17. M. Ionescu, B. Winton, T. Silver, S.X. Dou and R. Ramer "Large magnetoresistive effect in bulk Bi2212 with small additions of UsR_2CaO_6" *Journal of Physics D: Applied Physics* **37** 1727-1731 (2004)
18. M. Ionescu, Y. Zhao, M. Roussel, S.X. Dou, R. Ramer and M. Tomsic "Flux pinning in MgB_2 thin films grown by pulsed laser deposition" *Journal of Optoelectronics and Advanced Materials* **6,1,** 169-176 (2004)

19. M Ionescu[a)] B Winton, T Silver and S X Dou "Cryogenic magnetic field sensor based on the magnetoresistive effect in bulk Bi2212 +Usr_2 CaO_6 Applied Physics Letter ,vol 84, no. 26, pgs 5335 – 5337, (2004)
20. M. James, D. Cassidy, K.F. Wilson, J. Horvat and R.L. Withers "Oxygen vacancy ordering and magnetism in the rare earth stabilised perovskite form of $SrCoO_{3-\square}$" *Solid State Sciences* **6** 655-662 (2004)
21. Y.M. Kang, K.T. Kim, J.H. Kim, H.S. Kim, P.S. Lee, J.Y. Lee, H.K. Liu and S.X. Dou "Electrochemical properties of Co_3O_4, Ni-Co_3O_4 mixture and Ni-Co_3O_4 composite as anode materials for Li ion secondary batteries" *Journal of Power Sources* **133** 252-259 (2004)
22. S. Keshavarzi, M.J. Qin, S. Soltanian, H.K. Liu and S.X. Dou "Vortex dynamics in pure and SiC-doped MgB_2" *Physica C* **408-410**, 601-602 (2004)
23. K Konstantinov, S Bewlay, G X Wang, M Linsday, j Z Wang, H K Liu, S X Dou, J H Ahn/ "New approach for synthesis of carbon-mixed $LiFePo_4$ cathode materials", Electrochimica Acta 50, 421- 426, 2004
24. Kusevic, E. Babic, D. Marinaro, S.X. Dou and R. Weistein "Critical currents and vortex pinning in U/n treated Bi2223 /Ag tapes" *Physica C* **408-410,** 524-525 (2004)
25. R.A. Lewis, Y.J. Wang, F. Gao, X.L. Wang and S.X. Dou "Phonon spectra of cobaltite/manganites in strong magnetic fields" *Journal of Magnetism and Magnetic Materials* **272-276** 616-617 (2004)
26. R A Lewis, Y J Wang, "Magnetospectroscopy of Zn-Doped InP TO 30 T" International Journal of Modern Physics B, Vol 18, Nos 27, 28 & 29 (2004) 3839-3842
27. R.A. Lewis, Y.J. Wang and M. Henini "Zeeman spectroscopy of Be impurity in GaAs to 30T" *Physica B* **346-347** 483-487 (2004)
28. H.K. Liu "Magnesium-nickel nanocrystalline and amorphous alloys for batteries" *Encyclopedia of Nanoscience and Nanotechnology* **4** Ed: H.S. Nalwa, American Scientific Publishers, 775-789 (2004)
29. D.A. Luzhbin, A.V. Pan, V.A. Komashko, V.S. Flis, V.M. Pan, S.X. Dou and P. Esquinazi "The Origin of paramagnetic magnetization in field-cooled $YBa_2Cu_3O_{7-\square}$ films" *Physical Review B* **69** 024506-1 – 024506-7 (2004)
30. X.W.. Mi, J.C. Cao and C. Zhang "Optical absorption in terahertz-driven quantum wells" *Journal of Applied Physics* **95, 3** 1191-1195 (2004)
31. A V Pan, Yu A Genenko, S V Yampolski, "Virgin magnetization of a magnetically shielded superconductor wire: Theory and experiment" 0003-6951, Applied Physics Letters, Vol 84 no. 19, 3921/3 (2004)
32. A Pan, Pablo Esquinazi, "Decoupling transition of two coherent vortex arrays within the surface superconductivity state" 1098-0121 Physical Review B 70, pgs 184510(6) (2004)
33. A. V. Pan, S. Dou, and T. H. Johansen**,** *Magneto-Optical Imaging of Magnetic Screening in Superconducting Wires,* NATO Science Series II: Mathematics, Physics and Chemistry, Vol. 142: *Magneto-Optical Imaging*, Ed. by T. H. Johansen and D.V. Shantsev (Kluwer A. P., Dordrecht, Boston, London), pp. 141-148 (2004).
34. A Pan, S X Dou "Overcritical state in superconducting round wires sheathed by iron"0021-8979, Journal of Applied Physics, vol 96 no. 2, pgs 1146-53, (2004)
35. A V Pan, Y Zhao, M Ionescu, S X Dou, V A Komashko, V S Flis, V M Pan "Thermally activated depinning of individual vortices in YBa_2 Cu_3O_7 Superconducting films" 0921-4534, Physica C, 407 (2004) 10-16
36. A.V. Pan, S. Zhou and S.X. Dou "Iron-sheath influence on the superconductivity of MgB_2 core in wires and tapes" *Superconductor Science and Technology* **17** S410-S414 (2004)
37. M.J. Qin, S. Keshavarzi, S. Soltanian, X.L. Wang, H.K. Liu and S.X. Dou "Sample-size dependence of the magnetic critical current density in MgB_2 superconductors" *Physical Review B* **69**, 012501-1 – 012507-4 (2004)
38. D. Shi, Y. Xu, H. Yao, Z. Han, J. Lian, L. Wang, A. Li, H.K. Liu and S.X. Dou "The development of $Yba_2Cu_3O_x$ thin films using a fluorine-free sol-gel approach for coated conductors" *Superconductor Science & Technology* **17** 1420-1425 (2004)
39. T. Silver, J. Horvat, M. Reinhard, P Yao, S. Keshavarzi, P. Munroe and S.X. Dou "Uranium doping and thermal neutron irradiation flux pinning effects in MgB_2" *IEEE Transactions on Applied Superconductivity* **14, 1,** 33-39 (2004)

40. M.S. Song, S.C. Han, H.S. Kim, J.H. Kim, K.T. Kim, Y.M. Kang, H.J. Ahn, S.X. Dou and J.Y. Lee "Effects of nanosized adsorbing materials on electrochemical properties of sulphur cathodes for Li/S secondary batteries" *Journal of the Electrochemical Society* **16,6,** A791-A795 (2004)
41. M.D. Sumption, M. Bhatia, S.X. Dou, M. Rindfliesch, M. Tomsic, L. Arda, M. Ozdemir, Y. Hascicek and E.W Collings "Irreversibility field and flux pinning in MgB_2 with and without SiC additions" *Superconductor Science & Technology* **17**, 1180-1184 (2004)
42. G.X. Wang, J.H. Ahn, J. Yao, S. Bewlay and H.K. Liu "Nanostructured Si-C composite anodes for lithium-ion batteries" *Electrochemistry Communications***6** 689-692 (2004)
43. G.X. Wang, S. Bewlay, J. Yao, H.K. Liu and S.X. Dou "Tungsten disulfide nanotubes for lithium storage" *Electrochemical and Solid State Letters* **7, 10**, A321-A323 (2004)
44. G.X. Wang, Z.P. Guo, X.Q. Yang, J. McBreen, H.K. Liu and S.X. Dou "Electrochemical and in situ synchrotron x-ray diffraction studies of $Li[Li_{0.3}Cr_{0.1}Mn_{0.6}]O_2$ cathode materials" *Solid State Ionics* **167** 183-189 (2004)
45. G.X. Wang, Jane. Yao, J.H. Ahn, H.K. Liu and S.X. Dou "Electrochemical properties of nanosize Sn-coated graphite anodes in lithium-ion cells" *Journal of Applied Electrochemistry* **34** 187-190 (2004)
46. G.X. Wang, J. Yao and H.K. Liu "Characterization of nanocrystalline Si-MCMB composite anode materials" *Electrochemical and Solid State Letters* **7, 8**, A250-A253 (2004)
47. G X Wang, Z P Guo, X Q Yang, J McBreen, H K Liu, S X Dou, "Electrochemical and in situ synchrotron X-ray diffraction studies of Li $\{Li_{0.3}$ Cr $_{0.1}Mn_{o.6}\}$ O_2 cathode materials", Solid State Ionics 167 183-189 (2004)
48. G X Wang, S Bewlay, K Konstantinov, H K Liu, S X Dou J H Ahn, "Physical and electrochemical properties of doped lithium iron phosphate electrodes" Electrochimica Acta 50, 443-447 (2004)
49. G X Wang, A A M Prince, S Mylswamy, T S Chan, R S Liu, B Hannoyer, M Jean, C H Shen, S M Huang, J F Lee. "Investigation of Fe valence in $LiFePo_4$ by Mossbauer and XANES spectroscopic techniques". Solid State Communications 132 (2004) 455-458
50. G X Wang, Jane Yao, H K Liu, S X Dou, Jung-Ho Ahn,"Electrochemical characteristics of tin-coated MCMB graphite as anode in Lithium-ion cells", Electrochimica Acta 50, 517-522 (2004)
51. G X Wang, Steve Bewlay, Jane Yao, J H Ahn, S X Dou and H K Liu "Characterization of LiM_x Fe_{1-x} PO_4 (M=Mg, Zr, Ti) Cathode Materials Prepared by the Sol-Gel Method" Electrochemical and Solid-State Letters, **7** (12),A503-A506) 2004
52. J Wang, G X Wang, Y Chen, C Y Wang, H K Liu, "A novel cureless pure lead oxide plate for valve-regulated lead-acid batteries" Journal of Applied Electrochemistry **34** 1127-1133 2004
53. X.L. Wang, S. Soltanian, M. James, M.J. Qin, J. Horvat, Q.W. Yao, H.K. Liu and S.X. Dou "Significant enhancement of critical current density and flux pinning in MgB_2 with nano-SiC, Si, and C doping" *Physica C* **408-410** 63-67 (2004)
54. X.L. Wang, E. Takayama-Muromachi, A.H. Li, Z.X. Cheng, S. Keshavarzi, M.J. Qin and S.X. Dou "Growth, microstructures and superconductivity of $Bi_{2-x}Pb_xSr_2Ca_{1-y}Gd_yCu_2O_{8+z}$ single crystals" *Journal of Applied Physics* **95 No 11,** 6699-6701 (2004)
55. X.L. Wang, Q.W. Yao, J. Horvat, M.J. Qin and S.X. Dou "Significant improvement of critical current density in coated MgB_2Cu short tapes through nano-SiC doping and short-time *in situ* reaction" *Superconductor Science & Technology* **17** L21-L24 (2004)
56. W. Xu, R.A. Lewis, P.M. Koenraad and C.J.G.M. Langerak "High-field magnetotransport in a two-dimensional electron gas in quantizing magnetic fields and intense terahertz laser fields" *Journal of Physics Condensed Matter* **16** 89-101 (2004)
57. Q.W. Yao, X.L. Wang, J. Horvat and S.X. Dou "Cu and nano-SiC doped MgB_2 thick films on Ni substrates processed using a very short-time in situ reaction" *Physica C* **402** 38-44 (2004)
58. Q.W. Yao, X.L. Wang, S. Soltanian, A.H. Li, J. Horvat and S.X. Dou "Fabrication, microstructure and critical current density of pure and Cu doped MgB_2 thick films on Cu, Ni and stainless steel substrates by short-time in-situ reaction" *Ceramics International* **30,** 1603-1606 (2004)
59. W.K. Yeoh, J. Horvat, S.X. Dou and V. Keast "Strong pinning and high critical current density in carbon nanotube doped MgB_2" *Superconductor Science & Technology* **17**, S572-S577 (2004)

60. Y.H. Yu, S.C. Lee, D.C. Kim. C. Zhang and P. Harrison "Optical losses in dielectric apertured terahertz VCSEL" 20-21 October 2004 - Paris *Optics & Laser Tec+hnology* **36** 575-580 (2004)
61. C. Zhang and J.C. Cao "Calculation of the nonlinear free-carrier absorption of terahertz radiation in semiconductor heterostructures" *Physical Review B* **70** 193311-1 – 193311-4, 2004
62. Y. Zhao, M. Ionescu, J. Horvat and S.X. Dou "Comparative study of in situ and ex situ MgB_2 films prepared by pulsed laser deposition" *Superconductor Science & Technology* **7**, Ss482-S485 (2004)
63. Z W Zhao, K Konstantinov, L Yuan, H k Liu and S X Dou, "In-Situ Fabrication of Nanostructured Cobalt Oxide Powders by Spray Pyrolysis Technique", Journal of Nanoscience and Nanotechology, Vol 4, No 7, 861 -866, (2004)
64. Y. Zhao, M. Ionescu, J. Horvat, A.H. Li and S.X. Dou "Si addition in insitu annealed MgB_2 thin films by pulsed laser deposition" *Superconductor Science & Technology* **17** 1247-1252 (2004)
65. Y Zhao, S X Dou, M Ionescu, P Munroe, "Significant improvement of activation energy in the MgB_2/Mg_2Si multilayer film" – Applied Physics Letters, 1 – 6 (2004)
66. S.H. Zhou, A.V. Pan, J. Horvat, M.J. Qin and H.K. Liu "Effects of precursor powders and sintering processes on the superconducting properties of MgB_2" *Superconductor Science & Technology* **17**, S528-S532 (2004)

Conference Proceedings

1. K Konstantinov, Z W Zhao, L Yuan H K Liu, S X Dou, "In-situ production of Nano-structured ceramics by spray solution technique", 14 – 18 March 2004, North Carolina ,Advanced materials for Energy Conversion Vol 11, 331-338 (2004)
2. B C Lough, R A Lewis, C Zhang, "Principles of charge and heat transport in thermionic devices", 13-15 December 2004 – Sydney Australia, Smart Structures, Devices and Systems ll, Proceedings of SPIE Vol 5649, 332-343, (2004)
3. *D.A. Luzhbin, A.V. Pan, V.A. Komashko, V.S. Flis, S.X. Dou, P. Esquinazi, and V.M. Pan, The origin of paramagnetic magnetization in field-cooled $YBa_2Cu_3O_7$ films, Proc. 6th European Conference on Applied Superconductivity*, *Inst. Phys. Conf. Ser. No 181 (2004 IOP Publishing Ltd), pp. 2125-2132 (2004).*
4. M Roussel, A V Pan, R Zeng, H K Liu, S X Dou, T H Johansen, " Optimization of BI-2223 tape fabrication procedure with help of magneto-optical imaging" , *NATO Science Series II: Mathematics, Physics and Chemistry, Vol. 142: Magneto-Optical Imaging, Ed. by T. H. Johansen and D.V. Shantsev (Kluwer A. P., Dordrecht, Boston, London), pp. 125-132 (2004).* 28-30 August 2004 Norway, Magneto-Optical Imaging 125-132 (2004)
5. A V Pan, S X Dou, Tom H Johansen, "Magneto-optical imaging of magnetic screening in superconducting wires" NATO Advanced Research Workshop, 28-30 August 2003, Norway, Magneto-Optical Imaging 141-148 (2004)
6. A.V. Pan, M.J. Qin, X.L. Wang, H.K. Liu and S.X. Dou "Effects of Si and C doping on the superconducting properties of MgB_2" *Advances in Cryogenic Engineering, International Cryogenic Materials Conference*, Anchorage, Alaska 22-26/9/2003, Ed: U. Balachandran, 554-560 (2004)
7. A V Pan, Sihai Zhou, S X Dou, "Overcritical state as a result of the magnetic interaction between iron sheath and MgB_2 core in superconducting wires and tapes" Institute of Physics Conference Series No. 181, (2004 IOP Publishing Ltd, pp. 2542-2549 (2004) Paper presented at 6th European Conference of Applied Superconductivity, 14-18 Sept 2003
8. V Pan, C Tretiatchenko, V Komashko, Yu Cherpak, E Pahitskii, A Semenov, S Ryabchenko, A Pan, S Dou, V Svetchnikov, H Zandbergen, "Nature of critical current limitation in HTS $YBa_2Cu_3O_{7-d}$ films", Institute of Physics Conference Series No. 181, (2004 IOP Publishing Ltd, pp. 2542-2549 (2004) Paper presented at 6th European Conference of Applied Superconductivity, 14-18 Sept 2003
9. L Yuan, K Konstantinov, G X Wang, H K Liu, "Nano-structured SnO_2 Anodes For Lithium Ion Batteries", 20-21 October 2004 Paris, ASME Nanotechnology Institute, European Micro and Nano Systems 2004
10. C. Zhang, S. Hessami Pilehrood, "Nonlinear free carrier absorption in semiconductor heterostructures in terahertz regime" *Proc of International Society for Optical Engineers"* 10-12/12/2003, Perth, Australia, 284-291 (2004)

Australian Research Council Grants

ARC Large/Discovery Scheme Grants

S.X Dou J. Horvat	First principles for development of high temperature superconducting wires	$217,899	
S.X. Dou M.J.Qin	Control of nano-structure for enhancing the performance of magnesium diboride superconductor by chemical doping	$100,000	
X.L. Wang	Enhancement and elucidation of flux pinning in doped Bi-Sr-Ca-Cu-O high temperature superconducting single crystals	$62,967	
C. Zhang, R.A. Lewis	Analysis, simulation, fabrication and characterization of reliable, robust and salable compact cooling elements based on semiconductor nonostructures	$80,000	
X.L.Wang, M.Ionescu Z.X. Cheng	Fabrication, Charge and Spin Ordering, Magnetoresistance, and polaron effects in nano-size and single crystals of novel transition metal perovskite oxide	$77,000	
H K Liu Z.P.Guo	Hydrogem storage materials for energy conversion appplications	$85,000	
A V Pan	Development of hight-temperature superconducting coated conductors by pulsed-laser deposition for future long-length applications	$70,000	
C Zhang R.A.Lewis X.Zhang R.E.Vikers	Non-linear dynamics in electronic systems and devices under intense terahertz radiation	$120,000	
			$812,866

ARC Centre of Excellence Grants

H.K. Liu	Nano-materials for energy storage	$198,174	
			$198,174

Strategic Parnterships with Industry – (SPIRT) Scheme - Linkage Projects & Linkage APAI

S.X. Dou GX. Wang	Developing new cathode materials for lithium-ion batteries using Australian mineral resources	$84,000	
S.X. Dou X.L.Wang, M.Ionescu	Fabrication and characterisation of magnesium diboride superconducting wires	$100,000	
R. Lewis C. Zhang	Experimental development of thermionic cooling for domestic refrigeration	$60,000	
X.L. Wang	Fabrication of Magnesium Diobride (MgB_2) thick films	$22,545	
H K Liu	Lithium/sulphur rechargeable batteries for power applications	$75,000	
G X Wang	Large-scale rechargeable lithium battery for power storage and electric vehicle applications	$110,000	
			$451,545

Total this page **$1,462,585**

Brought Forward			**$1,462,585**
ARC linkage-infrastructure			
R.A Lewis C. Zhang H.H. Tan A.M. Sanagavarapu A.R.Hamilton	T-ray factory: a new Australian souce of strong, pulsed, broadband, terehertz radiation	$113,190	
Total this page			**$113,190**
Linkage International Awards			
H.K. Liu, D. Shi	Investigation of a series of metallic substrate materials suitable for developing long Y-Ba-Cu-O superconductors	$17,596	
S X Dou	Magneto-Optical imaging of super current flow in superconducting tapes and wires	$14,140	
C. Zhang R.A.Lewis K.A.Chao	Simulation and characterisation of opto-thermionic cooling devices	18,700	
			$50,436
Research Infrastructure Block Grants			
S X Dou,	Electrochemical Workstation for research on	$74,000	
G X Wang	Dynamics of Electrode Materials	$35,000	
			$109,000
Systemic Infrastructure Initiative Grants			
S.X. Dou	Nanofabrication facilities for processing of novel multiplayer materials	$487,000	
			$487,000
Small Grants & Indicative Near Miss Grants			
G.X.Wang H. Liu K. Konstantinov S. Zhong	Novel lithium phospho-olivines for lithium storage electrodes	$10,000	
C. Zhang	Magnetoresistance in high mobility electronic systems under a microwave radiation	$12,000	
	Diluted Magnetic Semiconductor (DMS) Materials for Spintronics	$8,000	
G. Wang	An investigation of the transition metal disulfide nanotubes for hydrogen and lithium storage	$9,000	
J. Horvat	Current transport in MgB2 superconductor	$10,350	
			49,350
Total this page			**$2,271,561**

Brought forward			**$2,271,561**

Australian Institute of Nuclear Science & Engineering

D. Marinaro/SX Dou	Special Postgraduate Award	$5,500	
T.Silver	Thermal neutron irradiation of uranium-doped superconductors	$1,710	
X.L. Wang	Studies of novel perovskite cobalt compounds	$10,818	
X.L. Wang	Studies of magnetic properties of doped Y-Sr-Co-O perovskite cobalt compounds	$27,818	
X.L. Wang	Enhancement of critical current density in newly discovered MgB_2 superconductors using hot isostatic press and hot press techniques	$2,300	
			$48,146

Industry Grants

Metal Manufactures Ltd	$70,000	
Lexel Battery Co Ltd	$19,500	
Sons of Gwalia Ltd	$30,000	
Hyper Tech Research Inc	$20,000	
Australian Battery Technology Ltd	$15,000	
OMG Group	$10,000	
Alphatech International Ltd	$6,000	
FSL Enterprises Ltd	$5,000	
		$175,500

University of Wollongong Support

ISEM Performance Indicators	$102,309	
Faculty of Engineering funding	$20,000	
URC contribution	$125,000	
Postgraduate student maintenance funds	$23,625	
Scholarships	$189,000	
		$459,934

TOTAL 2004 funding	**$2,955,141**

Professor SX Dou
Director
e-mail: shi_dou@uow.edu.au

Prof. C. Zhang
Assoc. Director
Telephone: 61 + 2 4221 3458
Facsimile: 61 + 2 4221 5944
e-mail:

Ms Christine O'Brien
Administration Officer
e-mail: cobrien@uow.edu.au

Telephone: 61 + 2 4221 5730
Facsimile: 61 + 2 4221 5731
web site: http://www.uow.edu.au/eng/ISEM

Northfields Avenue
Wollongong NSW 2522
Australia

Applied Superconductivity

Dr. J Horvat
Telephone: 61 + 2 4221 5725
Facsimile: 61 + 2 4221 5731
e-mail: jhorvat@uow.edu.au

Spintronic & Electronic Materials

Dr. X.L. Wang
Telephone: 61 + 2 4221 5766
Facsimile: 61 + 2 4221 5731
e-mail: xiaolin@uow.edu.au

Energy Materials

Prof. H.K.Liu
Telephone: 61 + 2 4221 4547
Facsimile: 61 + 2 4221 5731
e-mail: hua_liu@uow.edu.au

Dr. G.X. Wang
Telephone: 61 + 2 4221 5726
Facsimile: 61 + 2 4221 5731
e-mail: gwang@uow.edu.au

Thin Film Technology

Dr A.V.Pan
Telephone: 61 + 2 4221 4729
Facsimile: 61 + 2 4221 5731
e-mail: pan@uow.edu.au

Nanostructured Materials

Dr. K. Konstantinov
Telephone: 61 + 2 4221 5765
Facsimile: 61 + 2 4221 5731
e-mail: kostan@uow.edu.au

Terahertz Science, Thermionics & Solid State Physics

Prof. C. Zhang
Telephone: 61 + 2 4221 3458
Facsimile: 61 + 2 4221 5944
e-mail: chao_zhang@uow.edu.au